Forschungszentrum Karlsruhe

Technik und Umwelt

Wissenschaftliche Berichte

FZKA 6721

TRePro 2002

Modelling of Coupled Transport Reaction Processes

Workshop of the Forschungszentrum Karlsruhe

held at 20th and 21st of March 2002

Editors:

V. Metz, W. Pfingsten*, J. Lützenkirchen and W. Schüßler

Institut für Nukleare Entsorgung

* Paul-Scherrer-Institut, Labor für Endlagersicherheit

Forschungszentrum Karlsruhe GmbH, Karlsruhe

2002

Impressum der Print-Ausgabe:

Als Manuskript gedruckt

Forschungszentrum Karlsruhe GmbH
Postfach 3640, 76021 Karlsruhe

Mitglied der Hermann von Helmholtz-Gemeinschaft
Deutscher Forschungszentren (HGF)

ISSN 0947-8620

Preface

A wide variety of geochemical processes including the migration of radiotoxic and chemotoxic materials are intimately related to reactive transport processes. The relevant rock-water systems can be regarded as open geochemical reactors where chemical changes occur via the transient interactions between the aqueous, solid and gas phases. The evolution of these open systems is affected by diverse processes including fluid flow, transport of solutes and colloids, and chemical reactions.

Reactive transport codes may be used to simulate the chemical interactions and the transient migration of relevant species in one-, two- or even three-dimensional spatial configurations. The ability to model reactive transport in natural systems and the near- and far-fields of waste repositories has advanced considerably over the past decade. Numerous comprehensive reactive transport codes have been developed and applied. However, all modelling approaches implicitely apply certain simplifications. At the present stage of process understanding and the state of computational capabilities, it is still impossible to predict the evolution of a natural system or a repository. Nevertheless, reactive transport modelling may provide insight into some of the relevant phenomena.

TRePro 2002 deals with “Modelling of Coupled **T**ransport **Re**action **Pro**cesses”. The field of reactive transport involves a number of diverse scientific disciplines, such as those related to advective, convective, dispersive and diffusive transport of solutes and colloids, and interactions among aqueous species, redox reactions, dissolution/precipitation, surface complexation and ion exchange, as well as radioactive decay and biochemical reactions, and those scientific disciplines related to the required numerical aspects of the modelling.

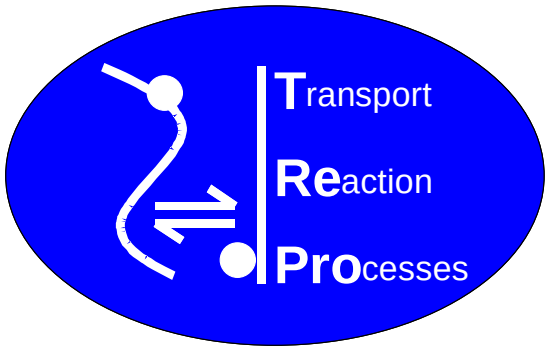

The workshop focuses on the following major topics:

- Coupling of sorption processes and transport
- Coupling of redox processes and transport
- Coupling of dissolution / precipitation processes and transport
- Influence of colloids on transport phenomena

Coupled transport reaction modelling may become one of the cornerstones to evaluate the performance of a geological repository for radiotoxic and chemotoxic wastes. Therefore, the challenge of involving coupled transport reaction processes in the frame of performance assessment is included in **TRePro 2002.** Indeed, it is one of the objectives of the workshop to learn to what extent this may be done at present. The workshop is an attempt to bring together researchers from the disciplines mentioned above, experimentalists and modellers, for stimulating discussion on the latest developments in modeling of coupled transport reaction processes and their relevance to performance assessment.

TRePro 2002 is the third meeting in the series of the Karlsruhe Geochemical Workshops. The first workshop was held in 1997 at the Forschungszentrum Karlsruhe. Its main topic was “Geochemical Modelling - Radio Toxic and Chemical Toxic Substances in Natural Aquatic Systems”. The second workshop was held in 1999 in Speyer focusing on “Mineral / Water Interactions Close to Equilibrium”. The present workshop was jointly organized by Institut für Nukleare Entsorgung, Forschungszentrum Karlsruhe (FZK-INE) and Labor für Endlagersicherheit, Paul Scherrer Institut (PSI-LES). This book of abstracts contains the contributions presented at **TRePro 2002** held at the Forschungszentrum Karlsruhe, March 20-21, 2002.

The organizing committee thanks all the authors for their efforts to prepare their extended abstracts in advance of the workshop. Moreover, we would like to thank the numerous persons behind the scenes who contributed in whatever way to the workshop. Especially, the support by FZK-INE director Prof. J.-I. Kim and PSI-LES director Prof. J. Hadermann is acknowledged. Special thanks are also due to Mrs. G. Endreß for her administrative assistance.

PAUL SCHERRER INSTITUT

Forschungszentrum Karlsruhe
Technik und Umwelt

Content

TOWARDS OBTAINING THE EXCHANGE COEFFICIENTS OF SYNTHETIC ZEOLITE NaP1; MULTICOMPONENT ION EXCHANGE TO BE COUPLED TO TRANSPORT

J. Cama, A. Garrido, X. Querol, and C. Ayora
Institute of Earth Sciences "Jaume Almera", CSIC, Barcelona, Catalonia;
E-mail: jcama@ija.csic.es, agarrido@ija.csic.es, xavier.querol@ija.csic.es, ayora@ija.csic.es

INTRODUCTION

Na-exchanger zeolite NaP1 is synthesized at the Institute of Earth Sciences "Jaume Almera" from fly ash by conventional and microwave-assisted hydrothermal alkaline activation experiments (Querol et al., 1997). This zeolitic material has been proposed as candidate to remove metal cations in solution from acid mine and industrial waste waters (Moreno et al., 2001). Furthermore, ground-water remediation using NaP1 exchanger is expected to be carried out either by mixing the zeolitic material with contaminated soil or as a permanent reactive barrier. At the laboratory, column experiments are designed to simulate field conditions, i.e., circulation of solutions with known pH and metal concentration through a mixture of NaP1 zeolite and soil. The reactive transport code RETRASO (Saaltink et al., 2000), which incorporates cation-exchange reactions coupled to transport equations is suitable to evaluate the change in composition through the columns. For the precise evaluation of the exchange process that takes place during transport with NaP1, the exchange coefficients ($K_{i/j}$) of each cation exchange reaction between Na and the exchangeable cations in solution ought to be found out. The exchange coefficients account for the competition between exchangeable cations for the exchanger sites, the exchangeable cation-charge character as well as the possible temperature effect.

We present experimental results regarding cation exchange reactions between Na^+ of NaP1 and monovalent and divalent exchangeable cations in solution K^+, Ag^+, Ca^{2+}, Ba^{2+}, Cu^{2+}. The results obtained up to now allow us to understand the mechanism by which the multicomponent exchange reactions may take place. These results are also the basis to obtain the appropriate values of selectivity coefficient required to coupling exchange reactions with zeolite NaP1 to transport.

NaP1 EXCHANGE EQUATIONS

Equilibrium between zeolite NaP1 and exchangeable cations is calculated with the law of mass action as the reaction is considered as

$$\frac{1}{z_i} i^{z+} + Na - X \leftrightarrow \frac{1}{z_i} i - X + Na^+$$

$$K_{i/Na} = \frac{\{i - X\}^{\frac{1}{z_i}} \left[Na^+\right]}{\{Na - X\}\left[i^{z+}\right]^{\frac{1}{z_i}}}$$

where $K_{i/Na}$ is the exchange coefficient, z_i is the valence of the cation i, and braces and brackets indicate the activity of the exchangeable and aqueous species, respectively. The values of exchange coefficients for smectite rich sediments are listed in Appelo (1996).

SYNTHETIC ZEOLITIC MATERIAL AND PRETREATMENT

The synthesized raw material contains about 65 % of zeolite NaP1 whose structural formula is $Na_{5.7}(Si_{9.98}Al_{6.12}O_{32})\cdot 9.64H_2O$. The rest of the sample is formed by remaining amorphous glass (rich in Si and Al) and crystalline phases as quartz (SiO_2), mullite ($Al_6Si_2O_{13}$), calcite ($CaCO_3$), tobermorite ($Ca_5Si_6O_{16}(OH)_2$) and magnetite (Fe_3O_4). The specific surface area was 18.1 $m^2\ g^{-1}$ (± 5%). Along with these phases dried NaOH (used as a reagent in the production of the zeolite from the fly ash) is present in about 5 % of weight. Experimentally found CEC is about 2.7 meq/g.

The presence of 5 % of NaOH might hinder the cation exchange reactions since its removal of the sample may interfere the exchange with the solution cations competing for Na sites. To release the dry NaOH, different amounts of raw material are washed with 0.01 M HCl solution. For example, 20 g of zeolitic material are added to 1 L of double deionised water (DDW) and stirred. Immediately, the solution pH rises up to 11 as NaOH is being dissolved. Accordingly suitable amounts of HCl solution are continuously poured to the mixture to maintain pH about 7. After 1 h, the solution is decanted and the solid is filtered through a Whatman 0.45 μm filter. Afterwards the solid is added to another 1L of DDW to maintain the pH at about 5, following the same procedure. After 40 min, the pH remains constant. Then the solution is decanted and the solid is filtered and let dry for 24 h at 90 ºC in the oven. The recovered sample -pretreated NaP1- is used in all the cation exchange experiments. Similarity between XRD patterns before and after the pretreatment indicates that the bulk NaP1 sample remains practically unaltered.

EXPERIMENTAL RESULTS AND DISCUSSION

All the experiments have been carried out by adding 1 g of pretreated NaP1 into 100 mL of desired exchangeable cation solution in 250 mL capped beakers partially immersed in water-baths to totally cover the mixture at the desired temperature. Well-stirred mixtures are ensured placing a magnetic Teflon bar that is agitated with a submersible magnetic plate. Initial solutions' pH is approximately 5.6. In general, as the powder is added to the aqueous solution, the pH decreases to about 4.9. Concentrations of all the cations involved in the exchange are measured. Total Al and Si concentrations in solution released during the experiment due to NaP1 dissolution are also measured. Nevertheless, Al concentration in solution is undetectable at the experimental pH due to precipitation of Al-bearing solids (e.g., Al-oxyhydroxides).

The experiments are conducted to evaluate the kinetics, temperature and charge effects on the exchange reactions. Cation exchange isotherms for the binary systems Na^+ - K^+ and Na^+ - $Ca^{2+}$are presented.

Exchange kinetics

Several experiments have been carried out to estimate the kinetics for the binary exchange reactions. The time to closely approach ion exchange equilibrium is within 4 h as shown in Fig. 1 (a). For K, Ba and Cu exchange experiments additional experiments run for 24 h have been conducted. The exchanged concentration is approximately the same within error to that of 4 h, which indicates that the exchange equilibrium is closely reached. Si release increases with time as the sample is being dissolved. Cama et al. (2001) calculated the dissolution rate of NaP1 at pH 5 and 25 ºC. Accordingly after 24 h (1440 min) and assuming that the reactive surface area is the same as that measured by BET, about 5 μM of Si should be released to solution due to NaP1 dissolution. Fig. 1 (b) shows that the measured concentration is two orders of magnitude higher. This important difference may be attributed to amorphous glass

dissolution and to the existence of very reactive ultrafine particles. Therefore, we safely assume no cation interference due to zeolite dissolution.

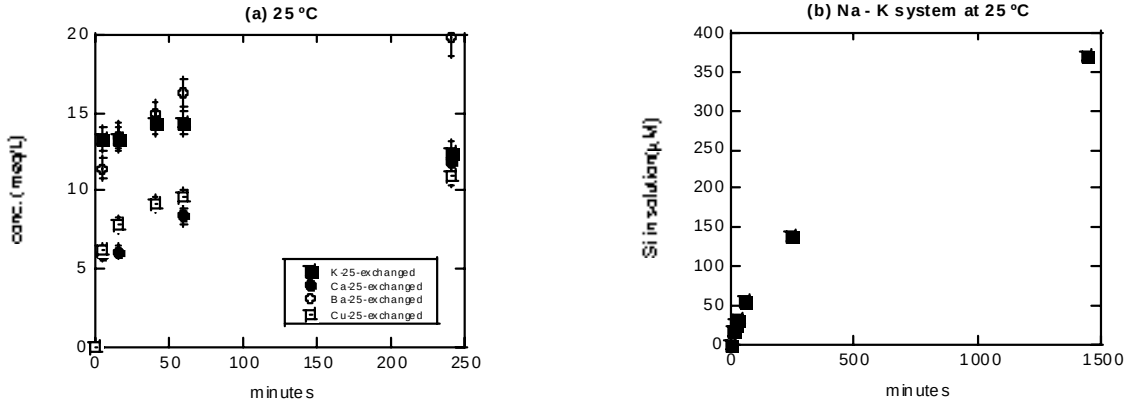

Figure 1. (a) Evolution of the cation exchange for the binary systems and (b) Si release to solution in the system Na^+ - K^+.

Temperature effect

Experiments are conducted at 25, 50 and 70 ± 0.1 ºC to examine the temperature effect on the exchange reactions for the binary systems Na^+ - K^+ and Na^+ - Ca^{2+}. Temperature seems not to affect the reaction between monovalent cations, whereas it seems to affect between monovalent and divalent cations as observed in Fig. 2.

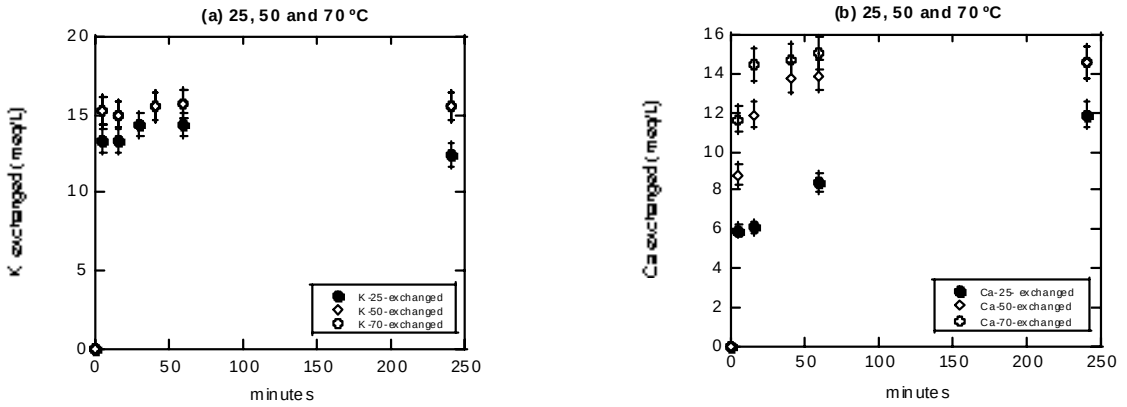

Figure 2. Temperature effect on the kinetic behaviour and exchange capacity of the binary systems (a) Na^+ - $K^+$and (b) Na^+ - Ca^{2+}.

Exchange isotherms

Cation exchange isotherms at 25 ºC for the binary systems Na^+ - K^+ and Na^+ - Ca^{2+} are plotted in terms of Na^+ released to solution versus the exchangeable cation in solution in Fig. 3. To model the experimental isotherm Langmuir type regressions are used:

$$C_{Na(sol)} = 14.3 \pm 0.7 \cdot \frac{0.65 \cdot C_{K(sol)}}{1 + 0.65 \cdot C_{K(sol)}} \text{ and } C_{Na(sol)} = 10.2 \pm 0.6 \cdot \frac{46 \pm 21 \cdot C_{Ca(sol)}}{1 + 46 \pm 21 \cdot C_{Ca(sol)}}.$$

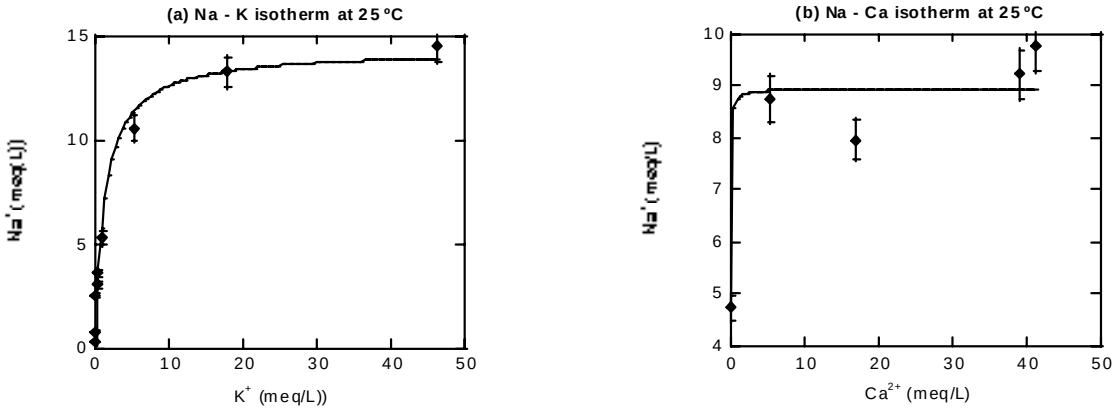

Figure 3. Exchange isotherms associated to binary systems: (a) $Na^+ – K^+$ and (b) $Na^+ – Ca^{2+}$. R^2 values for the respective Langmuir type regressions are 0.98 and 0.91.

Experimental work for cation exchange at pH 5 is carried out to assess the final values of exchange coefficients related to zeolite NaP1 exchange. Additional experiments, which are being currently conducted and the obtained results are going to be discussed during the meeting.

REFERENCES

Appelo, C. A. J. 1996. Multicomponent ion exchange and chromatography in natural systems. *Reactive transport in porous media. Reviews in Mineralogy* 34, 193-225.

Cama, J. Querol, X., Sanz, E., and Ganor, J. 2001. pH effect on synthetic zeolite dissolution under acidic conditions. *European Journal of Mineralogy* 13, 33.

Moreno, N., Querol, X., Alastuey, A., López-Soler, A., and Ayora, C. 2001. Immobilization of heavy metals in polluted soils by the addition of zeolitic material synthesized from coal fly ash. *International Ash Utilization Symposium, Lexington, Kentucky, USA*

Querol, X., Alastuey, A., López-Soler, A., Plana, F., Andrés, J.M., Pedro-Ferrer, R..J. & Ruiz, C. 1997. A fast method for recycling fly ash, microwave-assisted zeolite synthesis. *Environmental Science & Technology* 31, 2527-2533.

Saaltink, M.W., Ayora C. & Carrera, J. 1998. A mathematical formulation for reactive transport that eliminates mineral concentration. *Water Resources Research* 34, 1649-1656.

ACKNOWLEDGEMENTS

This work is partially funded by an European Research project PIRAMID and by a Research and Development contract with the Spanish Government CICYT. JC is also supported by a grant from the Catalan government. The analytical assistance of S. Toro, R. Bartrolí and J. Elvira is gratefully acknowledged.

FULLY COUPLED MODELING OF RADIONUCLIDE MIGRATION IN A CLAYEY ROCK DISTURBED BY ALKALINE PLUME

Laurent De Windt[1], Delphine. Pellegrini[2] and Jan van der Lee[1]

1-Ecole des Mines de Paris (EMP/CIG), 35 rue Saint-Honoré, 77305 Fontainebleau, France; E-mail: dewindt@cig.ensmp.fr, vanderlee@cig.ensmp.fr

2-Institut de Protection et de Sûreté Nucléaire (IPSN/DES), BP6, 92265 Fontenay-aux-Roses, France; E-mail: delphine.pellegrini@ipsn.fr

OBJECTIVES OF THE STUDY

The disposal of radioactive wastes in clayey formations may require the use of large amounts of concrete and cement as a barrier to minimize corrosion of steel containers and radionuclide migration and for supporting drifts and disposal vaults. In this context, reactive transport modeling of the interactions between cement or concrete and the argillaceous host rock aims at estimating the evolution in time of the containment properties of the multi-barriers system.

The objectives of the paper are to demonstrate that integrating radionuclides migration in the modeling of strongly coupled geochemical processes of cement-claystone interactions is feasible and that it represents an efficient way to assess the sensitivity and modification of the classical Kd and solubility parameters with respect to the chemical evolutions. Two types of modeling are considered in the paper: i): calculation of intrinsic solubility limits and Kd values backing up on the results of modeling of cement/claystone interactions (radionuclides are assumed to be present over the whole domain at any time whatever the scenario), ii) full mechanistic modeling which explicitly introduces radionuclides in the calculation with ad hoc assumptions on radionuclide inventory, canister failure, migration pathway, etc.

The reactive transport code HYTEC (van der Lee and De Windt, 2001), based on the geochemical code CHESS (van der Lee, 1998), is used to simulate both the cement-claystone interaction processes and the radionuclide migration in 1D and 2D configurations. Convective/dispersive and diffuse transport can be simulated for solutes and colloids. A wide range of processes such as aqueous chemistry, redox, dissolution/precipitation, surface complexation and ion exchange can be modeled at equilibrium or with kinetic control. In addition, HYTEC is strongly coupled, i.e. the hydrology (flow and diffusion) may change when mineral precipitation or dissolution changes the local porosity (Lagneau, 2000).

CONTEXT AND MODELING ASSUMPTIONS

The studied system is a simplified representation of a potential repository site of intermediate level radioactive wastes in a deep claystone formation (De Windt et al., 2001). The waste disposal design consists of long horizontal tunnels (100 m long, 6 m in diameter) perpendicular to handling drifts. For simplicity, it is assumed that the tunnels are entirely filled with a young Portland Cement (pH = 13.3 with CSH1.8, portlandite and ettringite as principal minerals). The claystone mainly contains clay minerals (illite, montmorillonite) with cation exchange properties (CEC = 20 meq/100g), but also quartz, calcite and dolomite. The porewater has a pH of 7.7 with sodium, chloride and sulfate as major ions. Diffusion is predominant over the whole system and an excavation damaged zone is considered around the tunnels.

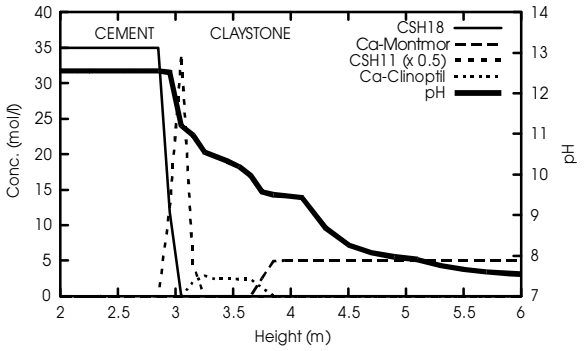

Figure 1. Evolution after 10000 y. Extension of the pH disturbance and distribution of the mineral with radionuclide retention properties (hyp. C).

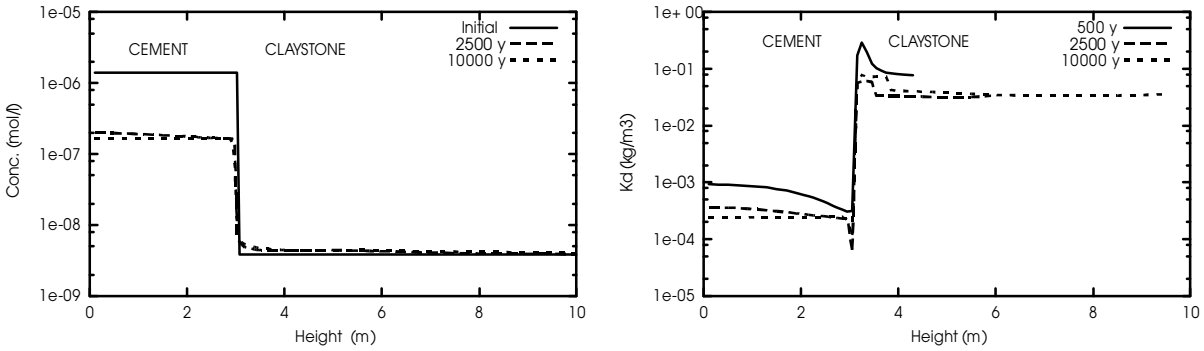

Figure 2. Modification of the solubility limit of technetium (hyp. A, intrinsic calculation) and of the Kd value of caesium (hyp. C, mechanistic calculation) during the first 10000 years.

One of the most problematic issues in cement/rock interactions is to select secondary minerals which will be allowed to precipitate in the simulations. Keeping in mind performance assessment requirements, we have analyzed in previous studies the effect of the mineralogical hypothesis on the extension of the alkaline plume and the claystone degradation [see for instance De Windt et al (2001)]. Globally, after 10000 years, the pH is always strongly buffered and important mineral transformations occur at the interface, both in cement and host rock, over several decimeters. Even beyond the zone of intense mineral transformations, the pore water chemistry is disturbed due to an attenuated but continuous flux of OH^-, K^+ and Ca^{2+} ions over many meters. Four interdependent mechanisms control the pH profile in the whole system: diffusion of the alkaline plume, mineralogical buffering, ion exchange and sealing of the pore space. Two mineralogical hypotheses are considered in the present paper: i) CSH of low Ca/Si ratio, hydroxides and carbonates are introduced in the thermodynamic database in addition to the initial minerals of cement and claystone (hyp. A); ii) zeolites, cation exchange and surface complexation are introduced too (hyp. C). The EQ3/6 (V8-R6) dataset (Wolery, 1992) is selected, but enriched with specific data for the rather well documented radionuclides Cs, Sr, Tc and U. As a typical example, Figure 1 provides some details on pH and mineralogy around the interface after 10000 years of cement – claystone interactions.

INTRINSIC AND MECHANISTIC SIMULATIONS

The solubility of technetium has been calculated according to the intrinsic approach over the entire domain for hypothesis A using the NEA thermodynamic database (Rard et al., 1999). As shown in Figure 2, there is initially a difference of more than two orders of magnitude between the theoretical maximum solubility of Tc in cement and claystone porewaters.

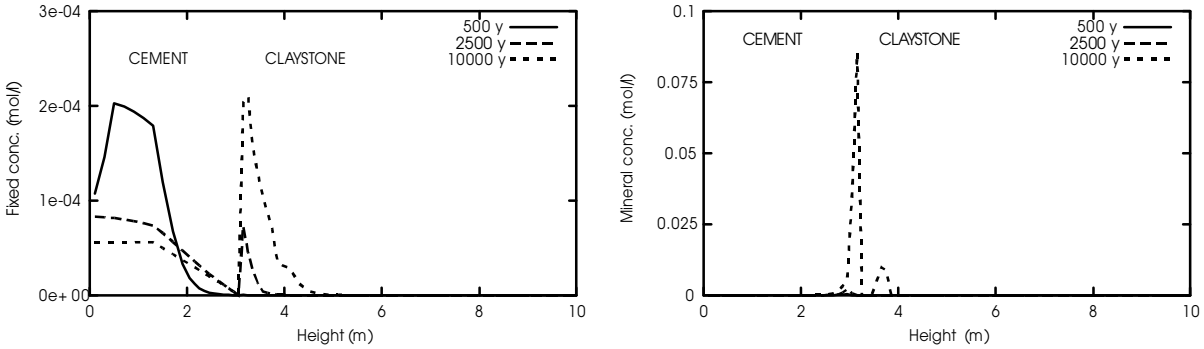

Figure 3. Examples of mechanistic processes. Evolution over 10000 years of the fixed caesium concentration in both cement and claystone and precipitation of strontianite, mostly at the cement-claystone interface, in case of strontium migration.

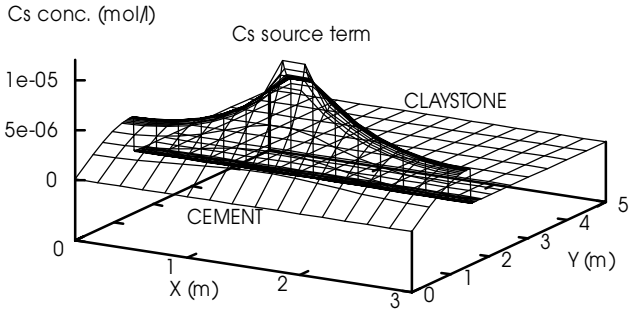

Figure 4. In a fully coupled simulation (e.g. feedback of chemistry on transport), the porosity drop at the cement-claystone interface leads to a significant decrease of caesium migration into the host rock (visualized here as a "wall" at y=1.50 m).

The calculated values are in good agreement with the compilation of Berner (1999). The solubility limit is progressively lessened inside the cement in parallel to the pH drop, whereas the propagation of the attenuated alkaline plume in claystone has no effect on solubility. Tc solubility is controlled by the balance between complexation with hydroxyl-carbonate ligands ($TcCO_3(OH)_3^-$ species) and oxide precipitation. A similar trend is observed with uranium. In both cases, the relation between redox and pH changes has a strong impact on the calculated solubility. Obviously, co-precipitation and organic matter complexation should be assessed in a further step.

The second type of modeling is illustrated through the calculation of caesium migration in the conservative hypothesis of an early waste package failure just after the resaturation of the near field. The simulations take into account cation exchange processes for clay minerals and zeolites and surface complexation for CSH (Ames, 1964; Poinssot et al., 1999; Viallis-Terrisse, 2000). Consequently, Kd profiles can be derived from the calculations in both cement and claystone (Fig. 2). In agreement with experiments (Bradbury and Baeyens, 1997), the retention of Cs is much less effective in cement than claystone. Within claystone, Cs is continuously fixed by illite and montmorillonite (Fig. 3). The competitive effect with calcium and potassium ions diffusing from cement leads to a small decrease of the Kd, decrease which is partly compensated by the precipitation of the zeolite clinoptilolite close to the interface. The diminution of the Kd in the cement is directly related to the re-protonation of silanol type sites and the increase of calcium concentration due to pH lessening. Strontium follows a similar reaction scheme regarding sorption, but the Sr migration is also coupled to the precipitation of carbonate minerals (strontianite, see Fig. 3), or in some cases by co-precipitation with CSH, at the cement-claystone interface.

Important precipitations of calcite or minerals with high molar volume (CSH and zeolites) may lead to a dramatic drop of the pore space volume at the cement-claystone interface, slowing down, or even stopping, further geochemical evolution of the system (Lagneau, 2000). Figure 4 gives a brief illustration of the process. The 2D profile of Cs concentration has been calculated along the gallery with a fully coupled simulation (feedback of chemistry on transport) of the cement – claystone interactions after 5000 y. A local permanent source of Cs is assumed in the cement, but sealing at the interface prevent it from migrating into the claystone (at least in this simplified but demonstrative theoretical calculation).

CONCLUSIONS

The paper demonstrates that integrating radionuclide migration in the modeling of strongly coupled geochemical processes of cement-claystone interactions is feasible. This represents an effective alternative to the traditional Kd and solubility limit approach, although there are still significant limitations due to the disponibility of relevant data. Meanwhile, it also helps to assess the sensitivity and modification of these transport parameters with respect to the evolution of the system in time and space.

REFERENCES

Ames, L. (1964). Some zeolite equilibria with alkaline metal cations, Americ. Mineral. 49, 127-145.

Berner, U. (1999). Concentration limits in the cement based Swiss repository for long-lived, intermediate-level radioactive wastes (LMA}, technical report 99-10, PSI (CH).

Bradbury, M.H. and B. Baeyens (1997). Far-field sorption data bases for performance assessment of a L/ILW repository in a disturbed/altered Palfris marl host rock, technical report 97-16, PSI (CH).

Poinssot C., B. Bayens and M.H. Bradburry (1999). Experimental and modelling study of the Cs sorption on illite, Geoch. Cosmoch. Acta 63(19-20), 3217-3227.

De Windt L., J. van der Lee and D. Pellegrini (2001). Reactive transport modeling of pH buffering in cement - clay systems, Water Rock Interaction Proc. (Sardaigne, Italy), Balkema Ed., 1315-1318.

Lagneau V. (2000). Influence des processus géochimiques sur le transport en milieu poreux ; application au colmatage de barrières de confinement potentielles dans un stockage de déchets en formation géologique, Ph.D. thesis from Ecole Nationale Supérieure des Mines de Paris.

Rard J.A., M.H. Rand, G. Anderegg and H. Wanner (1999). Chemical thermodynamics of technetium, North-Holland, Amsterdam (NL).

van der Lee J. (1998). Thermodynamic and mathematical concepts of CHESS, Technical Report LHM/RD/98/39, Ecole des Mines de Paris, Fontainebleau (France).

van der Lee J. and L. De Windt (2001). Present state and future directions of modeling geochemistry in hydrogeological systems, J. Cont. Hydr. 47, 265-282.

Viallis-Terrisse (2000). Interaction des silicates de calcium hydratés, principaux constituants du ciment, avec les chlorures d'alcalins. Analogie avec les argiles, Ph.D. Thesis from Université de Bourgogne (France).

Wolery T. (1992). EQ3/6. A software package for geochemical modelling of aqueous systems: package overview and installation guide (version 7.0), Technical Report UCRL-MA-110662 PT I ed., Lawrence Livermore National Laboratory, USA.

REACTIVE TRANSPORT MODELLING OF RADIONUCLIDES ALONG A SINGLE FRACTURE IN GRIMSEL (CRR PROJECT).

A. Delos, L. Duro and J. Guimerà.
Enviros QuantiSci S.L., Av. Universitat Autònoma, 3, Parc Tecnològic del Vallès,
Cerdanyola del Vallès,08290 Barcelona, Spain; Email: adelos@quantisci.es

SUMMARY

This article presents the interpretation of several tracer tests carried out at the Grimsel Test Site. They were undertaken with Uranine as conservative tracer, and a cocktail containing Th and Hf as homologues of tetravalent actinides and Tb as analogue of trivalent actinides aiming at predicting the behaviour of radionuclides in an in situ test. Hydrodynamic parameters were obtained by automatic calibration of flow and conservative solute transport. The set of parameters resulting from the flow simulation have been fed into a reactive transport model together with Kd values obtained from laboratory experiments. Our work presents the calibration of the model with the conservative tracer tests, the hydrogeochemical conceptual model, the implementation in a 2D multicomponent reactive transport code, and the predictions for the in situ injection of active cocktails with and without colloids.

INTRODUCTION:

The performance assessment of the storage of radioactive waste in deep geological repositories needs understanding of the detailed processes, which affect the transport of radionuclides in a real scale. With this aim in mind, a lot of experiments were carried out in field and in laboratories but few of them used radionuclides with a high specific activiy.

In order to reinforce our knowledge about the behaviour of these elements in the geosphere, the CRR project (Colloids and Radionuclides Retardation) focuses on fundamental processes, which affect the radionuclide transport. An in situ experiment is planned, which consists in injecting a cocktail of radionuclides (U(VI), Sr(II), Cs(I), Tc(IV), Th(IV), Np(V), Pu(IV) and Am(III)) at low concentrations in order to study their behaviour in the geological environment of the possible repository, with and without the presence of bentonite colloids. The redox state of the system will remain unchanged. Previous studies determined geochemical solubilities of radionuclides and the composition of the radionuclide cocktail, dealt with the interpretation of laboratory and field experiments to calibrate the hydrodynamic parameters of the model, and the design of the experiments using reactive transport codes. These field experiments take place in the MI fracture of the Grimsel Test Site in Switzerland.

The objective of this article is to present the results of the prediction of the behaviour of several radionuclides that will be included in the injection cocktail, and to assess the effect of added bentonite colloids into the cocktail.

METHODOLOGY

The in situ experiments will take place between two boreholes separated by 2.5 m in a well-characterised fracture.

PHAST (Parkhust et al., 2000), a 3-dimensional multicomponent reactive transport code, has been used to model the tracer tests. As a first step, the calibration of the model has been done with the interpretation of the conservative tracer test with uranine. Because PHAST solves direct problem, in a first stage the automatic inverse modelling has been carried out with Transin II (Medina et al., 1996). The resulting heads and set of hydraulics parameters have been used to build up the conceptual model with PHAST, whose domain is far more restricted

around the dipole of interest, which enables a finer discretisation (Figure 1 and Figure 2). The simulations are steady state, in a homogenous domain. The final set of hydraulic parameters obtained is $T=8.8\cdot10^{-7}$ $m^2\cdot s^{-1}$, $\alpha_L=2\cdot10^{-1}$ m, $\alpha_T=1.5\cdot10^{-2}$ m, $\phi=9\cdot10^{-3}$, which agrees with previous studies (Meier et al., 1998).

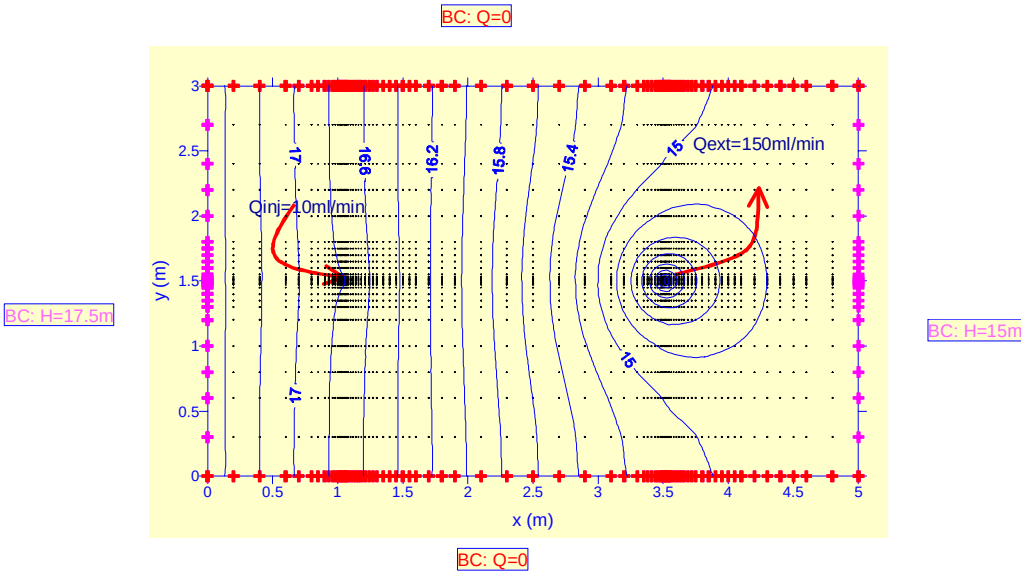

Figure 1: Model structure implemented in PHAST with the piezometric results. The boundary conditions are extracted from a larger scale model.

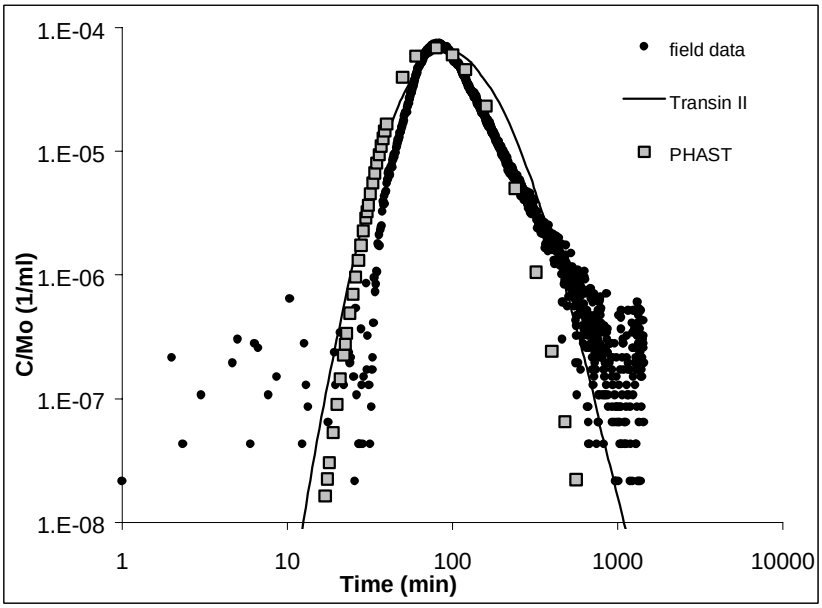

Figure 2: Breakthrough curve for the calibration of the conservative tracer test with a large scale model using Transin II, and with a finer model using PHAST.

Several tracer tests were undertaken with Th and Hf as analogues of tetravalent actinides and Tb as analogue of the trivalent actinide Am. The homologues' breakthrough curve occurs at the same time as uranine, probably transported by naturally occurring colloids. Only 40% of the total injected mass is recovered. The remaining mass is thought to be reversibly retained on the surface of the fracture filling material, resulting in too low concentrations in the outflowing solution as to be detected by the analytical technique. Kd values obtained from laboratory experiments (Geckeis et al., 2000) and (Missana et al., 2000) were introduced in PHAST. The results of the simulations indicate that the recovery of the sorbing tracers

affected appear below the detection limits of the technique used in the analysis, in agreement with the experimental observations.

Two cases have been studied for the reactive transport modelling, with and without the addition of bentonite colloids in the injection cocktail.

The surface complexation processes considered are:

$>X\text{-}OH + Am(OH)_2^{2+} => X\text{-}O\text{-}Am(OH)_2^{+} + H^{+}$	$\log K_{FFM}=-5.76; \log K_{colloids}=-1.81$
$>X\text{-}OH + Pu(OH)_4(aq) => X\text{-}O\text{-}Pu(OH)_4^{+} + H^{+}$	$\log K_{FFM}=-6.52; \log K_{colloids}= -3.02$
$>X\text{-}OH + UO2(OH)_3^{-} => X\text{-}O\text{-}UO2(OH)_3^{2+} + H^{+}$	$\log K_{FFM}=-6.67; \log K_{colloids}=-5.27$
$>X\text{-}OH + Th(OH)_4 => X\text{-}O\text{-}Th(OH)_4^{+} + H^{+}$	$\log K_{FFM}=-6.52; \log K_{colloids}=-3.02$
$>X\text{-}OH + TcO(OH)_2 => X\text{-}O\text{-}TcO(OH)_2^{+} + H^{+}$	$\log K_{FFM}= -6.36; \log K_{colloids}= -5.62$

These chemical equilibria are based upon the study of the speciation of each radionuclide under the conditions of the Grimsel groundwater (pH = 9.5, log[HCO3-] = -3.54) and on the determination of the distribution coefficients (Kd) in laboratory conditions (Missana et al., 2000) and (Geckeis et al., 2000).

With the addition of bentonite colloids, radionuclides may be sorbed onto the surface of the fracture filling material (FFM) as well as onto the surface of the bentonite. The largest colloids are filtered off within the fracture, whereas the smallest ones are transported with the water flow, as the conservative tracer (Fierz et al., 2001). These processes are depicted in Figure 3. Given that those colloids travelling with the water flow do not have any influence on the radionuclide migration behaviour, we have only considered the colloid fraction retained in the fracture.

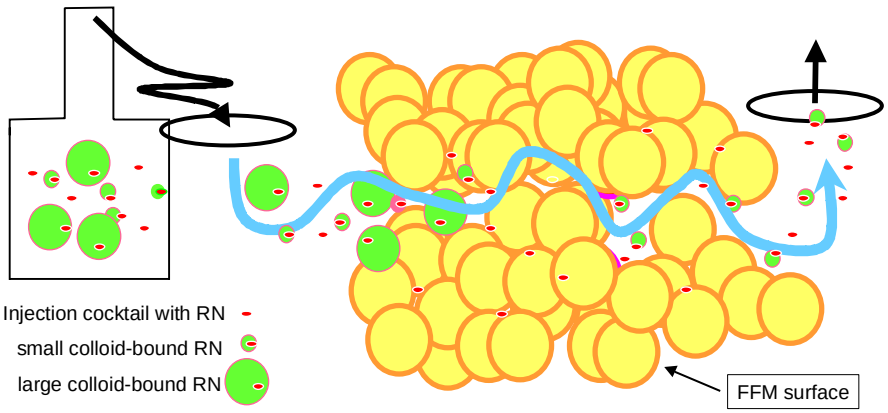

Figure 3: Conceptual model of the radionuclide behaviour, when bentonite colloids are added into the injection cocktail.

RESULTS

Figure 4 shows the results of the simulation of the injection of the active cocktail without bentonite colloids. Np is considered to behave as conservative, because no sorption is assumed in our simulation (Möri, 2001). Under the simulation conditions, the maximum concentration of Np is at 80 min and a total recovery is achieved after 28 hours. On the contrary, sorbing radionuclides are not totally recovered after 21 days. The stronger is the sorption constant, the later, the lower and the wider is the peak of the breakthrough curve. As expected, the first arrival of the hexavalent uranium will occur before the first arrival of the tetra and trivalent actinides. The model reproduces the sorption characteristics derived in previous equations since U, Th and Pu display a similar behaviour. However, since the limit of detection of the analytical technique is higher than the maximum concentration of the peak,

Pu could be detected before one hour of pumping time, and Am and U will be detected after 4 hours of pumping provided that our assumptions are correct.

In the case of the injection of the active cocktail with bentonite colloids (Figure 4), we can compare the behaviour of radionuclides in the fracture with and without the presence of colloids. We can conclude that the strength of sorption is very similar for U, Th and Pu in the two cases, whereas Am has not reached the extraction borehole after 21 days of simulation yet. The effect of colloids is noticeable because the difference between the sorption constants is of several orders of magnitude. Otherwise, the breakthrough curve is not affected, because the quantity of colloids present in the domain is small. If we compare the logarithmic constants in the two cases, we realize that: the higher the oxidation state of an actinide, the lower is the difference between the logarithmic sorption constant onto FFM surface and onto bentonite colloid surface; also, the larger the difference in the normalised concentrations of the sorbed radionuclides onto the two surfaces, the lower the influence of the sorption onto bentonite colloids on the breakthrough curve of the element.

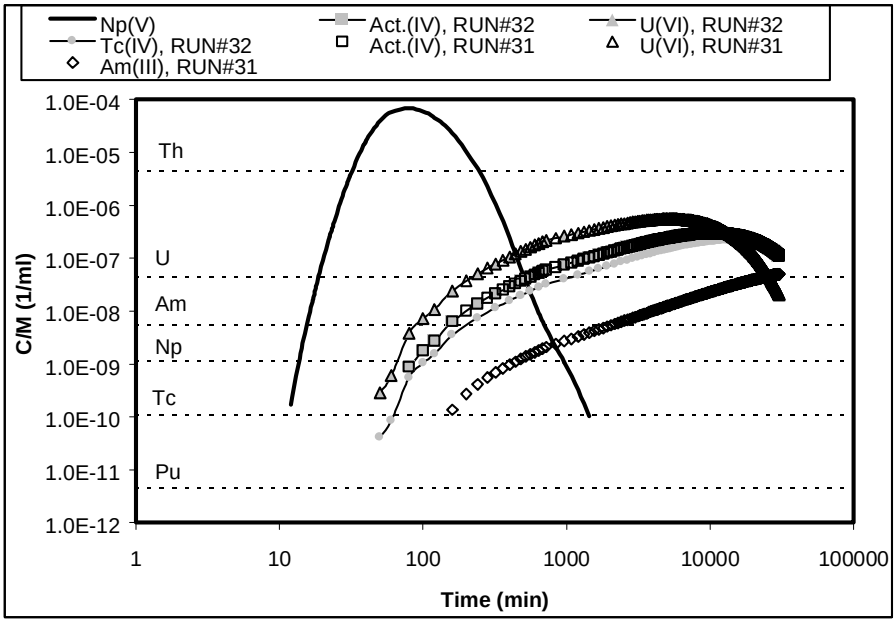

Figure 4: Injection of the cocktail without bentonite colloids (Run#31) and with bentonite colloids (Run#32). Simulation of the breakthrough of Am, Pu, U, Th, Tc and Np. Horizontal lines stand for the limit of detection of the technique used in the analysis of the outflowing solution, either radiochemical (Am, Np, Tc and Pu) or ICP-MS (Th and U).

CONCLUSIONS

The presence of colloids introduces two kinds of behaviour in the chemical transport of the homologues, which have been reproduced by means of a multicomponent reactive transport model. On the one hand, "small-size" colloids accelerate the transport of the attached sorbates. On the other hand, the "large-size" colloids that suffer from filtration increase the duration of the test and eventually may prevent the recovery of some radionuclides such as Am, regardless the duration of the experiment.

REFERENCES

Fierz, T., Geckeis, H., Götz, R., Geyer, F.W. and Möri, A. (2001): GTS V/ CRR, Tracer tests #1-#16, internal report NAGRA 01-06.

Geckeis, H. (2000): Tentative nuclide composition of injection solutions for the CRR experiment. Technical Note of the CRR project.

Medina, A., Galarza, G. and Carrera, J. (1996): TRANSIN II. Fortran code for solving the coupled flow and transport inverse problem in saturated conditions. El Berrocal Project, Volume IV Hydrogeological modelling and code development, Topical Report 16, ENRESA,217-422.

Meier, P., Carrera, J. and Sánchez-Vila, X. (1998): An evaluation of Jacob's method for the interpretation of pumping tests in heterogeneous formations. Water Resources Research, 34, 1011-1025.

Möri, A., editor (2001): GTS V /CRR Scoping calculations, base data set V-3.

Missana, T. and Mingarro, M. (2000): Summary of the results of sorption experiments for CRR Project. CRR Technical Report CIEMAT/DIAE/54221/4/00

Parkhurst, D.L., Kipp, K.L. and Engesgaard, P. (2000): PHAST. A Program for Simulating Ground-Water Flow and Multicomponent Geochemical Reactions. User's guide. USGS, 154 pp.

CHARACTERIZATION OF NONLINEAR TRANSPORT BEHAVIOR IN HETEROGENEOUS POROUS MEDIA BY MEANS OF BREAKTHROUGH CURVES

J. Dimitrova, , S. Attinger and W. Kinzelbach
Institute of Hydromechanics and Water Resources Management, ETH Hönggerberg, HIL G 34.2, 8093 Zürich, Switzerland; E-mail: dimitrova@ihw.baug.ethz.ch

ABSTRACT

We focus our investigations on the large scale transport behavior of nonlinear reactive transport processes in heterogeneous aquifers. The adsorption process is described by an equilibrium isotherm of Freundlich type. In a stochastic modeling approach we analyze temporal moments of breakthrough curves and evaluate large scale parameters, in which the influence of small scale variations is appropriately considered. In linear transport theory the large scale transport is characterized by the same type of homogeneous transport equation as on the smaller scale, replacing the transport parameters by equivalent effective parameters. In the nonlinear transport case, we will demonstrate that the large concentration gradients at the front cause an additional dispersive flux, resulting in a decrease of peak concentrations and less steeper profiles of averaged breakthrough curves in the heterogeneous realization. We propose to modify the equivalent large scale transport equation by a supplementary term.

INTRODUCTION

Transport through heterogeneous aquifers is often investigated with stochastic models. The stochastic theory is well established and linear transport phenomena have been studied using analytical and numerical methods (Dagan, 1984; Attinger et al., 1999; Cirpka, 2000).

Although nonlinear adsorbing transport quite often occurs in natural environment, these processes are less investigated so far (Bosma, 1996; Berglund, 1996; Attinger, 2000). The objective of this work is to characterize the large scale behavior of nonlinear adsorbing transport by analysis of temporal moments of breakthrough curves. Our method sets a useful link to many field studies, where in only few monitoring wells current depth averaged concentrations are measured.

IDENTIFICATION OF TRANSPORT PARAMETERS BY MEANS OF TEMPORAL MOMENTS

Adsorbing transport of solute cloud in a heterogeneous porous medium is described by an advection-dispersion equation:

$$\theta\,\partial_t c(\mathbf{x},t) + \rho\,\partial_t c_{ads}(\mathbf{x},t) + \partial_{x_i}\left(u_i(\mathbf{x})c(\mathbf{x},t) - D_{ij}\partial_{x_j} c(\mathbf{x},t)\right) = 0 \qquad (1)$$

Here θ is the porosity of the medium, $c(\mathbf{x},t)$ the dissolved and $c_{ads}(\mathbf{x},t)$ the adsorbed concentration. D_{ij} denotes the entries of the local dispersion tensor. Due to fluctuations of the permeability, the Darcy velocity $u_i(\mathbf{x})$ varies spatially. It can be split into the large scale flow field $\bar{\mathbf{u}}$ and its deviation from that value, $\mathbf{u}(\mathbf{x}) = \bar{\mathbf{u}} + \tilde{\mathbf{u}}(\mathbf{x})$.

The tracer is injected into the domain over the inflow boundary pulse like in space and time. The flux concentration in the inflow is uniformly distributed over the inflow boundary. The concentration gradient normal to the outflow boundary is assumed to be zero. We model the adsorption by an equilibrium isotherm of Freundlich type,

$$c_{ads}(\mathbf{x},t) = K_D c^p(\mathbf{x},t) \quad \bullet \tag{2}$$

with a Freundlich exponent $1>p\geq 0$ and a Freundlich distribution coefficient K_D. The nonlinear adsorption leads to a concentration dependent retardation. Smaller concentrations are more strongly retarded than larger ones. As shown in figure 2, it results an asymmetric concentration profile with a self-sharpening front and a long tailing behind the front.

Transport behavior on scales much larger than the scale of heterogeneity can be analyzed using a stochastic modeling approach: A spatially fluctuating parameter is considered as single realization of a stochastic process defined by the ensemble of all possible realizations. If the stochastic properties of the process are known, appropriate ensemble average values can be evaluated. These ensemble average values describe the ensemble of all realizations in a probabilistic way. However, a stochastic process sampling a representative part of the heterogeneous medium might approach its own mean value if the medium is assumed to be ergodic.

It is convenient to characterize the transport behavior on large scales by the same type of transport equation as on smaller scales, replacing the transport parameters by equivalent large scale transport parameters. An appropriately defined averaging procedure yields the equivalent transport parameters.

For nonlinear transport we propose a new identification method of transport parameters. We analyze generalized temporal moments of cross-sectional averaged breakthrough curves, which express especially the nonlinear transport character. Equivalent transport parameters can be defined as an adept combination of first and second moments of both the dissolved and adsorbed concentrations integrated over the outflow boundary of the domain.

NUMERICAL QUASI ONE–DIMENSIONAL RESULTS

In order to determine the large scale transport behavior we consider a two-dimensional numerical test case with a log-normal distributed permeability field (mean value: $\bar{k}_f = 10^{-4} m/s$, variance: $\sigma_f^2 = 0.12$ and correlation length: $l_x = 1m$). Assuming a constant head gradient we construct a spatially variable flow field with $\bar{u} = 10^{-4} m/s$ in **x**-direction. The domain contains 360 by 200 cells, resolved by elements of grid size $\Delta x=\Delta y=0.1$m, and covers 36 correlation lengths in longitudinal direction. The nonlinear adsorption is parameterized by a Freundlich exponent $p=0.75$ and a Freundlich coefficient $K_D=7.5\cdot10^{-5}\ (g/m^2)^{1-p}$. The transport problem is solved with the method of upstream finite differences with a Courant number equal to 0.5.

For illustration, figure 1 shows the concentration distribution after time $t=9.5\cdot10^6$ s. The fluctuating velocity field leads to travel time differences between solute particles in different streamlines and the originally uniformly distributed line source is irregularly deformed. The heterogeneous structure of the domain causes an enhancement of the longitudinal dispersion coefficient. This is illustrated in figure 2, where we compare averaged breakthrough curves in the heterogeneous domain with those in the homogeneous small scale one. Different as in linear transport theory, enlarged longitudinal macrodispersion coefficients have a different impact on concentration profiles. The spreading of the plume is mainly caused by nonlinear adsorption effects.

As described above, we use the first and second moment of averaged breakthrough curves for identification of large scale transport parameters. According to our approach, the large scale velocity corresponds to the mean groundwater velocity,

- $$u_i^{ens} = \overline{u}_i \delta_{i1} \tag{3}$$

In figure 3 we plot the numerical results for the macrodispersion coefficient. Due to ensemble mixing the dispersion increases continuously. After about five correlation lengths the plume has spread over a representative part of the medium and reaches the asymptotic regime. The results for nonlinear transport are compared with our calculations for nonreactive transport. As expected from theoretical investigations by perturbation theory [Attinger et al. (2000)], the asymptotic value is equivalent to the result in linear transport theory:

$$D_{ii}^{ens}(t) \quad \xrightarrow{t\to\infty} \quad D_{ii}^{ens}(\infty)\Big|_{linear} = \sigma_f^2 l_x \overline{u}\sqrt{\Pi}/2 \quad >> \quad D_{ii} \tag{4}$$

EQUIVALENT HOMOGENEOUS TRANSPORT MODEL

Assuming self-averaging property, we are allowed to replace the heterogeneous transport system by an equivalent homogeneous one. Instead of small scale transport parameters we insert the evaluated effective parameters. For many practical applications it is significant, whether the equivalent homogeneous equation reproduces properly the heterogeneous transport. In case of linear adsorption the macrodispersion coefficients exactly approximate the heterogeneous transport. The large scale transport is given by the same type of differential equation.

In case of nonlinear adsorption the situation differs. In figure 4 we compare the breakthrough curve averaged over the outflow boundary in the stochastic realization and the breakthrough curve in the equivalent homogeneous domain. As we can see, the tailing is quite well reproduced. In contrast, the peak concentration in the heterogeneous medium is lower and also the front steepness decreases. This effect does not depend on the magnitude of longitudinal dispersion.

We can show that this so-called “nonlocal” effect originates from local effects at the self-sharpened front. We assume that high concentration gradients generate an additional dispersive flux at the Freundlich front. Accordingly, the macrodispersion consists of two different processes: a Fickian macrodispersion and a local mass transfer at the front, proportional to the current peak concentration.

Thus, the corrected equivalent homogeneous transport equation can be written as:

$$(\overline{c} + \frac{\rho K_D}{\theta}\overline{c}^{\,p}) + \overline{u}\partial_x \overline{c} - \partial_x D^{ens}\partial_x \overline{c} \pm \alpha(x^*_{\pm\varepsilon})\overline{c}(x^*,t) = 0 \tag{5}$$

Here $\overline{c}$ are upscaled homogeneous concentrations and D^{ens} corresponds to the macrodispersion coefficient in (4). The last term in (5) affects only the front at x^*, which is defined as the position on the front edge with half peak concentration. It causes a reduction of the maximal peak concentration. Mass is transferred from regions at the front smaller than x* to regions greater than x*.

CONCLUSION

Temporal moments are a useful tool for characterization of both linear and nonlinear adsorbing transport in heterogeneous media. Knowledge of the actual magnitude of transport parameters and processes can be essential in risk assessment and remediation schemes for estimation of first arrival and cleanup times, peak concentrations etc. In a stochastic sense one can replace the heterogeneous transport equation by a homogeneous one with appropriately

averaged large scale transport parameters. In linear transport, equivalent transport parameters can be identified by means of averaged breakthrough curves. They consistently reproduce the heterogeneous medium. In case of nonlinear adsorption dispersive fluxes at the Freundlich front causes an additional front broadening and reduction of peak concentrations. Consequently, equivalent transport is given by a modified transport equation.

REFERENCES

Attinger, S., Dentz, M, Kinzelbach, H. and W. Kinzelbach (1999):, Temporal behaviour of a solute cloud in a chemically heterogeneous porous medium. J. Fluid Mech., 386, 77-104,

Attinger, S., Dimitrova, J. and W. Kinzelbach (2000): Nonlinear adsorbing transport behavior in heterogeneous porous media: Asymptotic behavior. Submitted to Water Resour. Res.

Berglund, S. and V. Cvetkovic(1996): Contaminant displacement in aquifers: Coupled effects of flow heterogeneity and nonlinear sorption. Water Resour. Res., 32, 23-32

Bosma, J.P. and S.E.A.T.M. van der Zee (1996): Plume development of a nonlinearly adsorbing solute in heterogeneous media. Water Resour. Res., 32, 1569-1584

Cirpka, O.A. and P.K. Kitanidis (2000): Characterization of mixing and dilution in heterogeneous aquifers by means of local temporal moments. Water Resour. Res., 36, 1221-1236

Dagan (1984): Solute transport in heterogeneous porous formations. J. Fluid. Mech., 145, 151-177

FIGURES

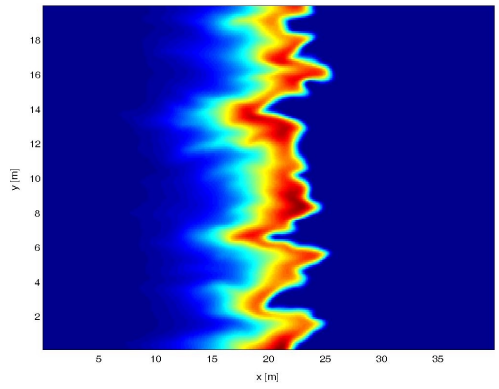

Figure 1: Concentration profile for $t=9.5 \cdot 10^6$ s

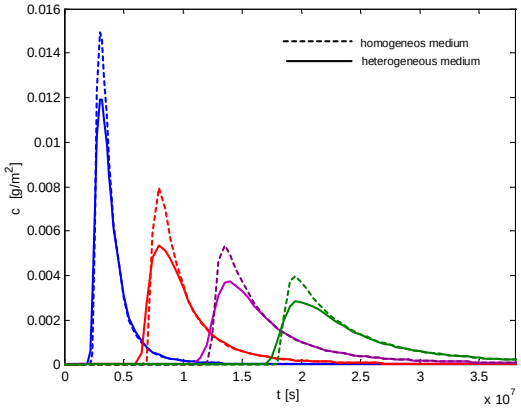

Figure 2: Averaged breakthrough curves

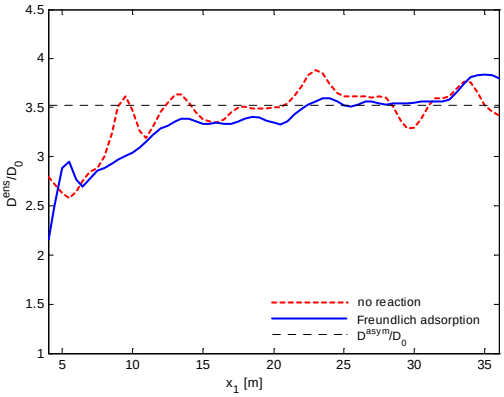

Figure 3: Dispersion of ensemble mixing for transport without reaction and with Freundlich adsorption

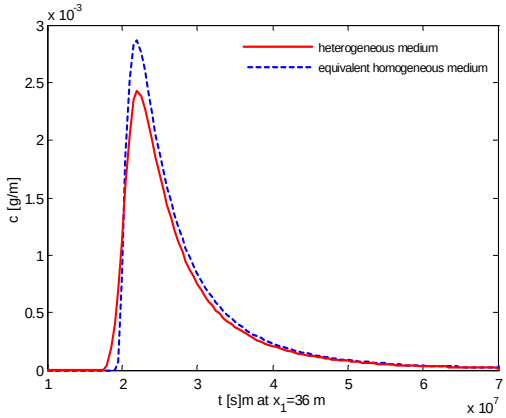

Figure 4: Breakthrough curves in averaged heterogeneous realization and in equivalent homogeneous medium

A MICROSCOPIC SCALE LOW PARAMETER MODEL FOR SIMULATION OF FLOW AND TRANSPORT IN POROUS MEDIA

Frieder Enzmann, Michael Kersten and Thilo Hofmann
University of Mainz, Institute of Geosciences, Becherweg 21, DE-5099 Mainz, Germany
enzmann@mail.uni-mainz.de, michael.kersten@uni-mainz.de, thilo.hofmann@uni-mainz.de

ABSTRACT

A simulation model has been developed in order to deduce the effective transport parameters from porous media. In a first approach the model delivers a 3D sphere agglomeration model with variable grain size distributions. In a second approach, real pore structures can be implemented from Micro-Computer-Tomography (µCT) data. In the negative space (3D pore structure), the model simulates multiphase flow and transport of dissolved components and particles based on the numerical solution of the Navier-Stokes-equation and the Lattice-Boltzmann method. Statistical analysis and homogenisation of simulation data delivers the effective transport parameters, such as specific and relative permeabilities, dispersivity and tortuosity. The simulations give an insight into complexity and heterogeneous dynamics of microscopic flow and transport in porous media.

INTRODUCTION

The flow and transport processes in porous media are linked directly to its pore space geometry, fluid properties and dissolved constituents (Dagan, 1989; Sahimi, 1993; Stockman, 1999; Martys et al., 2000). Although the pore space is the site of many relevant chemical reactions involving trace element partitioning between fluid and solid matrix, it is not adequately represented in conventional advective-dispersive transport models. The heterogeneity in pore space distribution and gas/fluid phase distribution, e.g., determines the sites of cement formation and, in feedback, the hydraulic flow distribution condition. A direct geometrical deduction of the effective hydraulic and transport parameters in complex natural subsurface environment with a high grade of heterogeneity is currently not possible. A microscopic view and simulation of pore scale processes gives an insight of the complexity and dynamics of these processes to understand the fluid/rock-interactions. This contribution discusses the development of a microstructural model of the pore space as a first step in a true physicochemical model of coupled transport reaction processes.

MODELING AND REPRESENTING POROUS MEDIA

For fluid and transport simulations, the model requires a 3D pore structure represented by a voxel system (domain). A granular porous media, such as sand or gravel, can be represented by an agglomeration of spheres with a specific and variable grain size distribution. Here we present a 3D sphere agglomeration model based on geometrical-mathematical solutions by sequentially solving sets of sphere-equations (eq. 1). The result is a sphere agglomeration with up to two million spheres approaching most dense packing with defined diameter distribution. With simple geometric operations, the model can directly derive fundamental parameters (porosity), generate porosity profiles and estimate a geometric tortuosity.

The mathematical formulation for this problem are sets of sphere equations to be solved:

$$\begin{aligned} U_A &:= (\vec{x}_A - \vec{x})^2 - (r_A + r_D)^2 = 0 \\ U_B &:= (\vec{x}_B - \vec{x})^2 - (r_B + r_D)^2 = 0 \\ U_C &:= (\vec{x}_C - \vec{x})^2 - (r_C + r_D)^2 = 0 \end{aligned} \qquad (1)$$

where x_A, x_B, x_C = vector of middle point of the spheres, r_A, r_B, r_C = radii of the spheres and r_D = radius of the new sphere for agglomeration. The results of the equation system are two possible vectors of middle point for the new sphere.

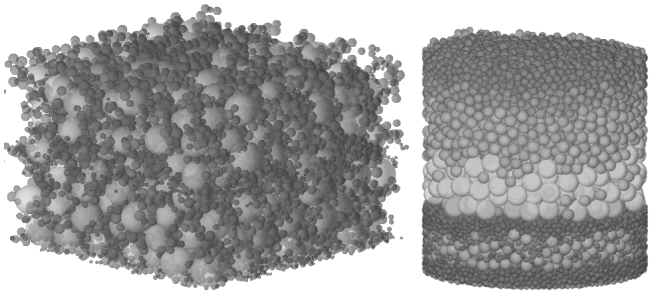

Figure 1. Sphere agglomerations with different agglomeration conditions (bidisperse distribution, graded stratification)

Figure 1 shows two examples of sphere agglomerations with different grain-size distributions. Any size distribution function can be built to generate a hypothetical agglomeration. Simple geometric calculation delivers the overall geometric porosity referring to a vector space. The inner surface and specific surface can be calculated analogous over the sum of sphere surfaces.

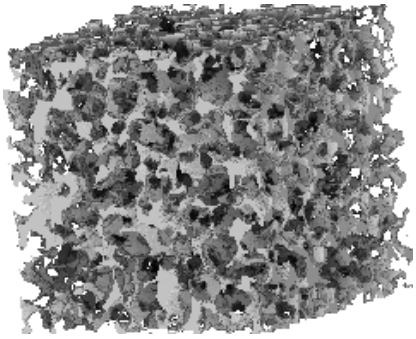

Figure 2. 3D voxel system (pore system) of Fontainebleau sandstone (Biswal et al., 1999)

Another approach is the representation of porous structures calculated from analysis of real sample geometry by Micro-Computer-Tomography. This data presents the porous structure more realistic than models. Figure 2 shows a sample of a Fantainebleau sandstone from the image processing data. With the help of percolation theory and special algorithms, the pore network can be derived (Hilfer, 1996; Turek, 1999; Lindquist and Venkatarangan, 1999; Martys et al., 2000).

MODELING FLUID FLOW AND TRANSPORT

The fundamental equation for fluid flow in microscopic scale is the time depended Navier-Stokes equation for incompressible fluids:

$$\underbrace{\frac{\partial \vec{v}}{\partial t} + (\vec{v} \cdot \nabla)\vec{v}}_{\text{fluid acceleration}} = \underbrace{-\frac{1}{\rho}\nabla p}_{\text{fluid pressure gradient}} + \underbrace{\frac{\eta}{\rho}\nabla^2 \vec{v}}_{\text{viscose friction}} + \underbrace{\frac{\vec{f}}{\rho}}_{\text{external force}} \qquad (2)$$

where v = fluid velocity vector, ρ = fluid density, η = fluid viscosity, p = fluid pressure and f = external force vector. To solve the Navier-Stokes equation, the porous media must be discretized. Our model uses a finite difference marker and cell method (3D voxel system).

The velocity vector field is to be solved by an explicit update scheme, and the pressure field by a successive overrelaxation scheme for every time step (Rage, 1996; Turek, 1999). Under constant flux boundary conditions the iteration stops after development of a steady state velocity vector field, with equal flux into and out of the model space, and a linear pressure gradient results in the mean flow direction of the overall pressure field. The accuracy of this

solving scheme can be tested in simple geometric configurations (like Hagen-Poiseuille) (Enzmann, 2000).

In this model, no input hydrodynamic material parameters are required. The flow conditions in model space are only dependent on pressure drop, external forces and viscose friction. The pressure drop and viscose friction is dependent on the inner boundaries of the model space, such as grain surfaces. The effective hydraulic parameters can be delivered from the velocity vector field and pressure drop. The pressure drop under constant flux on one boundary is almost linear in the profile of the cylinder (cf. Figure 5) and does not correlate with average local porosity. On the other hand, there is a strong negative correlation between average fluid velocity and local porosity due to the Hagen-Poiseuille equation as shown in Figure 4. This is the prerequisite to calculate permeability from Darcy's law (Figure 4 and 5).

The Lattice-Boltzmann method is applied to model multiphase flow and transport. This method is based on the kinetic gas theory and is a powerful alternative computational fluid dynamic (CFD) method (Martys et al., 2000; Stockmann, 1999; Martys and Chen, 1996). The Lattice-Boltzmann equation for each phase α can be written as:

$$\underbrace{f_i^{\alpha}(x+e_i,t+\Delta t)}_{\text{progradation}} - \underbrace{f_i^{\alpha}(x,t)}_{\substack{\text{distribution}\\ \text{on lattice sites i}}} = \underbrace{-\frac{1}{\tau^{\alpha}}\left[f_i^{\alpha}(x,t) - \underbrace{f_i^{\alpha(\text{eq})}(x,t)}_{\text{equilibrium distribution}} \right]}_{\text{single time relaxation approximation}} \qquad (3)$$

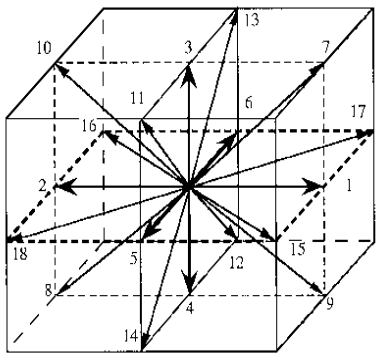

Figure 3. 3d element (voxel) with 19 velocity vectors (D3Q19)

We use a D3Q19 model (3D voxel and 19 velocity vectors field, Figure 3). For each time step, a particle distribution is calculated on each vector (progradation). The collision term on the right side of the equation is based on an equilibrium (Maxwell) distribution. The relaxation parameter τ is coherent with the viscosity of each phase or diffusion coefficient for each species. Macroscopic variables (density, pressure and velocity) are obtained from simple additivity principle (momentum sums). Mass and momentum conservation achieves the incompressible Navier-Stokes equation.

Surface tension forces and body forces (fluid acceleration) can be easily integrated. Also any kind of boundary conditions (von Neumann, Dirichlet) are possible.

SIMULATION RESULTS

First simulation results in profiles through a hypothetical pore geometry show the strong negative correlation expected between porosity and average fluid velocity (Figure 4).

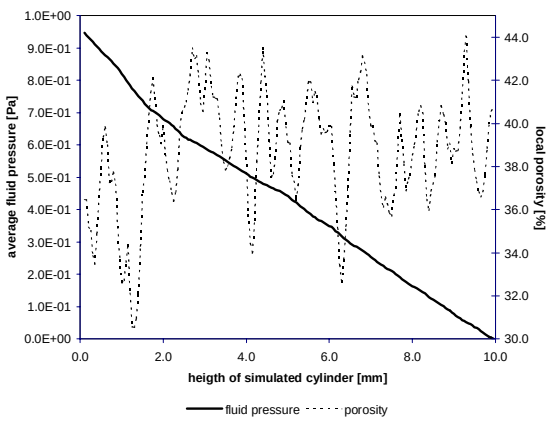

Figure 5. Average fluid pressure of simulated media in cylinder profile (mean flow direction)

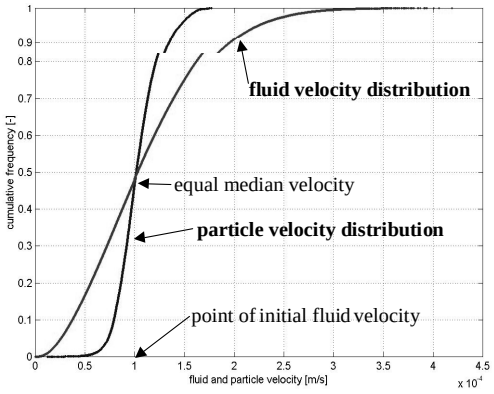

Figure 6. Distribution of particle and fluid velocity

The statistical variance of velocity vectors and particle velocity correlates with hydrodynamic dispersion (Figure 6). Results of various pore models are compared with results from flow and tracer experiments with real columns filled with glass beads. The simulated data shows a high dependence on the variance in pore space geometry. The same qualitative relationship can be found with the experimental results (Enzmann 2000). Moreover, colloidal latex particle breakthrough calculated by the pore model is comparable with analytical solutions of the conventional advective-dispersive transport equation (Enzmann 2000).

FUTURE WORK

The extension by coupling with geochemical reactions such as pore cement formation or trace element adsorption is the next step of physicochemical model sophistication. This is facilitated due to the fact that the surfaces of porous media are exactly defined from sphere agglomeration or 3D image processing data (µCT).

REFERENCES

Biswal, B., Manwart, C., Hilfer, R., Bakke, S. and Oren, P.E. (1999): Quantitative analysis of experimental and synthetic microstructures for sedimentary rock. Physica A 273, 452-475

Dagan, G. (1989): Flow and Transport in Porous Formations. Berlin-Heidelberg, Springer

Enzmann, F. (2000): Modellierung von Porenraumgeometrien und Transport in korngestützten porösen Medien. Dissertation, Inst. f. Geowissenschaften, Universität Mainz

Hilfer, R. (1996): Transport and Relaxation Phenomena in Porous Media. Adv. Chem.- Phys., 92, 299-424

Lindquist, W.B. and Venkatarangan, A. (1999): Investigating 3D geometry of porous media from high resolution images. Phys. and Chem of Earth, Part A 24, 593-599

Martys, N. and Chen, H. (1996): Simulation of multicomponent fluids in complex three-dimensional geometies by lattice Boltzmann method. Phys. Rev. E 43, 743-750

Martys, N., Masad, E., and Muhunthan, B. (2000): Simulation of fluid flow and permeability in cohesionless soils. Water Resource Res. 36, 851-864

Rage, T. (1996): Studies of Tracer Dispersion and Fluid Flow in Porous Media. Dep. of Physics. Oslo, Norway, PhD Thesis, University of Oslo

Sahimi, M. (1993): Flow phenomena in rocks: from continuum models to fractals, percolation, cellular automata, and simulated annealing. Rev. Mod. Phys. 65, 1393-1534

Stockman, H. (1999): A 3D lattice Boltzmann code for modeling flow and multi-component dispersion. Sandia National Lab., Sandia Report, SAND99-0162, Albuquerque, New Mexico, USA.

Turek, S. (1999): Efficient solvers for incompressible flow problems: An algorithmic and computational approach. Berlin-Heidelberg, Springer.

SPREADING OF REACTIVE CHEMICALS IN NATURAL POROUS MEDIA: FROM THE ATOMIC TO THE FIELD SCALE.

Daniel Grolimund,[1] Jeffrey A. Warner,[2] Xavier X. Carrier,[3] and Gordon E. Brown, Jr.[4]

1- Swiss Light Source (SLS) and Waste Management Laboratory (LES), Paul Scherrer Institute, CH-5232 Villigen PSI, Switzerland; E-mail: daniel.grolimund@psi.ch
2- Lawrence Berkeley National Laboratory, Chemical Sciences Division, Berkeley, CA 94720, USA
3- Université Pierre et Marie Curie (Paris VI), Laboratoire de Reactivité de Surface, Paris, France
4- Stanford University, Geological & Environmental Sciences, Stanford, CA 94305-2115, USA; Stanford Synchrotron Radiation Laboratory, SLAC, Stanford, CA 94309, USA

In natural systems, the fate as well as the potential hazard of chemicals is controlled to a notable extent by their affinity for solid phases or by chemical transformations mediated by solid surfaces. Consequently, physicochemical reactions occurring at the solid-liquid interface are of central importance to a broad variety of environmentally relevant phenomena including the transport of contaminants in the subsurface zone, waste water treatment, or bioavailability of nutrients.

Focusing on the spreading of chemicals in subsurface systems, substantial progress has been made in understanding and predicting the transport of non-reactive (inert) chemicals in heterogeneous subsurface systems. Our ability to quantify transport phenomena involving reactive chemicals, however, is by far less advanced. '*Predictive*' reactive transport models require an adequate description of chemical processes occurring at the solid-liquid interface as well as in solution. Despite their importance, the structure of interfacial systems as well as the mechanisms and pathways of chemical reactions taking place at the solid-solution interface are not yet well understood on a 'molecular' level. Such a detailed level of understanding, however, corresponds to a fundamental prerequisite in order to be able to predict the reactivity of interfacial systems and resulting reactive transport phenomena.

Our predictive capabilities are further hampered by the chemical complexity of natural systems. Natural porous media are not only structurally (physically) but also chemically extremely complex. Generally, various chemicals can be involved – in a competitive manner – in a single process and the coupling of several simultaneous chemical processes must be considered. Consequently, a microscopic, mechanistic approach is required in order to be able to understand the interfacial reactivity and reactive transport phenomena in complex natural systems.

Various novel applications of modern spectroscopic methods – in particular synchrotron-based techniques – provide unique opportunities for probing interfacial systems on a molecular-level. By applying these forefront techniques one is capable to gain fundamental insights into atomic structure of solid-solution interfaces. Furthermore, by identifying reactive functional surface groups (reactants) and interfacial species (products), these techniques are able to elucidate – on a molecular level – mechanisms and pathways of reactions occurring at interfaces. Consequently, using synchrotron radiation, molecular-level information becomes experimentally accessible that has hitherto been impossible to obtain. This allows identifying the key geochemical processes – even in complex natural systems.

Based on the example of the field-scale subsurface migration of Strontium at the Chalk River Nuclear Laboratory site (Figure 1), we demonstrate the importance of molecular level information as essential 'interior condition' in reactive transport modeling. In the past, various

studies attempted to explain the transport behavior of Strontium in the Chalk River Aquifer based on bulk mineralogical properties of the geologic media or on equilibrium-based chemical speciation in the aqueous solution. However, transport models using chemical sub-models building up on such approaches and generally deduced from macroscopic studies were not able to reproduce the main characteristics of the observed Strontium transport.

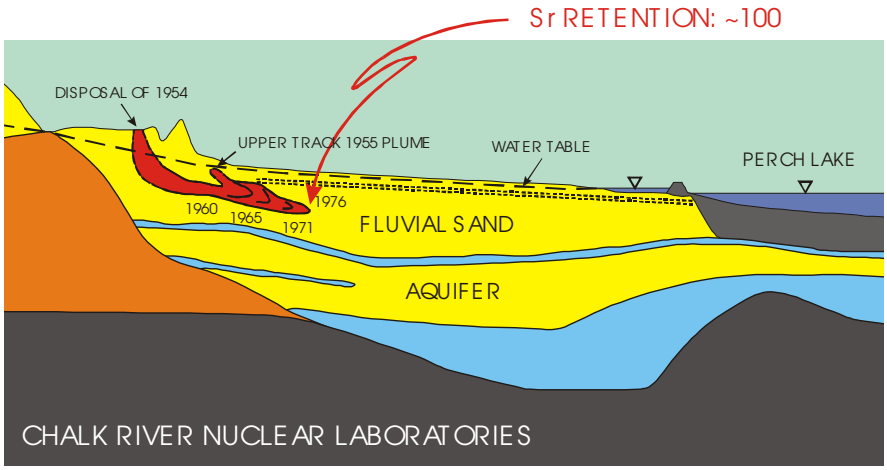

Figure adapted from Jackson and Inch, 1980

Figure 1: Spreading of aqueous Strontium in the Chalk River aquifer following disposal.

Most recent, we employed different X-ray absorption spectroscopy (XAS) techniques to gain new insights into the interfacial chemistry of Sr. The experimental data obtained permit the molecular-level (mechanistic) rationalization of the observed field-scale transport phenomena.

Our findings demonstrate the importance of coupling physical transport to chemical models which were based on (micro)spectroscopic, mechanistic information and accordingly represent ‘physical reality’.

QUANTITATIVE MODELLING OF COLLOID FACILITATED TRANSPORT IN NATURAL POROUS MEDIA

Daniel Grolimund[1] and Michal Borkovec[2]
1- Swiss Light Source (SLS), Paul Scherrer Institute, 5232 Villigen, Switzerland
2- Analytical and Biophysical Environmental Chemistry (CABE), University of Geneva, Sciences II, 30 Quai Ernest-Ansermet, 1211 Geneva 4, Switzerland;
E-mail: michal.borkovec@cabe.unige.ch

Mobile colloidal particles have been identified to be involved in a broad variety of environmentally relevant processes (Jenny and Smith, 1935, Muecke, 1979, Khilar and Fogler, 1987, Ryan and Elimelech, 1996). A considerable number of these processes may have hazardous consequences. Most recently, mobile colloidal particles have been reported to be a potentially relevant transport pathway for strongly sorbing contaminants (Vinten et al., 1983, Grolimund et al., 1996, Grolimund and Borkovec, 2001, Grolimund et al., 2001). Thereby the colloidal particles act as highly mobile contaminant carries and enhance in such a way the spreading of sorbing pollutants in subsurface systems. Therefore, considering potential hazardous incidents due to mobilized colloidal particles should represent a critical task in risk assessment of any subsurface contamination problem, in the development of remediation strategies, as well as in recharge and waste water management. In order to judge or predict the susceptibility of a subsurface system to the phenomena of enhanced contaminant transport by mobile colloidal particles, a detailed understanding of the following processes is required (Ryan and Elimelech, 1996): (i) the generation of mobile colloidal particles, (ii) the life-time of these particles within the system, and (iii) the association of the contaminant with the mobile particles. In the present paper various aspects of the diverse problem of enhanced contaminant transport by *in-situ* mobilized colloid particles will be addressed.

A comprehensive set of laboratory-scale column experiments was performed in order to investigate relevant fundamental processes such as particle mobilization, particle deposition and transport, as well as multicomponent contaminant transport phenomena. In addition, dynamic light scattering techniques were used to study the aggregation behavior of in-situ mobilized colloidal particles over a wide range of solution conditions. Complementary analytical techniques were applied in order to enlighten the physical and chemical properties of the mobilized particles. The knowledge about structure and dynamic of each process obtained by these individual experimental investigations were compiled and incorporated into an extended contaminant transport model. The resulting set of coupled, non-linear partial differential equations was solved numerically and used to simulate and analyze contaminant transport experiments where in-situ mobilized colloidal particles have been proven to be a dominant transport pathway (Grolimund et al., 1996).

Information about the general nature of the particle release process was obtained by studying mobilization phenomena in natural porous media under well-controlled conditions. A pronounced non-exponential release behavior, the finite supply of colloidal particles and the strong dependence of the observed release kinetic on chemical system parameters turn out to represent general characteristics of the release process. The non-exponential release behavior can be rationalized in terms of a broad distribution of populations of particles. This heterogeneity of the colloidal particles initially present in the system results in characteristic release pattern (Grolimund and Borkovec, 2001, Grolimund et al., 2001). Further, as a consequence of the sensitivity of the release process on the present chemical conditions, a distinct interplay between mobilization of colloidal particles and multicomponent transport phenomena could be established. An illustrative example is depicted in Figure 1. The outflow

pattern for an experiment with variations in the ionic strength and simultaneous presence of different components (sodium and calcium) is shown. The sequence of feed solutions is summarized in Figure 1a. The corresponding breakthrough patterns of sodium and calcium are shown in a semilogarithmic representation in Figure 1b. The breakthrough behavior of these two major cations governs the particle release pattern shown in Figure 1c. Each reduction in ionic strength results in a sudden increase of the particle concentration in the outflow. Furthermore, the observed tail of this peak ends abruptly with the arrival of the retarded exchange front (compare course of the calcium concentration, Figure 1b).

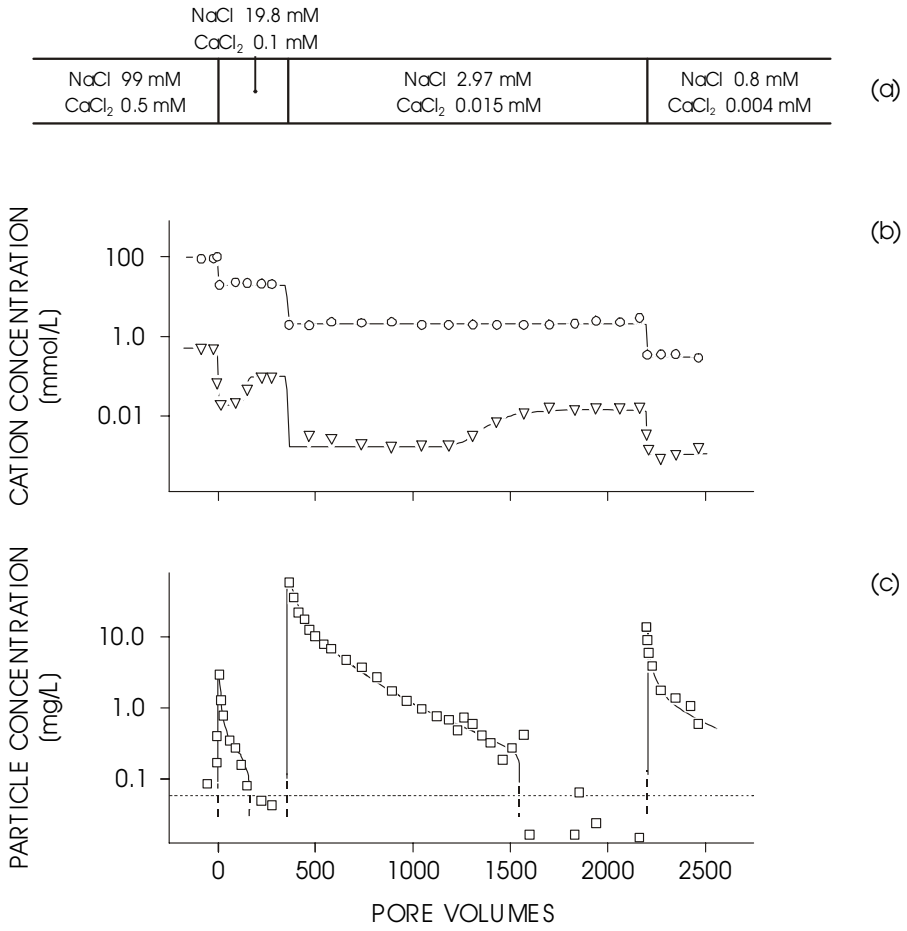

Figure 1: Release of colloidal particles in the simultaneous presence of sodium and calcium. The feed solutions (a) contain a constant sodium/calcium molar ratio of 200:1. The mobilization is induced by step-wise changes in normality. (b) Resulting outflow pattern of sodium and calcium in a semi-logarithmic scale. (c) Concentration of colloidal particles suspended in the outflow in a semi-logarithmic representation. In spite of the presence of divalent cations in the outflow mobilization of particles can be observed.

After mobilization, the life-time of colloidal particles is mainly determined by convective transport, particle (re-)deposition, and the aggregation behavior. The morphology and structure of the porous media influences the convective transport of the mobile particles which can be distinctly different from a conservative tracer. The processes of particle (re-)deposition and aggregation turned out to be dominantly influenced by solution chemistry as well as the surface chemical properties of the colloidal particles and the porous media. As an

example, the influence of the electrolyte concentration, counterion valence, and solution pH on the deposition rate coefficient is shown in Figure 2.

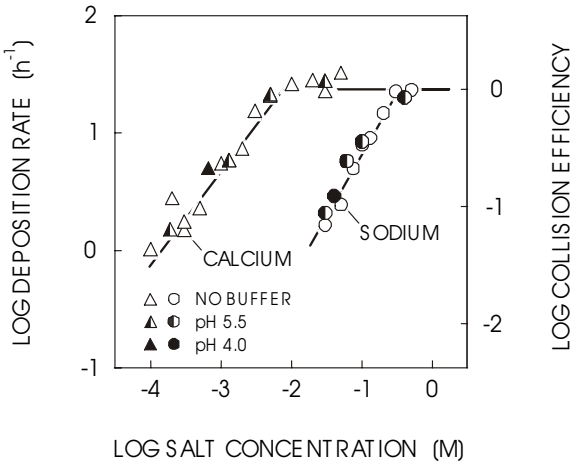

Figure 2: Influence of solution chemistry on particle deposition kinetics in packed soil columns. Effect of electrolyte (NaCl or $CaCl_2$) concentration, counterion valence (Na^+ and Ca^{2+}), and solution pH (pH 4.0 or 5.5, controlled by azide buffer) on deposition rate coefficients and experimental collision efficiencies for *in-situ* mobilized soil particles in their parent porous medium.

The three processes of particle mobilization, deposition and aggregation occur in general simultaneously. However, the relative importance of each of these processes is strongly dependent on the present chemical and physical conditions.

An extended transport model considering colloidal phenomena was formulated based on various independent experiments, each focusing on one particular process in an isolated fashion. This model was successful in the description of coupled multicomponent transport and particle mobilization phenomena taking place simultaneously in natural porous media. This modeling attempt clearly demonstrated the pronounced impact of ionic strength, solution and surface composition on particle release rates. Furthermore, the model was able to predict the observed breakthrough pattern of complex contaminant transport experiments, including the phenomena of enhanced contaminant transport by *in-situ* mobilized colloidal particles.

In conclusion, experiments and model calculation clearly demonstrated the potential importance of *in-situ* mobilized colloidal particles as a predominant transport vector of contaminants in natural subsurface systems. The experimentally simulated situations and the observed processes are likely to be operational in the field. Nevertheless, one has to be careful in translating the results obtained in laboratory column studies into actual field situations. Additional systematic investigations concerning mobilization and transport phenomena including natural, heterogeneous systems as well as well-characterized model systems are needed. Especially the combination of experimental investigations and mathematical modelling corresponds to a powerful tool in order to achieve a refined understanding of the chemical or physical system parameters controlling particle release under field conditions. Such efforts would result in an improved ability to understand and predict the susceptibility of natural systems for hazardous phenomena induced by mobilized colloidal particles such as enhanced transport of contaminant associated with mobile particles.

REFERENCES

Grolimund, D.; Borkovec, M.; Barmettler, K.; Sticher, H. Environ. Sci. Technol. 1996, 30, 3118-3123.

Grolimund, D.; Borkovec M. Water Resour. Res., 2001, 37, 559-570.

Grolimund, D.; Barmettler, K.; Borkovec M. Water Resour. Res., 2001, 37, 571-582.

Jenny, H.; Smith, G. D. Soil Sci. 1935, 39, 377-389.

Khilar, K. C.; Fogler, H. S. Reviews in Chemical Engineering 1987, 4, 41-108.

Muecke, T. W. Journal of Petroleum Technology 1979, 31, 144-150.

Ryan, J. N.; Elimelech, M. Colloids and Surfaces A. 1996, 107, 1 - 56.

Vinten, A. J. A.; Yaron, B.; Nye, P. E. J. Agric. Food Chem. 1983, 31, 662 - 664.

Diffusion limited sorption of strontium by microporous hydrous ferric oxide: modelling electrostatic constraints

Annette Hofmann[1], Wendy van Beinum[2], Johannes C.L. Meeussen[3] and Ruben Kretzschmar[1]

1- Institut f. Terrestrische Ökologie, Bodenchemie, ETH-Zürich, Grabenstr.3, CH-8952 Schlieren; Switzerland; E-mail: annette.hofmann@ito.umnw.ethz.ch, kretzschmar@ito.umnw.ethz.ch
2- Macaulay Institute, Craigiebuckler, Aberdeen, AB15 8QH, United Kingdom; E-mail: W.Van-beinum@macaulay.ac.uk
3- Alterra Wageningen, PB 47, 6700 AA ,Wageningen, Netherlands; E-mail: J.C.L.Meeussen@Alterra.wag-ur.nl

Hydrous ferric oxide plays a significant role in the sorption of organic and inorganic contaminants in soils, aquifers and aquatic environments. This is due to its ubiquity, to the extremely high specific surface area and to the reactivity of the hydroxylated surface sites. Hydrous ferric oxide is made up of unit crystallites of nanometer size, aggregated to form microporous aggregates. To reach the surface sites, the sorbates must diffuse through pores of subnanometer to nanometer size. Diffusion slows down the sorption kinetics. Sorption equilibrium therefore depends on parameters such as aggregate size and ratio of micropores to larger pores. To reach complete equilibrium it can take several years.

Due to the hydroxylation reaction, hydrous ferric oxide surfaces carry variable, pH dependent charge. To balance the surface charge, a diffuse layer of counterions develops, that extends over several nanometers away from the surface. In a microporous aggregate, a « squeezed » diffuse layer establishes in the pore space, with ion concentrations that differ from those in the bulk solution. The objective of the present study is to describe the electrostatically controlled ion concentrations in the pores by a simple model and to investigate whether micropore diffusion can be defined as a function of the pore chemistry and the free ion diffusion coefficient.

Experiments are conducted with strontium as the sorbate. Strontium contamination originates mainly from Sr-90, a fission product of spent fuel. Compared to other heavy metals, strontium has low surface affinity and therefore it tends to accumulate in the aqueous phase. Hydrous ferric oxide is one of the more relevant sorbents.

To investigate the diffusion of strontium in hydrous ferric oxide, we have developed a method to produce compact microporous hydrous ferric oxide aggregates. These aggregates have an average size of 230 µm. The size distribution of the aggregates is narrowed to a range of 200-300 µm by wet sieving.

Experiments are conducted in a system of advective flow. A chromatographic column is filled with the hydrous ferric oxide aggregates. The material is equilibrated by pumping a 10^{-3} M $NaNO_3$ electrolyte solution with a given pH through the column, using an HPLC pump at a flow rate of 0.2 ml min^{-1}. Once equilibrium is reached, the inflowing solution is switched to a 10^{-4} M $Sr(NO_3)_2$ solution of identical background electrolyte and pH. The effluent is collected with a fraction collector. Strontium is analysed by ICP-MS on the mass 88, effluent pH is measured online. A $NaNO_3$ salt pulse, recorded by conductivity measurement is used to determine the mobile pore volume.

For a pH above 4, results show that the strontium breakthrough is retarded, indicating sorption to hydrous ferric oxide. The breakthrough curves show a significant tailing indicating that sorption is diffusion limited (Figure 1).

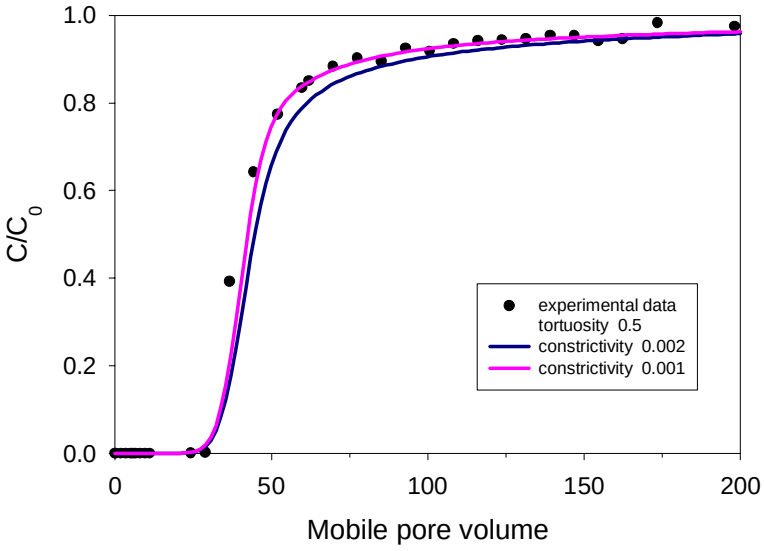

Figure 1 : Breakthrough curve of Sr^{2+} through a column of hydrous ferric oxide aggregates. Prior to the experiment, the column fill is equilibrated with an electrolyte solution of 10^{-3} M $NaNO_3$ at pH 6.7.The experiment is conducted with an inflowing solution of 10^{-4} M $Sr(NO_3)_2$ in 10^{-3} M $NaNO_3$ at pH 6.7. C/C_0 corresponds to the molar ratio of effluent to influent Sr^{2+} concentration.To fit the data, 60 % of sorption sites were defined as « accessible without diffusion ».

For quantitative assessment of the kinetic sorption experiment we have developed a transport model using ORCHESTRA (Meeussen, 2000), an object oriented framework for composing chemical speciation and transport models. In our model, sorption is described by the surface complexation two-layer model by Dzombak and Morel (1990). Transport is implemented as one-dimensional advective – dispersive flow. The slow ion diffusion into the micropores of the aggregates, responsible for the tailing of the strontium breakthrough curve, is described in terms of the free ion diffusion coefficient, a tortuosity factor and an « electrostatic constrictivity factor ». Spherical diffusion is solved numerically. The tortuosity factor is fixed at 0.5, based on the assumption that the particles in the aggregate can be described as packed monosize spheres. The electrostatic constrictivity is a fitting factor that expresses the influence of the pore chemistry on the ion diffusion process. Under conditions of pH 6.7 the experimental data are best fitted with a constrictivity factor of 0.001 (Figure 1). Combining with tortuosity, the overall factor lowers the micropore diffusion coefficient by a factor 2000 relative to the free diffusion coefficient. As the charge at the hydrous ferric oxide surface changes, the distribution of counter ions in the pore space changes too. Additional experiments are now being performed at conditions of higher pH, where we expect higher counter cation concentrations in the micropores, and therefore a lower electrostatic constrictivity factor for strontium diffusion.

We are in the course of developing an electrostatic model to replace the empirical constrictivity factors by a mechanistic concept that describes the average chemical conditions in the pore. This is achieved by considering the overall electroneutrality condition of the system « inner aggregate surfaces / micropore solution » and by describing the transition of ion concentrations in the pore solution and in the free solution by the Boltzmann factor. First results will be presented.

REFERENCES

Dzombak, D.A., and F.M.M. Morel (1990): Surface complexation modeling. Hydrous ferric oxide. John Wiley & Sons

Meeussen, J.C.L. (2000): Orchestra, a new framework for composing combined chemical reaction and transport models. International workshop on Surface Chemical Processes in Natural Environments, Monte Verità, Ascona, Switzerland, October 2000, p.37

MIGRATION OF AMD WATER IN CARBONATE BUFFERED AQUIFERS - COLUMN FLOW EXPERIMENTS AND THEIR MODELLING

Nils Hoth, Jan Hutschenreuter and Frieder Häfner
Institute of Drilling Engineering and Fluid Mining, Technical University of Freiberg
Agricolastr. 22, 09599 Freiberg, Germany; E-mail: Nils.Hoth@tbt.tu-freiberg.de

INTRODUCTION

The closure of brown coal opencast mines leads to the question of the future influence of the surrounding aquifers by dump waters. For an open cast mine in the northern part of the "Niederlausitzer Brown Coal District" a predictive 2D transport modelling study was carried out (Hoth et al. 2001). Therefore the reactive transport code PCGEOFIM (Sames, 1995; 2000) was used. The model shows an retention of the dissolved iron content of dump waters by iron hydroxide formation and exchanger buffering. The pH value was buffered by carbonate dissolution. A sulphate front arose in the gypsum level. Based on these modelling studies several column flow experiments were carried out to characterise the effectiveness of the predicted buffering systems. Dump water was infiltrated into cores originated from the surrounding aquifer. The paper points out results of the experiments and their modelling.

MATERIALS AND METHODS

Three column flow experiments were carried out at 60 cm long columns, with a 11.5 cm diameter. In the further text the experiment " SVJ 2 " is exemplary discussed. The column was filtrated by dump water with a constant rate of 6,04 ml/h. The infiltrating dump water was pumped from a dump water measuring point and conserved under nitrogen atmosphere. The total porosity of the column material amounts to 0.31. The effective porosity arose as a result of tracer experiments and is equal 0.2. Due to the non unique characteristics of salt tracers (comp. Postma & Apello) was it not possible to determine the longitudinal dispersivity. At the in- and outlet a continuous measurement of pH, EC and EH was realised. The outflowing water was also characterised by the measurement of the following parameters after filtration (0,45 µm): titremetric – alkalinity, acidity ; photometric - Fe2+, Feges , Siges, SO42-, Cl- ; ICP-OES - Na, K, Ca, Mg, Al, As, Cd, Co, Cr, Cu1, Fe, Mn, Ni, Pb, Zn, Si, S. Plausibility of analyses was checked by ion balance calculations with the program PHREEQC 2.0 (Parkhurst & Appelo, 1999). The ion balance errors of the analyses were in the range 4 to 8 %.

The initial and the final state of the filtrated core were characterised. Before the flow experiments at both ends a section was separated. After the experiments the core was separated into 4 sections. The following investigations were realised: grain size distribution analysis, indication of the pore water condition (GBL- extraction after VWV, 1995), sequential extraction as well as the investigation of TC/ TIC content by IR- detection. The sequential extraction after Zeien & Bruemmer (1989) was used in a simplified procedure. The fist step of the extraction was performed with 1M ammonium nitrate, the second step with 1M ammonium acetate (50% acetic acid) and the third step with 0,2 M di-ammonium-oxalat-monohydrat (oxalic acid, ammonia solution). The first step indicates the composition of CEC (cation exchange capacity) and easily soluble mineral phases (gypsum). Carbonates are indicated by the second step, while the third step summarises manganese oxides, organic matter and badly crystalline ferrihydroxides. Additionally the sand and pelite fraction was

[1] The content of trace metals of the used infiltrating dump water was at the level of the detection limit, while for the column outflow the values was below this limit. Therefore trace metals were not considered within the modelling.

investigated by means of SEM-EDX at selected samples. Because the lack of an ESEM the samples were dried and carbon-vaporised.

For the modelling of the experiments two models were used, the first is the 1D – transport tool within PHREEQC 2.0 (Parkhurst & Appelo, 1999). This code divides the transport calculation in convection, dispersion and hydrogeochemical interactions. The convective mass transport is based on "upstream weighting". The second model is PCGEOFIM. This Finite Volume- code solves the convection- dispersion equation in one step. Subsequently the hydrogeochemical interactions are calculated with PHREEQC (Sames,1995). The convective mass transport is based on a "Flux Limiter weighting".

The following hydrogeochemical processes were considered: mineral precipitation and dissolution processes, cation- exchange processes, complexation and redox processes. Reactive minerals were represented in the model by calcite, dolomite, siderite, rhodochrosite, gypsum, $Fe(OH)_3(a)$ and $SiO_2(a)$. The initial content of carbonate phases was derived from the second step of the sequential extraction. Step one of the extraction supplied the initial composition of the cation exchanger. The equilibrium state, necessary for the transport modelling, was calculated with the relevant thermodynamically constants of the database "phreeqc.dat" (Parkhurst & Appelo, 1999).

RESULTS AND DISCUSSION

Table 1 summarises the average chemical values of infiltrating solution and the initial pore water. The infiltrating dump water shows a high Fe, SO_4 concentrations (sulphide weathering) as well as sign of carbonate buffering (Ca, Mg, DIC- content), reductive processes (DIC) and silicate weathering (silicic acid = Si_{tot}).

Table 1 – Concentration of infiltrating solution (second row) and initial pore water (third row) [mmol/l] (Fe^{3+}, not detected – values calculated from pe, DIC calculated from acidity and alkalinity measurements)

pH [-]	pe[-]	Ca^{2+}	Fe^{2+}	Fe^{3+}	DIC	SO_4^{2-}	Mg^{2+}	Si_{ges}	Mn_{ges}	Cl^-	K^+	Na^+
6.6	2.37	12.5	1.37	$3.3*10^{-5}$	21.5	14.5	7.53	0.543	0.04	0.151	0.436	2.25
7.29	1.71	5.76	$8.9*10^{-3}$	$3.2*10^{-7}$	4.0	3.96	0.61	0.083	0.007	2.7	0.15	1.26

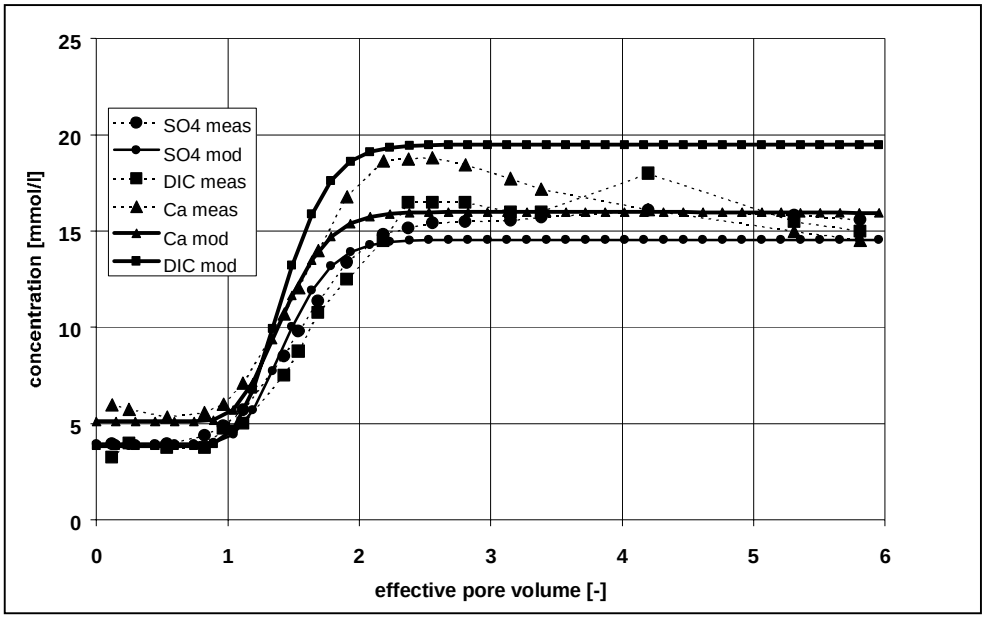

Figure 1: Comparison of PHREEQC results (variant 1)with observed values– SO_4^{2-}, DIC, Ca^{2+}

Figure 1 and 2 depict a comparison of the PHREEQC results and the observed values. The break-through of Ca, SO_4 and DIC occurs between an exchanged effective pore volume of 1 to 2. The model can not reconstruct the Ca and DIC curves exactly. The pH value (not shown) drops to a level of 6.7, which is well captured by the model. The measured concentration values for Fe_{tot}, Mn_{tot} and Si_{tot} can not be explained with the chosen model conception.

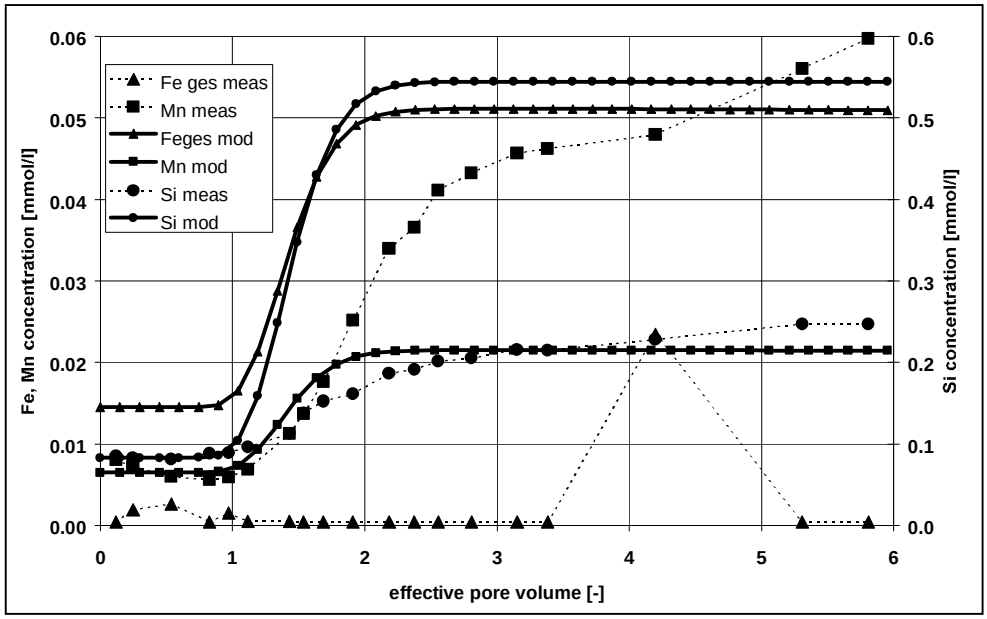

Figure 2: Comparison of PHREEQC results (variant 1) with observed values – Fe_{tot}, Mn_{tot}, Si_{tot}

In contrast to the modelling the measured Fe_{tot} values does not increase at the column outlet[2]. The measured Mn_{tot} concentrations rise continuously and achieve values above the infiltrate concentration. The silicic acid values (indicated as silicium) are during the entire experiment below the infiltrate concentration. This shows a significant retention of silicic acid. Again, this can not be explained by the used model conception.

That is why a second model uses a distinct conception. A manganese reduction was included, according to eq. 1. The rate definition in eq. 1 follows Postma & Appelo [2000]. The MnO_2 content was derived from the results of step 3 of the sequential extraction. Further the saturation index for $SiO_2(a)$ was assumed -0.8, resulting in a stronger retention of silicic acid.

Figure 3 shows the results of the second model. Obviously the Fe_{tot}, Mn_{tot} and Si_{tot} concentrations fits the observed values with a reasonable accuracy.

$$2\ Fe^{2+} + MnO_2 + 2\ H_2O \rightarrow 2\ FeOOH + Mn^{2+} + 2\ H^+ \qquad \text{(eq. 1)}$$

The influence of the manganese reduction on the Fe_{tot} and Mn_{tot} concentrations is confirmed by the pore water measurements following the experiment. The iron concentrations drops significantly from inlet to outlet of the core. This is accompanied with an increase of the Mn concentrations. The SEM investigations confirm the validity of the $SiO_2(a)$ saturation index adjustment. The retention of $SiO_2(a)$ occurs by a aggregation with carbonates. Due to the consideration of model minerals and equilibrium processes, this phenomena is only be explainable with adjustment of the saturation index. The generation of mass balances for the different components causes serious problems. The steps of the sequential extraction do not

[2] The measured value for 4.2 pore volumes is an exception.

exactly differentiate the bond type of the components. Additionally the heterogeneity of the solid phase is hardly to assure. Further the TIC solid phase analysis results deviate from the results of the sequential extraction (second step).

The modelling by means of PCGEOFIM show similar results to PHREEQC. The "upstream weighting" of the 1D PHREEQC transport tool causes a larger numerical dispersion.

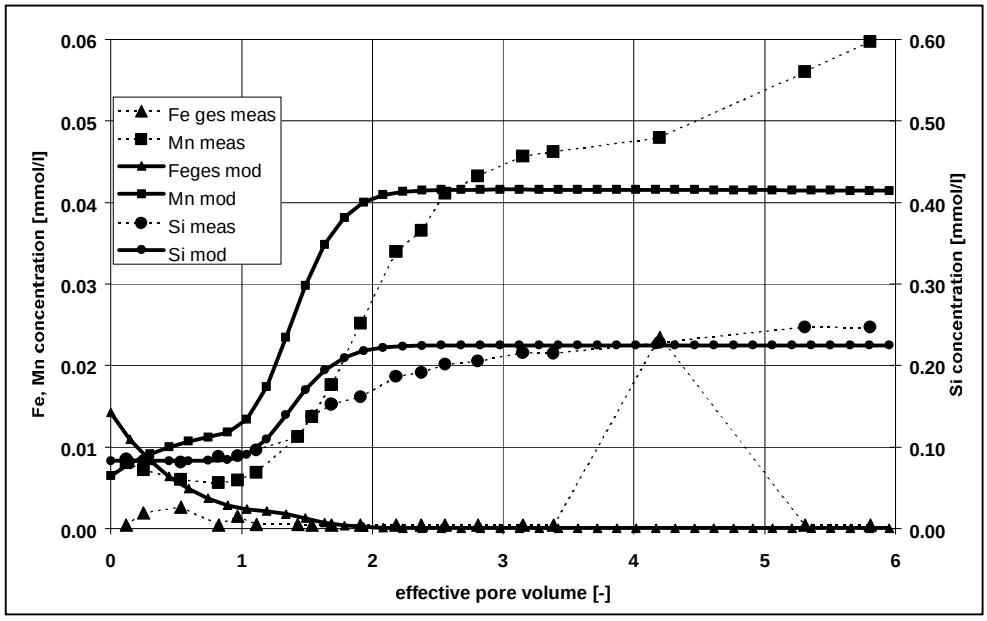

Figure 3: Comparison of PHREEQC results (variant 2) with observed values – Fe_{tot}, Mn_{tot}, Si_{tot}

However the sharper fronts of the PCGEOFIM modelling are accompanied with numerical oscillations.

CONCLUSIONS

The results of the column flow experiments confirm the conclusions of the predictive 2D model (Hoth et al., 2001). The modelling of the column flow experiments shows that the measured Mn, Fe values at the outlet can be explained by manganese reduction. This causes a retention of iron and simultaneously a manganese mobilisation.

A substantial difficulty of the modelling of reactive inorganic transport systems is the quantitative indication of the reactive mineral phases. For that purpose sequential extractions are essential investigation methods. The assignment of bond types to the different extraction steps is probably superimposed by kinetic effects. That is why the characterisation of the initial conditions and the generation of mass balances for the different components are difficult. The SEM investigations clarify that the formed mineral phases are often "solid solutions". This process can not exactly modelled with the thermodynamic equilibrium data of the used model minerals.

For the modelling of the transport processes the weighting scheme of convective mass transport is important. To improve the understanding of column experiments a parameter estimation considering cation exchange coefficients, saturation index etc. should be a next step. However a secured process understanding is therefore very substantial.

REFERENCES

Appelo, C.A.J. and Postma, D. (1999): Variable dispersivity in a column experiment containing MnO_2 and FeOOH- coated sand. J. of. Cont. Hydrology 40, 95 –106.

Hoth, N., Wagner, S., and Häfner, F. (2001): Predictive modelling of dump water impact on the surroundings of the lignite dump site. J. of Geochem. Exploration 73, 113 – 121.

Parkhurst, D.L. and Appelo, C.A.J. (1999): User's guide to PHREEQC 2.0- U.S. Geological Survey, Water Resour. Inv. Rep. 99-4259, Denver-Colorado,

Postma, D. and Appelo, C.A.J (2000): Reduction of Mn-oxides by ferrous iron in a flow system. Geochim. et Cosmochim. Acta 64, 1237 - 1247

Sames, D. and Boy, S. (1995): *User's guide to PCGEOFIM*. IBGW Leipzig, in German

VWV (1993): Verwaltungsvorschrift „Bodenproben" des Umweltministeriums Baden-Würtemberg", Anlage 4, in German.

Zeien, H. and Brümmer, G.W. (1989): Chemische Extraktionen zur Bestimmung von Schwermetallbindungsformen in Böden. Mitteilungen Dt. Bodenkundl. Gesellschaft 59/I, 505 – 510, in German.

COUPLING OF REDOX PROCESSES AND TRANSPORT: TRACER TESTS WITH ARSENIC (III) AND ARSENIC (V) AT THE CAPE COD SITE

Margot Isenbeck-Schröter[1], Susanne Stadler[1], Rouven Höhn[1] Steffen Jann[1], Douglas Kent[2], James Davis[2], Volker Niedan[1], Christian Scholz[1], Andreas Tretner[1], Stefan Rheinberger[1], Volker Wild[1] and Rasmus Jakobsen[3]

1- Institute of Environmental Geochemistry, University of Heidelberg,
Im Neuenheimer Feld 236, D-69120 Heidelberg, Germany;
Email: mischroe@ugc.uni-heidelberg.de

2- United States Geological Survey, Menlo Park, USA

3- Danish Technical University, Lyngby, Denmark

In groundwater redox processes mediate the transport behavior of numerous elements, e.g. heavy metals and arsenic. These elements can be divided into two groups, which react differently. The first group reacts directly during electron transfer and changes the redox state, whereas the second group reacts with typical products of redox processes consuming organic substance, as e.g. the sulfide anion. To predict the geochemical behavior, concentrations in water, and transport velocities of these compounds, redox processes have to be coupled to transport. This coupling cannot be obtained in batch systems and transport experiments have to be conducted.

Groundwater contamination of arsenic leads to severe health risks in drinking water supplies in India, Bangladesh and some other countries (e.g. Conference on Water Rock Interaction, Calgliari Sardengna 2001). The origin of the arsenic contamination is often geogenetic. Processes of arsenic mobilization and transport seem to be directly dependent on the redox processes as e.g. pyrite oxidation and degradation of organic substance. Since a couple of years, transport experiments in columns have been run in my team (and of course also by others) in order to improve knowledge of the transport behavior of the redox species As (III) and As (V) under various geochemical conditions (Haury et al. 2000**)**. In spring and summer 2000, large scale transport experiments at the Cape Cod Site near Boston (Mass., USA) were performed in close cooperation with scientist of the USGS. The project was funded by the DFG and supported by the USGS Toxic Substances Program. The experiments should show a redox-induced transport behavior under natural conditions.

The Cape Cod Site is a famous hydrogeological test site of the USGS and consists of an array of more than 900 multisampling wells which are built in a former gravel pit in a stratified sand and gravel aquifer of glacial origin. Following a long-term contamination by sewage waters, a redox zonation occurs in the aquifer. Whereas the upper 3-4 meters are oxic (pristine zone), a suboxic zone and in 20 meter depth also an anoxic zone have developed during decades due to the degradation of organic substance. Preliminary studies in German groundwaters showed that an oxidation of As (III) has to be expected under oxic and suboxic conditions, whereas As(V) is only reduced in an anoxic environment (Tretner et al. 2001). Thus, in each redox zone a specific tracer experiment was run. We injected arsenic (III) into the oxic and the suboxic zone using a pulse injection of high loads of As (III) in 900 m^3 water. Bromide was used as an ideal tracer to find out the physical transport properties. The results of redox-processes and transport behavior of the corresponding arsenic redox species are shown and discussed in the presentation. The different geochemical environments lead to different kinetics of the processes and result in huge differences of the arsenic mobility (Stadler et al. 2001). The reduction of As (V) under iron reducing conditions seems to be the most important scenario to mobilize arsenic (Hoehn et al. 2001). We studied this process coupled to transport injecting As (V) continuously over a period of 4 weeks into the anoxic

layer of the Cape Cod aquifer. The results of the As (V) tracer test indicate that the mobilization can be obtained by small amounts of sulfide (Hoehn et al. 2001). Further studies will focus on solid phase processes and the modelling of the tracer tests.

REFERENCES

Haury, V., Jann, S., Kofod, M., Scholz, Ch. & M. Isenbeck-Schröter (2000): Redox-induced species distribution of arsenic in a suboxic groundwater environment - column experiments. - in: Rosbjerg et al. (eds): Groundwater Research, Balkema, Rotterdam, ISBN 90 5809 133 3, S.

Höhn, R., Isenbeck-Schröter, M., Niedan, V. Scholz, C., Tretner, A., Jann, S., Stadler, S., Kent, D.B. , Davis, J.A. Jakobsen, R. (2001): Tracer test with arsenic (V) in an iron-reducing environment at the USGS Cape Cod Site (Mass. USA). – in: Cidu, R. (ed.): Water Rock Interaction.- Band 2, S. 1099-1102, Balkema

Stadler, S., Jann. S., Höhn, R., Isenbeck-Schröter, M., Niedan, V. Scholz, C., Tretner, A., Davis, J.A., Kent, D.B. (2001): Tracer test with As (III) in the oxic and suboxic groundwater zones at the USGS Cape Cod Site (Mass. USA). – in: Cidu, R. (ed.): Water Rock Interaction.- Band 2, S. 1013-1016, Balkema

Tretner, A., Kofod, M., Scholz, C., Isenbeck-Schröter, M. (2001): Einflüsse des geochemischen Milieus und der Eintragsform auf die Verteilung der anorganischen Redoxspezies des Arsens im Grundwasser.- Grundwasser 6/1: 3-7

REACTIVE TRANSPORT MODELLING OF INTERACTION BOOM CLAY – CEMENT WATER: EXPERIMENTAL DATA AND PRELIMINARY MODELLING RESULTS

Diederik Jacques
SCK•CEN, Boeretang 200, B-2400 B-Mol, Belgium; E-mail: djacques@sckcen.be

INTRODUCTION

A generally accepted concept of the deep disposal of radio-active waste is the concept of a multibarrier system in which different barriers guarantee the long-term confinement of the waste and a long-term protection of man and environment. A sequence of possible barriers is, e.g., the waste matrix, backfill material, concrete liner, and the geological host formation (clays, salt, granite). Of course, the pore water solution of the different barriers will interact with each other and this may significantly change the effectiveness of a barrier. For example, the chemical composition of the pore water in the concrete, used either as backfill material or as a liner, typically has a high pH-value and high concentrations of Na, K, and Ca and is not in equilibrium with the geological layer. Thus, migration of chemical components from the concrete water to the geological layer may cause significant alterations of its physical and chemical properties.

In the current Belgian research programme of deep disposal of high and intermediate level waste, the Boom Clay geological layer at Mol is the reference site. In this study, therefore, the interaction between so-called young concrete water (pH ~ 13) and Boom Clay is investigated. The objectives are to develop a conceptual geochemical model to simulate the interactions and to validate this geochemical model by means of the reactive transport code PHREEQC (Parkhurst and Appelo, 1999) using experimental data. In this paper, we present a first geochemical model and some preliminary model simulations.

MATERIALS AND METHODS

Experimental set-up

A clay core containing undisturbed samples of the Boom Clay was placed in a flow through experiment with water representative for young concrete water, called here alkaline water or plume (see below). The core was 0.032 m long and had a diameter of 0.038 m. At each side, a filter of 0.002 m was placed. At one side, the alkaline water was added with a flux of 0.431 m^3 day^{-1}. Outflow pH and concentrations of several elements such as Al, Ca, K, Mg, Na, and Si were measured at regular moments during more than 1000 days.

Geochemical model

The Boom Clay mineralogy was represented by 10 minerals: quartz, albite, microcline, calcite, and the clay minerals kaolinite, illite, chlorite, and three forms of montmorillonite. Formula, thermodynamic equilibrium constants and amount in 100 g Boom Clay are given in Table 1. The rate of dissolution and precipitation of these minerals are described with:

$$rate = A\,k\left(1-\frac{Q}{K}\right) \qquad (1)$$

where rate is the dissolution rate (mole sec^{-1}), A is the reactive surface area (m^2), Q is the ionic product, K the equilibrium constant, and k is the rate coefficient (mole sec^{-1} m^{-2}). In this study, the rate coefficient, k, is defined as a function of pH:

$$\log(k) = a + b\ pH \tag{2}$$

or

$$k = 10^{a}\ act(OH^{-})^{b} \tag{3}$$

where *a* and *b* are two mineral dependent parameters (see Table 1) and *act*(OH^-) is the activity of OH^-. Since the rate coefficient of calcite is much larger than those of the other minerals, equilibrium precipitation and dissolution of calcite is assumed. Reactive surface areas of the individual minerals are based on literature values and these values are then scaled to the measured surface area of the Boom clay, i.e., 44 $m^2\ g^{-1}$ (Table 1; log *K* values are from the database from PHREEQC).

Table 1: Names, formula, equilibrium constant (*K*), weight percentages (*W*), reactive surface areas (*A*) and number of moles (*n*) in 100g Boom Clay, and *a* and *b* coefficients for the model of the Boom Clay mineralogy.

Name	Formula	log K		*A* (m^2)	*n*	*a*	*b*
			(%)				
Quartz	SiO_2	-3.99	45	180	0.7450	-15.44[(1)]	0.3
Albite	$NaAlSi_3O_8$	2.76	2	0.12	0.0076	-14.10[(1)]	0.3
Microcline	$KAlSi_3O_8$	-0.28	8	1.20	0.0287	-15.10[(2)]	0.3
Calcite	$CaCO_3$	1.85	2	0.40	0.0199	-	-
Kaolinite	$Al_2Si_2O_5(OH)_4$	6.81	7	70	0.0271	-15.68[(1)]	0.3
Illite	$K_{0.6}Mg_{0.25}Al_{1.8}Al_{0.5}Si_{3.5}O_{10}(OH)_2$	43.3	5.5	909	0.0143	-12.31[(3)]	0.34
Chlorite	$Mg_5Al_2Si_3O_{10}(OH)_8$	71.75	4.3	711	0.0077	-12.31[(4)]	0.34
Montmor.-Ca	$Ca_{0.165}Mg_{0.33}Al_{1.67}Si_4O_{10}(OH)_2$	2.49	6	992	0.0164	-12.31[(4)]	0.34
Montmor.-Na	$Na_{0.33}Mg_{0.33}Al_{1.67}Si_4O_{10}(OH)_2$	2.48	4.3	711	0.0117	-12.31[(4)]	0.34
Montmor.-Mg	$Mg_{0.495}Al_{1.67}Si_4O_{10}(OH)_2$	2.39	5	826	0.0138	-12.31[(4)]	0.34

[(1)] Eq. 2, Walther, 1996; [(2)] Eq. 2, Blum and Stilling, 1995 stating the kinetics of microcline is one order of magnitude slower than that of albite; [(3)] Eq. 3, Huertas et al., 2001; [(4)]Eq. 3, set equal to parameters of illite.

Since there is a large amount of clay minerals, especially smectites, in the Boom Clay, exchange of cations between the water and the Boom Clay was taken into account. The cation exchange capacity of Boom Clay is 30 meq / 100 g. Ion exchange reactions are written as half reactions in the Gaines-Thomas convention (see Parkhurst and Appelo, 1999).

Typical secondary minerals formed in high pH solutions are so-called calcium silicium hydrate-phases (CSH). In this study, we used three CSH-phases with different Ca/Si ratios, represented by tobermorite14A (Ca/Si=0.833), hillebrandite (Ca/Si=1.333), and okenite (Ca/Si=0.5) (Table 2). Studies of Opalinus shale in high pH solutions showed that analcime (a Na zeolite) was formed with NaOH (Chermak, 1992), and phillipsite and K-feldspar (microcline) was formed with KOH (Chermak, 1993). These two secondary minerals were also included in the geochemical model (Table 2). In experimental studies of the interaction of Boom Clay with Ordinary Portland Cement, Read et al. (2001) observed the formation of a Mg-aluminate hydroxide and Mg-silicate hydroxide gel with a composition corresponding to hydrotalcite and sepiolite and are therefore included in the model (Table 2). Precipitation processes were treated kinetically with the rate coefficient equal to 10^{-9} mole sec^{-1} m^{-2}, i.e. faster than the kinetic reaction of the primary minerals. The latter two minerals (hydrotalcite and sepiolite) and analcime are assumed to be in equilibrium. Most *K*-values for the secondary minerals are from the HATCHES-database (Hatches, 2000).

Table 2: Formula and equilibrium constants for the secondary minerals.

Name	Formula	log K
Tobermorite14A	$Ca_5Si_6H_{21}O_{27.5}$	63.84
Hillebrandite	$Ca_2SiO_3(OH)_2(H_20)_{0.17}$	36.82
Okenite	$CaSi_2O_4(OH)_2.H_2O$	10.38
Analcime	$Na_{0.96}Al_{0.96}Si_{2.04}O_6.H_20$	6.14
Phillipsite	$Na_{0.5}K_{0.5}AlSi_3O_8.H_2O$	-19.87
Hydrotalcite	$Mg_4Al_2(OH)_{14}.3H_20$	75.34
Sepiolite	$Mg_2Si_3O_{7.5}OH.3H_20$	15.76

MODELLING

The PHREEQC-model (Parkhurst and Appelo, 1999) was used to model the transport of an alkaline plume through an intact Boom Clay sample. The composition of the initial water in the clay core and of the alkaline water were measured and are given in Table 3. The flow domain contained 18 cells of 0.002 m of which the first and the last one consist of inert material, and thus only homogeneous aqueous reactions are taken into account. In the remaining 16 cells, following additional reactions can occur: dissolution/precipitation of primary minerals, dissolution/precipitation of secondary minerals, and ion exchange. Water is moving with a velocity of 1.12 10^{-8} m sec^{-1}. Solute transport is described by the convection dispersion equation. The molecular diffusion and dispersion is described with an effective dispersivity of 0.023 m. Simulations were performed for a total duration of 1000 days.

Table 3: Elemental composition of initial water and the alkaline plume (mg l^{-1}).

	Initial composition Boom Clay water	Alkaline plume
Al	0.00027	8.07
Ca	1.3	8.28
K	8	5500
Mg	0.7	0.47
Na	447	1490
Si	8.8	97.6
pH	8.55	13.04
pCO_2	-2.42	equilibrium with calcite

PRELIMINARY MODELLING RESULTS

Some first modelling results are plotted in Figure 1. We show the simulated pH, K-, Si-, and Na-concentration of the outflow together with the experimental observations. The geochemical model predicts a faster increase in pH compared to the observations. This is also observed for K and Si. The model predicts a complete depletion of Na which is not in accordance with the observation. This may be due to immediate precipitation of analcime. Obviously, kinetic precipitation of analcime has to be considered in further research. For the pH, a fast modelled increase is observed in the beginning of the flow through and a small underestimation is observed at the end of the model simulations. Both the end concentrations of K and Si are reasonable close. This is especially important for Si given the difference between the inflow concentration (~100 mg l^{-1}) and the outflow concentration (~ 400 mg l^{-1}). The large difference between simulated and observed Na outflow concentration may be due to

the equilibrium precipitation of analcime, or to neglecting some important Na-controlling process.

As part of a sensitivity analysis, we increased the *a*-parameters in Eqs. 2 and 3 with a value of 1. Corresponding simulation results are also plotted in Figure 1. For this fast model, simulated outflow concentrations respond slower than the observations.

As a conclusion of these preliminary model result, we believe that this geochemical model is a good starting point for further adaptations, given the very complex interactions between an alkaline plume and Boom Clay. In further research, we will include/remove several other possible secondary minerals based on literature study until we get a similar behaviour between measured and calculated outflow concentrations. In addition, some more precise processes, such as changing reactive surface area and porosity changes and its effect on kinetics and flow and transport properties, respectively, will be included in the geochemical model.

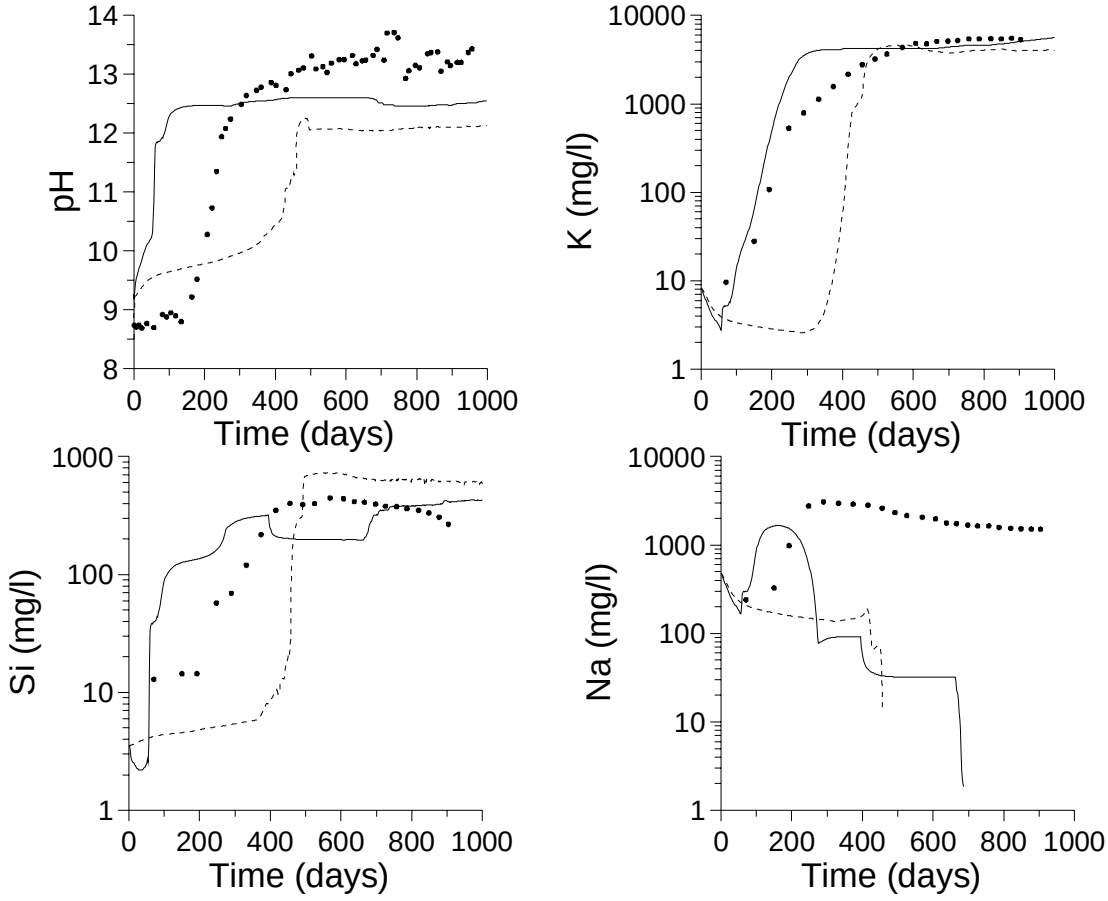

Figure 1: Comparison between observed outflow pH and concentration (dots), simulation results with the geochemical model (full line), simulation results with the 'fast' geochemical model (dashed line) of the pH, K-, Si-, and Na-concentration.

REFERENCES

Blum, A.E., and L.L. Stillings, 1995. Feldspar dissolution kinetics. In: *'Chemical weathering rates of silicate minerals*' (Eds. White, A.F., and S.L. Brantley), Reviews in Mineralogy 31, 291-351.

Chermak, J.A., 1992. Low temperature experimental investigation of the effect of high pH NaOH solutions on the Opalinius shale, Switzerland. Clays and Clay Minerals 40, 650-658.

Chermak, J.A., 1993. Low temperature experimental investigation of the effect of high pH KOH solutions on the Opalinius shale, Switzerland. Clays and Clay Minerals 41, 365-372.

HATCHES, 2000. HATCHES, The Harwell/Nirex Thermodynamic Dataase for Chemical Equilibrium Studies, version NEA13.

Huertas, F.J., E. Caballero, C. Jiménez de Cisneros, F. Huertas, and J. Linares, 2001. Kinetics of montmorillonite dissolution in granitic solutions. Applied Geochemistry 16, 397-407.

Parkhurst, D.L., and C.A.J. Appelo, 1999. *User's guide to PHREEQC (Version 2) – A computer program for speciation, batch-reaction, one-dimensional transport, and inverse geochemical calculations.* Water-Resources Investigation Report 99-4257, U.S. Dep. Of the Interior U.S. Geological Survey, Denver, Colorado, 312 p.

Read, D., F.P. Glasser, C. Ayora, M.T. Guardiiola, and A. Sneyers, 2001. Mineralogical and microstructural changes accompanying the interaction of Boom Clay with ordinary portland cements. Advances in Cement Research, accepted for publication.

Walther, J.V., 1996. Relation between rates of aluminosilicate mineral dissolution, pH, temperature, and surface charge. Am. J. Sci. 296, 693-728.

CODE DEVELOPMENT FOR MODELING OF COUPLED EFFECTS AT CORROSION OF CARBON STEEL CONTAINERS UNDER REPOSITORY CONDITIONS

E. Korthaus

Forschungszentrum Karlsruhe (FZK), Institut für Nukleare Entsorgungstechnik (INE), P.O.B. 3640, D-76021 Karlsruhe, Federal Republic of Germany; E-mail: korthaus@ine.fzk.de

The general corrosion of steel containers and the development of the pore-fluid chemistry in the adjacent backfill material are a result of several coupled processes:

- Electrochemical corrosion processes of the container surface
- Reactive transport of dissolved chemical species in the pore-fluid
- Changes of backfill porosity due to precipitation of corrosion products or other precipitation/dissolution effects
- Growth of (more or less) protective layers on the container surface
- Generation and build-up of hydrogen at the container surface

The 1-dimensional code TRANSAL is being developed as a numerical modelling approach to these effects. The main objectives are the support of the interpretation of corrosion tests and a prediction of long-term corrosion rates and near-field chemistry under repository conditions. The current version of TRANSAL consists of several iteratively coupled programm parts for the calculation of

- Saturated porous flow for porosities under the influence of precipitation/dissolution effects and of thermomechanic convergence/consolidation
- Diffusive and advective mass transport (with linear sorption)
- Thermodynamic equilibrium and precipitation/dissolution at high ionic strength and elevated temperatures (Pitzer's formalism for the calculation of activity coefficients).
- Parts of the THCC code (Carnahan, 1987) were used to develop this module.
- Kinetic effects in complexation and precipitation/dissolution with the aid of variable equilibrium constants
- Electrochemical corrosion rate and potential as a function of the composition and transport characteristics of the adjacent pore-fluid

Calculations were performed in order to test and to improve the numerical procedures. Most of them were focused on the reactive transport in the pore-fluid and used a fixed corrosion rate (assuming a constant source of Fe^{++}, OH^-) as a boundary condition. A considerable numerical effort was introduced when the oxidation kinetics of Fe^{++} by dissolved oxygen were taken into account under aerobic initial conditions. Some exemplary results, the development of pH and Eh distributions, are shown in figures 1 – 2 . A column of 0.1mol NaCl of 0.5m length at 25°C was considered in this test case. The aquatic species Na^+, Fe^{++}, Fe^{3+}, H^+, Cl^-, OH^-, $Fe(OH)_2(aq)$, $Fe(OH)_3(aq)$, $Fe(OH)_2^+$ and $O_2(aq)$ and the solids $Fe(OH)_2$, FeOOH, Fe_2O_3 and Fe_3O_4 were taken into account in the model.

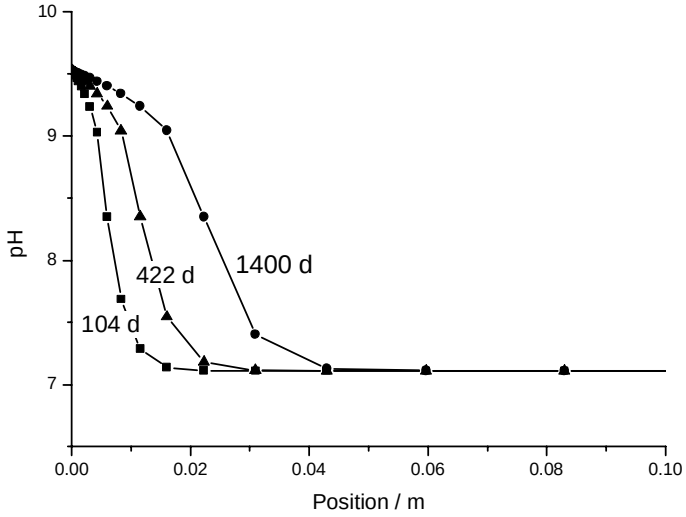

Fig. 1 Development of pH near the 'corrosion plane'

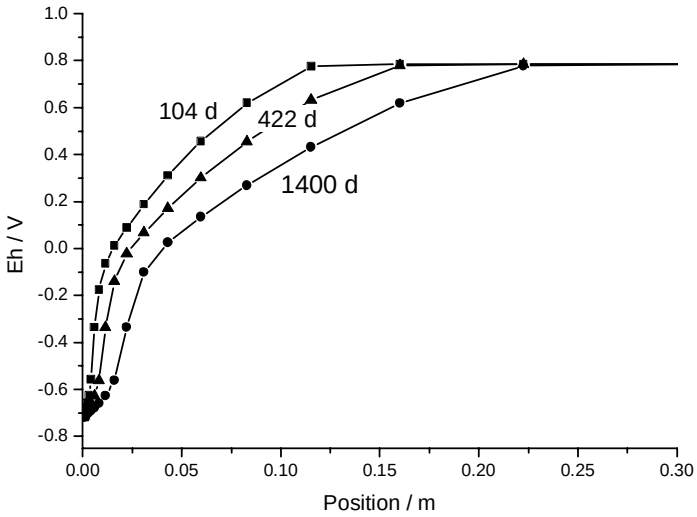

Fig. 2 Development of redox potential (from Fe^{3+}/ Fe^{++} ratio)

When the calculation of the electrochemical corrosion rate (based on kinetic data from Marsh, 1988) is introduced in this test case instead of using a fixed source term, it is found that the reduction of O_2 is the dominating cathodic reaction for a very short time only, because the supply of O_2 is limited by diffusion. In parallel, while the electrode potential is slightly decreasing, the water reduction reaction is rising to a small value remaining constant hereafter (Fig. 3). It is the dominating cathodic reaction because of the alkaline conditions prevailing near the corrosion plane in this test case. The situation would be quite different under acidic conditions as found in magnesium rich brines at elevated temperatures. The reduction of H^+ then will be the dominating cathodic reaction, giving rise to a more pronounced coupling between corrosion rate and pore-fluid chemistry.

Apart from the obvious need of additional data for an adequate modelling of the pore-fluid chemistry, it is well known that a more realistic prediction of long-term corrosion rates will not be possible without taking into account of the effects of protective layers. The search for a method to handle this problem will be started in the near future.

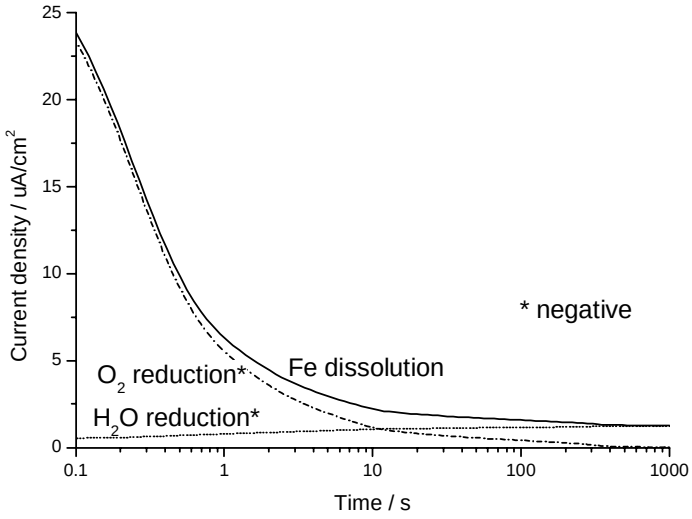

Fig. 3 Anodic and cathodic current densities of Fe corrosion in NaCl solution

REFERENCES

Carnahan, C.L., 1987. Simulation of Uranium Transport with Variable Temperature and Oxidation Potential: The Computer Program THCC. Mat. Res. Soc. Symp. Proc., 84 : 713-721.

Marsh, G.P., 1988. Progress in the Assessment of the Corrosion of Low and Intermediate Level Waste Containers under Repository Conditions. Harwell Laboratory, UKAEA, Report NSS/R126.

MODELLING OF COLLOID TRANSPORT IN A GRIMSEL SHEAR-ZONE

Georg Kosakowski

Waste Management Laboratory, Paul Scherrer Institute , CH-5232 Villigen PSI, Switzerland; E-mail: georg.kosakowski@psi.ch

Since more than 15 years tracer migration experiments are performed at Nagra's Grimsel Test Site. The recent Colloid and Radionuclide Retardation project (CRR) investigates the influence of bentonite colloids on radionuclide transport through a shear zone in the granitic host rock. Several tracer experiments were carried out in different hydraulic dipoles. After evaluation of the experiments one dipole (dipole 1) was chosen for the final experiments with colloids in February/March 2002.

The preliminary tests in dipole 1 are evaluated with a method already successfully applied during the Migration Experiments by Hadermann and Heer (1996) in a different part of the shear zone. Their method replaces the shear zone by a set of parallel fractures embedded in a porous rock matrix of finite thickness. Processes included are advection and dispersion in the fracture, diffusion from the fracture into the matrix (matrix diffusion), and sorption in the matrix. A comparison of the material parameters applied by Hadermann and Herr (1996) and those from the present study shows no significant differences.

The preliminary tests also showed a significant tailing in the breakthrough of colloids which cannot be explained by matrix diffusion or with the conventional model based on transport in a homogeneous domain. This observation could be interpreted as non-Fickian transport, which is characterized by non-Fickian scale-dependent spreading of contaminant plumes, unusually early breakthrough times or unusually long late time tails in measured breakthrough curves (e.g. Becker and Shapiro, 2000).

The limitations in describing non-Fickian solute and particle migration with conventional models was the reason to fit the colloid breakthrough with the Continuous Time Random Walk (CTRW) approach. The CTRW-approach was developed and applied to transport in fracture networks and heterogeneous porous media (Berkowitz and Scher, 1998; Berkowitz et al., 2001; Kosakowski et al., 2001).

REFERENCES

Becker, M.W., Shapiro, A.M., 2000. Tracer transport in fractured crystalline rock: Evidence of nondiffusive breakthrough tailing, Water Resour. Res., 36, 1677-1686.

Berkowitz, B., Scher, H., 1998. Theory of anomalous chemical transport in fracture networks, Phys. Rev. E, 57(5), 5858-5869.

Berkowitz, B., Kosakowski, G., Margolin, G. & Scher, H., 2001. Application of continuous time random walk theory to tracer test measurements in fractured and heterogeneous porous media. Groundwater, 39, 593-604.

Hadermann, J., Heer, W., 1996. The Grimsel (Switzerland) migration experiment: integrating field experiments, laboratory investigations and modelling, J. Cont. Hydrol., 21, 87-100.

Kosakowski, G., Berkowitz, B., & Scher, H., 2001. Analysis of field observations of anomalous transport in a fractured till. J. Cont. Hydrol., 47, 29-51.

COMPARISON OF DOUBLE LAYER MODELS IN TRANSPORT PROBLEMS

Johannes Lützenkirchen and Bernhard Kienzler
Forschungszentrum Karlsruhe GmbH, Institut für Nukleare Entsorgung, Postfach 3640,
D-76021 Karlsruhe, Germany; E-mail: johannes@ine.fzk.de

For the description of adsorption phenomena on oxide minerals a wide range of (semi)mechanistic surface complexation models are available. They have in common that they separate the free energy of adsorption into an intrinsic chemical and a coulombic contribution. By defining surface species in terms of surface chemical reactions and reactivities the intrinsic contribution is qualitatively defined. The coulombic term is determined by the structure of the electrical double layer, which forms at charged solid/water interfaces. The contributions to the overall free energy of the formation of surface species can be computed if one assumes a picture for the two aspects.

Unfortunately, a wide range of pictures exist how surface species are defined and how the electrical double layer is envisioned. This may for example be due to different objectives of the modelling i.e. a simple or a comprehensive model may be used to either just describe data or to attempt a structural representation on the macroscopic level, respectively.

There is at present no way to experimentally distinguish quantitatively between the contributions of the two terms and modellers are free to combine different complexities of the various components of surface complexation theory, which results in a wide range of model variations.

Thus the various existing models differ in the way the different components of the surface complexation approach are treated. The fundamental model is usually decided on when the sorbent acid-base properties are described, although some features still can be added in the subsequent modelling of the contaminant adsorption data. On the simplest level of surface complexation theory, any model encompasses decisions on:

- The proton ad(de)sorption mechanism: one may, for example, assume a 1-pK or a 2-pK protonation mechanism. The 1-pK approach involves only one proton ad(de)sorption step within the usual range of pH, so that surface groups will be present in no more than two states. The 2-pK approach generally involves two consecutive protonation steps (3 states) within a relatively narrow range of pH (the range is dependent on model parameterisation).
- The treatment of surface heterogeneity: one may distinguish between discrete and continuous heterogeneity of surface sites. Discrete heterogeneity involves the allocation of a specific affinity to a specific site type. The simplest case would be a one site model with a defined stability constant for all species formed on this site. Continuous heterogeneity involves a distribution function for the reactivities. The most complex case would be a multi-site model with distribution functions of the reactivities of all species formed on all sites.
- Electrical double layer: one has to account for the contribution of charge formation at the oxide/electrolyte interface. This is possible by defining a model for the structure of this interface. Different models of various degree of complexity exist which allow a more or less detailed picture (see figure 1).

With the complexity of the model, the number of parameters required usually increases. From various modelling exercises it has become clear that parameters are frequently correlated with each other and that a unique model parameter set can rarely be obtained. Combination of methods (i.e. macroscopic adsorption data with structural “microscopic” data) may improve that issue to some extent in particular for well-defined sorbents.

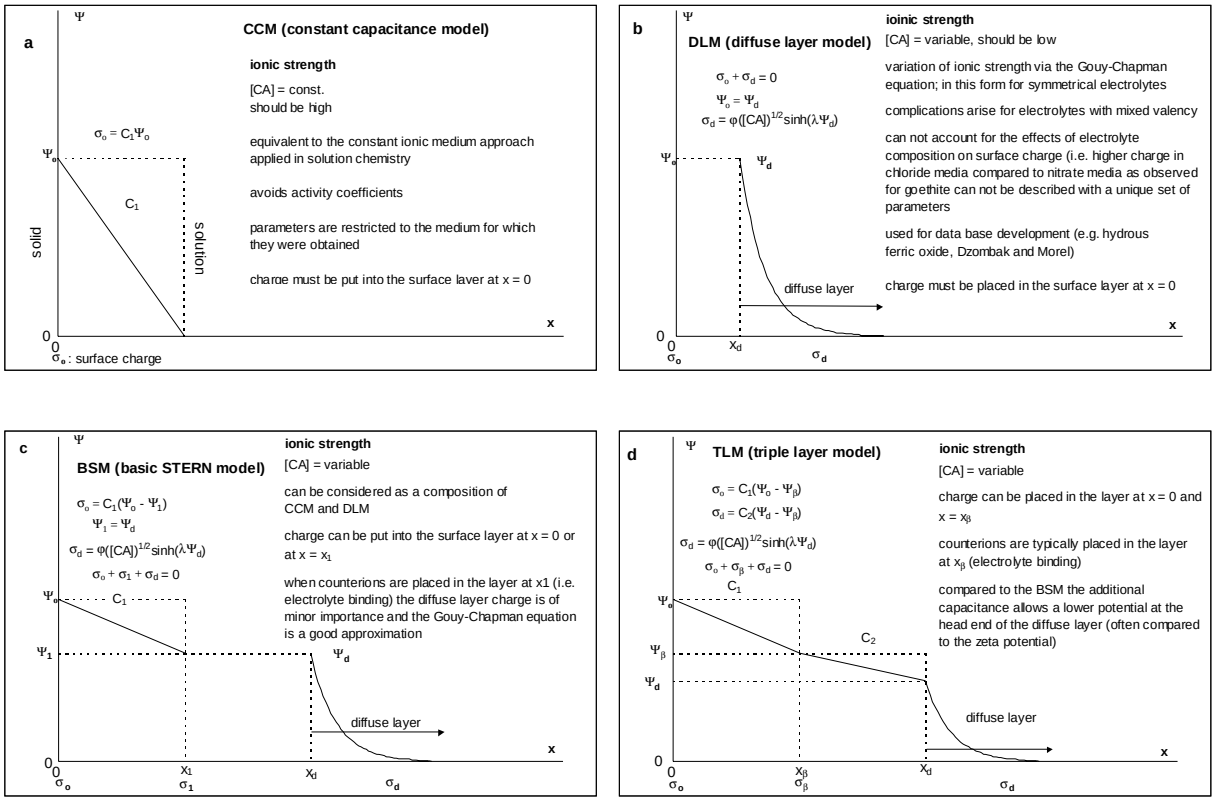

Figure 1: Electrostatic standard models as they are used in standard speciation codes handling surface complexation models.

In general however, many models will yield good descriptions of one data set. This is shown for goethite surface charge in figure 2. In this example two advanced approaches to handle multi-site features (discrete heterogeneity) with predicted proton affinities (Hiemstra et al., 1996) based on goethite bulk structure; Rustad et al. (1996) based on molecular modelling) allow a very similar description of goethite surface charge, although the individual contributions to the charge are very different in the two models.

Approaches to compare the respective model performances are desirable. In this contribution an attempt is made to compare the performance of various models in transport problems. This attempt encompasses model calibration on available batch adsorption data and subsequent application in predicting breakthrough curves with the individual models under identical hydrodynamic conditions.

In a first step the surface complexation models tested are applied to a set of adsorption data. This encompasses the respective modelling of the acid-base properties of the sorbent and the use of the extracted model parameters in the fitting of the adsorption data.

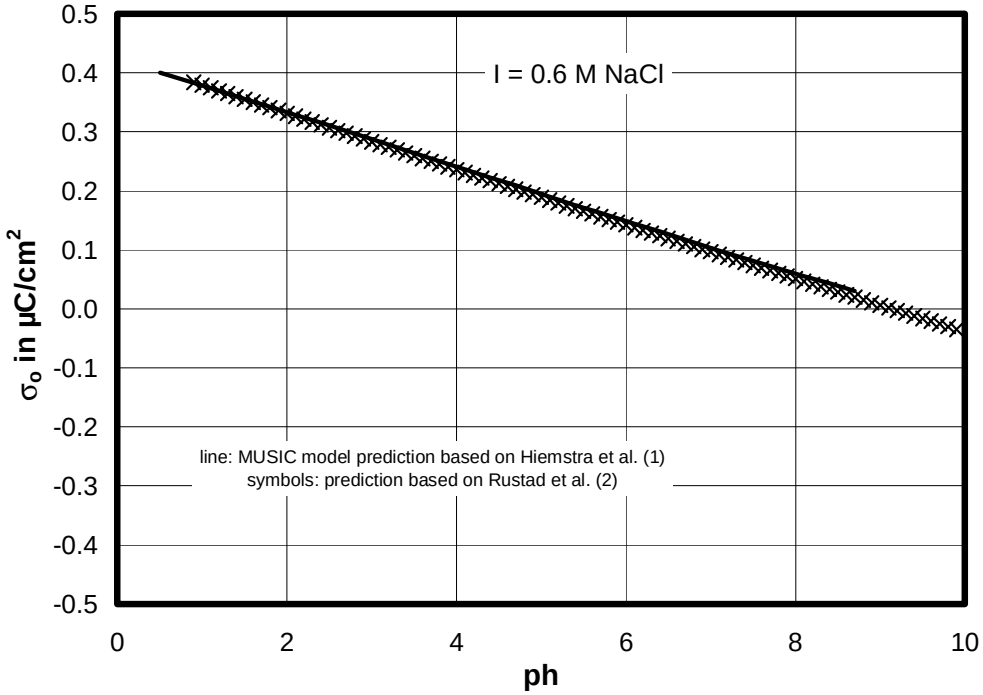

Figure 2: Prediction of goethite surface charge based on two different approaches. ph is the negative logarithm of the free proton concentration.

The descriptions of the adsorption data are usually in good agreement. However, the underlying proton data (i.e. surface charge vs. pH curves) may show differences concerning the goodness of fit. In the description of static batch adsorption experiments this is not crucial since the outcome of interest (i.e. the description of the adsorption curves) is similar. However, concerning dynamic column experiments two situations may be discussed:

- situations where the system is buffered with respect to the pH: here it is expected that models which are equally successful in describing batch experimental data will result in comparable breakthrough curves.
- situations where a pH front moves through the system: in such cases it is expected that the quality of the underlying acid-base model (i.e. the description of surface charge vs. pH curves) will strongly influence the breakthrough curve.

Different surface complexation models have been used to obtain a good model for batch titration and adsorption data sets measured under various conditions.

Using a reactive transport code these models have been applied to the above cases. Results and consequences are discussed.

REFERENCES:

Hiemstra, T., Venema, P., and Van Riemsdijk, W.H. 1996, J. Colloid Interface Sci. *184*, 680. Venema, P., Hiemstra, T., P. G. Weidler, and van Riemsdijk, W.H. 1998. J. Colloid Interface Sci. *198*, 282.

Rustad, J.R., Felmy, A.R., and Hay, B.P. 1996, Geochim. Cosmochim. Acta *60*, 1553. Rustad, J.R., Felmy, A.R. , and Hay, B.P. 1998, Geochim. Cosmochim. Acta *60*, 1563.1996 Felmy, A.R. , and Rustad, J.R.. Geochim. Cosmochim. Acta *62*, 25.

MONTE CARLO SIMULATION OF THE SWELLING BEHAVIOUR OF MX-80 WYOMING MONTMORILLONITE

Artur Meleshyn and Claus Bunnenberg
Center for Radiation Protection and Radioecology (ZSR), University of Hannover,
Herrenhauser Str. 2, 30419 Hannover, Germany;
E-mail: meleshyn@zsr.uni-hannover.de

INTRODUCTION

The excellent sealing properties of bentonites have made them primary candidate materials for backfill purposes and technical barriers in the multibarrier design of radioactive waste repositories in many countries. It is the strong swelling property that provides the unique sealing qualities of bentonite. As the clay hydrates and swells, the path for water flow becomes complex, as the clay platelets intersperse. The very common and most commercially available bentonites are composed primarily of the clay mineral montmorillonite, and it determines crucially the swelling behaviour of bentonite. It is also responsible for its excellent ability to adsorb cationic radionuclides, preventing their dispersion out of the waste disposal site. One of the bentonites, considered for the use in geological disposal facilities, is MX-80 Wyoming bentonite, consisting to 75 mass percents of MX-80 Wyoming montmorillonite. In this work we present results of a Monte Carlo (MC) simulation of the MX-80 Wyoming montmorillonite – water system.

METHODS

Model of the clay mineral

To start MC simulation of the clay mineral-water system, information is necessary about the coordinates of atoms constituting the clay mineral. As these coordinates are not experimentally available, we have used the method of structural modelling for their determination (Smoliar-Zviagina, 1993). On the basis of the unit-cell parameters and of the mineralogical composition this method allows computing atomic coordinates to a precision of 0.01 Å. The unit-cell parameters have been taken from (Tsipursky and Drits, 1984; Mueller-Vonmoos and Kahr, 1983): a=5.16 Å, b=8.98 Å, c=9.6 Å, α=90°, β=99.5°, γ=90°. The unit-cell formula has been derived from suggestions of (Tsipursky and Drits, 1984; Mueller-Vonmoos and Kahr, 1983; Kasbohm et al., 1998) to be:

$$Na_{0.6}\left(Si_{7.9}Al_{0.1}\right)\left(Al_{3.1}Fe^{3+}_{0.4}Mg_{0.5}\right)O_{20}\left(OH\right)_4$$

We have taken 10 unit cells (5 in crystallographic direction *a* and 2 in direction *b*) as a representative portion of a clay mineral layer in our simulation. The resulting simulation box thus occupies a 25.8x17.96 Å^2 patch of basal area and has a *c*-dimension starting from 9.6 Å for the dehydrated state and increasing, depending on the amount of interlayer water.

Three dimensional periodic boundary conditions are applied to the simulation box, in order to model the whole clay mineral, which means that the computational box is surrounded in a space-filling way by replica boxes with identical contents. Although such a procedure results in an infinite stack of infinite clay platelets, it should still have the same swelling and intercalation properties as a real clay mineral. It was shown that the properties of such a relatively small simulation box are still representative of the macroscopic system and are not influenced by artificial long-range symmetry of the imposed periodic lattice (Skipper et al., 1995).

Model of the interactions

Potential energies of interactions in the resulting system of an infinite number of atoms are calculated with help of Eq. (1).

$$U = \sum_{i=1}^{\infty}\sum_{j=1}^{\infty} U_{ij} = \sum_{i=1}^{\infty}\sum_{j=1}^{\infty}\left(U_{ij}^{Coloumb} + U_{ij}^{MCY}\right) = \sum_{i=1}^{\infty}\sum_{j=1}^{\infty}\left(q_i q_j \Big/ \left(4\pi\varepsilon_0 r_{ij}\right) + A_{ij}e^{-B_{ij}r_{ij}} - C_{ij}e^{-D_{ij}r_{ij}}\right) \qquad (1)$$

where the MCY potential model (Matsuoka et al., 1976) is used to represent short-range interactions. The Ewald technique (Ewald, 1921) is used to handle the Coulomb interaction part and the cut-off distance of 9 Å is used to manage calculation of short-range interactions.

Monte Carlo Simulation

A Fortran 90 program of MC simulations in isothermal-constant stress ensemble was written according to the methodology described in (Skipper et al., 1995). A Monte Carlo move in this ensemble consists of either: 1) a change of volume of the simulation box, thus allowing to model clay mineral swelling; or 2) a change of the center of mass coordinates of a randomly selected atom/molecule; or 3) a change of the orientation of a randomly selected molecule. MC moves are organised in cycles, during which a MC move of type 2 or 3 is applied to every interlayer atom/molecule once per cycle on the average. Moves involving a change in volume were attempted once per 5 cycles.

Equilibration in the system was assumed, when the average potential energy and the average layer spacing in the system had reached constant values. This typically took 15,000 MC cycles, which, for example, corresponds to about 1,000,000 Monte Carlo moves for 64 water molecules and 6 Na^+ cations in the interlayer space of the simulation box. The simulation was then allowed to proceed for another 5,000 cycles for data sampling. From these data, average potential energies, average layer spacings, interlayer atomic density profiles and radial distribution functions were calculated.

A series of simulations with different numbers of interlayer water molecules was carried out. A stress of 10^5 Pa normal to the clay mineral layers was applied, and the temperature was fixed at 300 K in all simulations.

RESULTS AND DISCUSSION

Interlayer water structure

To describe the structure of a system consisting of atoms or molecules, the radial distribution function g(r) is commonly used, which gives the probability of finding a pair of atoms a distance r apart, relative to the probability of finding such a pair with distance r for a chaotic distribution of atoms at the same density (Figure 1). The oxygen-oxygen (O-O), hydrogen-oxygen (H-O), and hydrogen-hydrogen (H-H) radial distribution functions obtained in simulation show principal agreement with those for the bulk water obtained from neutron diffraction experiments (Soper et al., 1997). Detailed comparison reveals, that the position of the peaks for the O-O curve did not change, whereas those for the H-O and H-H curves were shifted by about 0.1 Å. The position of the peak of the H-O curve indicates longer hydrogen bonds (1.9 Å) as compared to the bulk liquid (1.8 Å). It is also interesting that interlayer water in contrast to bulk water shows another rather sharp peak at 5.2 Å, which can be contributed to the interlayer cation solvation effects. According to diffraction experiments (Skipper and Neilson, 1989) the first peak in the Na^+-O curve occurs at 2.35 Å, a value perfectly coinciding with that obtained in our simulation (Figure 1).

From the data as given in Fig. 1, coordination numbers can be calculated, which yield information on the hydration state of interlayer atoms. For example, the Na^+-O coordination

number was found to be 2.6 in the montmorillonite, whereas for bulk water, it is 6 (Soper et al. 1997). Basal oxygen atoms can also participate in the hydration of interlayer species. The coordination number of Na^+ with basal oxygen O_b atoms is equal to 0.8, giving a total coordination number $n_{Na\text{-}O,Ob}$=3.4.

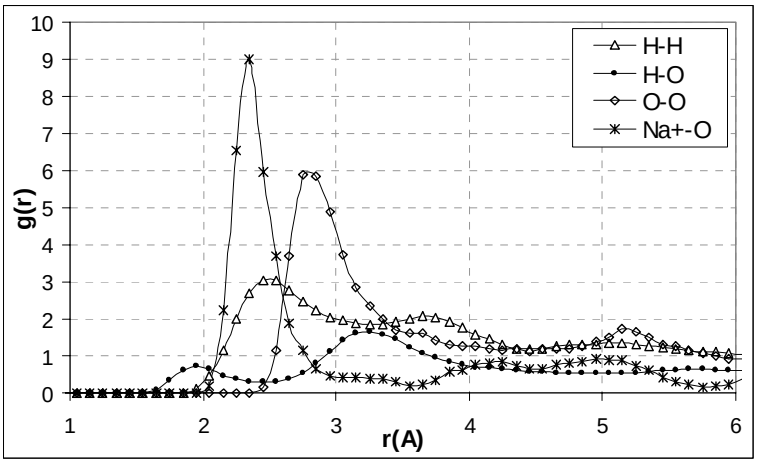

Fig. 1: Radial distribution functions for MX-80 Wyoming montmorillonite. Water content 160 mg/g clay

These findings indicate some differences in the structure of interlayer water and of bulk water, and show that Na^+ cations are not fully hydrated at the given water content. The latter observation is supported also by interlayer density profiles of water atoms as given in Figure 2. This Figure shows the probability g(z) of finding an H or O atom at distance z from one of the clay layer surfaces. It follows that at the given water content, water is concentrated in one single layer in the middle of the interlayer space, whereas the full hydration of interlayer cations would require at least two distinct water layers.

Swelling curve

Figure 3 presents the swelling curve obtained in a series of our simulation experiments with different initial amounts of interlayer water as well as the swelling curves obtained in the experiment of Kraehenbuehl et al. (1987), carried out with different amounts of pre-adsorbed water on MX-80 Wyoming montmorillonite, and in the experiment of Calvet (1973), carried out with a Na-montmorillonite. The swelling behaviour of montmorillonites is characterised by a stepwise change in layer spacing at certain water contents. This behaviour has been successfully simulated in our experiment and the layer spacings obtained in our simulations have values that are very close to those obtained by Calvet (1973). However, there are differences in the values of layer spacing between simulated swelling curve and swelling curve in (Kraehenbuehl et al., 1987), which may be explained by the fact that the MX-80 Wyoming montmorillonite used by obtained by Kraehenbuehl et al. contained 4% Mg^{2+}, 10% Ca^{2+} and 86% Na^+ as exchangeable interlayer cations (Mueller-Vonmoos and Kahr, 1983) compared to a 100% Na^+ content in our simulations.

The experimental layer spacings for a montmorillonite with only Mg^{2+} and Ca^{2+} cations in the interlayer space (Kraehenbuehl et al., 1987) were very similar to those obtained in the experiment with MX-80 Wyoming montmorillonite. Thus, the presence of these cations in the interlayer space of the montmorillonite affects significantly its swelling behaviour and we consider it to be a source of the differences between the experimental and simulated swelling curves.

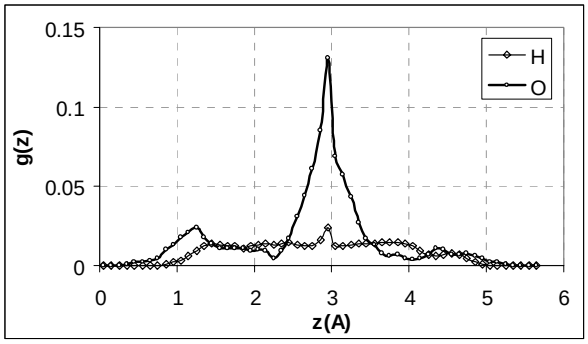

Fig. 2: Interlayer density profiles for MX-80 Wyoming montmorillonite. Water content 160 mg/g clay

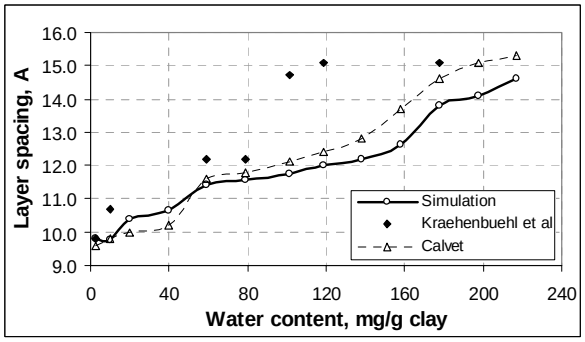

Fig. 3: Experimental and simulated swelling curves.

CONCLUSIONS

The interlayer water structure, hydration characteristics of interlayer cations and the swelling behaviour of MX-80 Wyoming montmorillonite can be reliably simulated with help of the Monte Carlo method. This provides the possibility to also simulate the adsorption of different cationic radionuclides by this clay mineral and thus to predict behaviour of the bentonite-water-cationic radionuclides system. It is also expected that our Monte Carlo approach is capable to additionally simulate the behaviour of the bentonite-water-cationic radionuclides system under the condition of saturated salt solutions in view of the concept of waste repositories in geological salt formations. Further developments are possible, to make predictions about the long-term stability of the adsorption of radionuclides by bentonites in technical barriers.

ACKNOWLEDGEMENTS

This work is supported by the Deutsche Forschungsgemeinschaft (DFG) under project No. BU 420/2.

REFERENCES

Calvet, R. (1973): Hydratation de la montmorillonite et diffusion des cations compensateurs. Ann. Agron. 24, 77-133

Ewald, P. (1921): Die Berechnung optischer und electrostatischer Gitterpotentiale, Ann. Phys. 64, 253-287

Kasbohm, J., Henning K.-H. and Herbert H.-J. (1998): Transmissionelektronenmikroskopische Untersuhungen am Bentonit MX80. Jahrestagung der DTTG, Greifswald, p.228

Kraehenbuehl F., Stoeckli H.F., Brunner F., Kahr G. and Mueller-Vonmoos M. (1987): Study of the water-bentonite system by vapour adsorption, immersion calorimetry and X-Ray techniques: I. Micropore volumes and internal surface areas, following Bubinin's theory. Clay Min. 22, 1-9

Matsuoka, O., Clementi, E. and Yoshimine, M. (1976): CI study of the water dimer potential surface. J. Phys. Chem. 64,1351-1361

Mueller-Vonmoos, M. and Kahr, G. (1983): Mineralogische Untersuchungen von Wyoming Bentonit MX-80 und Montigel. Technischer Bericht 83-12, NAGRA, p.9

Skipper, N.T. and Neilson G.W. (1989): X-Ray and neutron diffraction studies on concentrated aqueous solutions of sodium nitrate and silver nitrate. J. Phys. Condens. Matter 1, 4141-4154

Skipper, N.T., Chang, F.-R.C. and Sposito, G. (1995): Monte Carlo simulation of interlayer molecular structure in swelling clay minerals. 1. Methodology. Clays Clay Miner. 43, 285-293

Smoliar-Zviagina, B.B. (1993): Relationships between structural parameters and chemical composition of micas. Clay Min. 28, 603-624

Soper, A.K., Bruni, F. and Ricci, M.A. (1997): Site-site Pair Correlation Functions of Water from 25 to 400 ^{o}C: Revised Analysis of New and Old Diffraction Data. J. Chem. Phys. 106, 247-254

Tsipursky, S.I. and Drits, V.A. (1984): The distribution of octahedral cations in the 2:1 layers of dioctahedral smectites studied by oblique-texture electron diffraction. Clay Min. 19, 177-193

COLUMN EXPERIMENTS WITH HEAP MATERIAL OF KUPFERSCHIEFER MINING AND THERMODYNAMIC INTERPRETATION

Jens Mibus
Forschungszentrum Rossendorf e.V., P.O. Box 510 119, D-01314 Dresden, Germany
E-mail: J.Mibus@fz-rossendorf.de

INTRODUCTION

Mining dumps and industrial tailings mostly emit toxic substances, thus representing an only hardly calculable hazard for human and environment. The practiced assessment based on total or short-time leachable concentrations (e.g. DEV S4 test in Germany) does barely permit a firm prognosis of the long-term behavior and is discussed controversially at present (Vehlow et al., 2001). Dynamical techniques (column or lysimeter tests) facilitate a better approximation to real conditions like solid/solution ratio, the transport of dissolved or colloidal components and diffusive gas exchange in the vadose zone. Such experiments are indispensable for parameter estimation and verification of reactive transport models at least at laboratory scale.

The following investigations were carried out at the Freiberg University of Mining and Technology and funded by Federal Ministry of Education and Research (02WA9366/1).

MATERIALS AND METHODS

Material of a mine waste dump of Kupferschiefer mining in the south-eastern Harz foreland was investigated. The dump of the shaft "Zirkel-Schacht" is situated about 10 km north of the town of Eisleben and was built up from 1891 to 1927. It consists of a base of mainly carbonatic caprock (Zechsteinkarbonat Ca1) and thereupon deposited low-grade ore. The total volume of the dump is 3.5 million m³, the height is 60 m.

A borehole of 18 m depth was sunken in the low-grade ore. Samples were taken in 2-meter-intervals. One sample of caprock material was taken from the surface. Representative aliquots were air dried, sieved (mesh size 2 mm) and milled < 30 µm. The mineralogical (XRD) and chemical composition (total digestion, ICP-OES) were analyzed.

Laboratory columns (polypropylene, inner diameter 40 mm, length 200 mm) were filled with material of grain size < 10 mm: column 1 to 4 with low-grade ore (allocation of depth cf. table 1) and column 5 with caprock. The material was wetted to the originally measured water content ($\theta \approx 0.05$) and conditioned for two months at 10.0 ± 0.8 °C. After that the columns were unsaturated flown through with MilliQ water at a temperature of 10.0 ± 0.8 °C, applying a Darcy-velocity of $v = 1.8 (\pm 0.1) \cdot 10^{-6}$ m s^{-1}. A recirculation technique of a total volume of 150 ml was applied over a time period of 64 days. This part of experiment, percolation, is indicated with "P" furthermore. Equilibrium experiments were carried out with 50 g solid in 25 ml MilliQ over 90 days in closed bottles (equilibrium experiment indicated with "E").

Samples of 2 ml were taken at the columns outflow beginning after 0.5 d with steady doubling of time distance up to 64 days (additional samples at 12 and 24 days) and immediately replaced with aliquot volumes of MilliQ in the reservoir. pH and dissolved oxygen were measured with combination electrodes, alkalinity by acid capacity titration (standard deviation s = 5 %), concentrations of chloride, sulfate (IC, s = 15 and 20 % respectively), Mg, Ca, Mn, Zn (ICP-MS, s = 5 %), and Cu, Cd, Pb (ICP-MS, s = 10 %).

Geochemical modeling was done using the speciation code EQ3/6 (Wolery, 1992). The data base "HMW" from Harvie et al. (1984) extended by data for heavy metals (from different sources, documented in Mibus, 2001) was utilized.

RESULTS AND DISCUSSION

Composition of solids: The mineralogical composition over the profile is shown in table 1. The rock matrix consists of about 50 % silicate phases, less than 50 % carbonates and gypsum, few percent of residual sulfides (mainly pyrite FeS_2 and sphalerite ZnS), and a small amount of the crystalline secondary phase cerussite ($PbCO_3$). An elution of the karstifyable material by infiltrating water occurs in the upper part of the profile (0 to 4 m) where the more resistant silicates are enriched. Moreover the dissolution of dolomite proceeds faster than that of calcite inducing a calcite/dolomite ratio increasing with depth. In karst hydrogeology this phenomenon is known as dedolomitization (Bischoff et al., 1994). In calcium rich pore waters (due to gypsum dissolution) dolomite dissolves incongruently precipitating calcite. Magnesium and sulfate become enriched in solution.

Table 1. Mineralogical composition in a vertical profile of low-grade ore and a sample of caprock material from mining dump Zirkel-Schacht (in wt.-%), grain size < 2 mm

depth [m]	quartz	muscovite	albite	calcite	dolomite	gypsum	pyrite	sphalerite	galena	cerussite	column
0 - 2	26,9	37,8	8,3	16,5	6,0	1,4	0,5	0,8	< 0,5	1,2	1
2 - 4	21,3	34,3	4,5	20,8	12,5	3,4	< 0,5	1,5	< 0,5	1,0	
4 - 6	18,7	29,1	4,4	21,5	14,4	7,7	< 0,5	2,1	< 0,5	1,1	2
6 - 8	17,9	29,2	5,7	19,9	13,5	8,5	0,7	2,5	0,6	1,3	
8 - 10	20,3	28,6	5,5	19,7	16,1	6,1	1,1	1,4	< 0,5	1,0	3
10 - 12	18,5	29,2	5,7	22,9	12,3	7,0	1,0	1,9	< 0,5	1,2	
12 - 14	18,6	29,0	4,9	21,4	14,7	7,4	1,2	1,4	< 0,5	0,8	4
14 - 16	18,7	29,9	5,3	23,6	12,4	6,1	1,3	1,7	< 0,5	0,8	
16 - 18	17,6	31,5	6,3	21,1	12,2	6,2	1,8	1,8	< 0,5	1,0	
caprock	19,5	35,1	5,7	27,8	8,7	2,6	< 0,5	< 0,5	< 0,5	< 0,5	5

Beside the above mentioned cerussite there exist other secondary minerals that are not detectable in the whole rock sample: X-ray amorphous phases like ferrihydrite ($Fe_2O_3 \cdot nH_2O$) and $Zn(OH)_2$(amorph) or small amounts of basic copper sulfate (brochantite $Cu_4SO_4(OH)_6$).

Column experiments: The circulating waters are of neutral to weak alkaline and oxygenated character. Selected concentration-time-curves at the outflow are shown in figure 1. There are significant differences between the solution in contact with low-grade ore (column 1 to 3; also 4, but not shown) and that with carbonatic caprock (column 5) in pH and concentration of HCO_3^-, but also heavy metals (e.g. zinc) due to mineralogical and geochemical composition

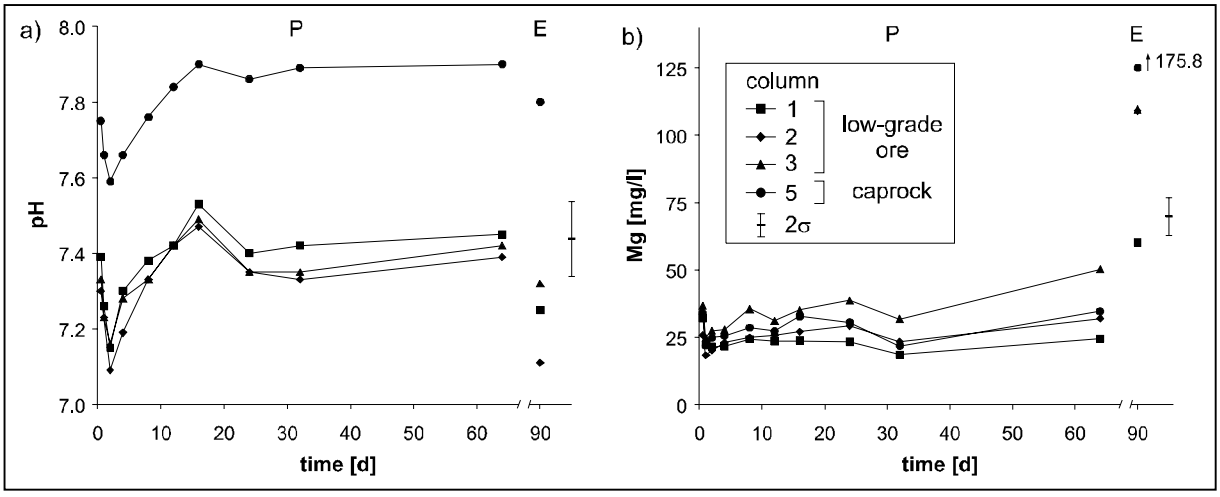

Figure 1. pH and Mg concentration as function of time in percolation (P) and equilibrium (E) experiment

The time development of pH is characterized by three stages:

- decrease of pH until t = 2 days
- steep increase until t = 16 days
- slight decrease and equilibration

The initial decrease traces back to displacement of equilibrated pore waters, the following increase by carbonate dissolution. The striking transient pH-maximum at t = 16 d suggests a temporary oversaturation by decomposition of a metastable phase.

The concentration of HCO_3^- developed similarly to pH. Calcium and sulfate concentration (not shown) are only little variably over total experimental time due to gypsum equilibrium, thus providing a nearly constant ionic strength in solution of about $7 \cdot 10^{-2}$ molal. Magnesium concentration, in contrast, continuously increases with time not attaining a steady state within percolation time. The mole fraction of magnesium in solution is thus increasing from 0.09 after 24 hours to 0.13 after full percolation time of 64 days and 0.26 in equilibrium experiment. In connection with the found mineralogical peculiarities the development of the Ca/Mg-ratio in solution and the transient maximum of pH (and HCO_3^- concentration) are attributed to the dedolomitization reaction.

The theoretical description and graphical representation of the solubility of binary solid phase systems in aqueous solution is possible based on the total solubility product ΣΠ according to Lippmann (1980). For the system $CaCO_3$-$MgCO_3$-H_2O applies:

$$\Sigma\Pi = a_{Ca^{2+}} \cdot a_{CO_3^{2-}} + a_{Mg^{2+}} \cdot a_{CO_3^{2-}}$$

where a_{Ca2+} denotes activity of Ca^{2+} in solution etc. Figure 2 presents the solubility of the system mentioned above. The soluti of calcite, magnesite and dolomite are calculated as follows (Lippmann, 1980): $\Sigma\Pi_{calcite} = K_{calcite}/(1-X_{l,Mg})$, $\Sigma\Pi_{magnesite} = K_{magnesite}/X_{l,Mg}$, and $\Sigma\Pi_{dolomite} = (K_{dolomite}/((1-X_{l,Mg})\cdot X_{l,Mg})))^{1/2}$ where K is the solubility product of the respective mineral phase taken from Harvie et al. (1984) and $X_{l,Mg}$ is the mole fraction of magnesium in solution. In this diagram the development of solution composition (ion activity product, IAP) in column 3 (P) and respective equilibrium experiment (E) is plotted (circle symbols) neglecting the initial phase of pore water displacement.

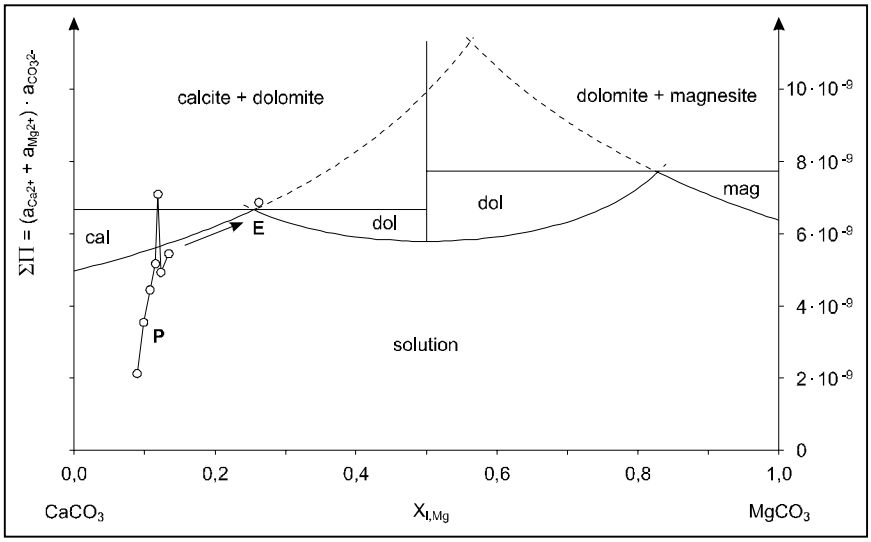

Figure 2. Development of solution composition (IAP) in the Lippmann diagram (column 3)

The IAP coming from the solution field converges the solutus of calcite to exceed it, i.e. solution is oversaturated with calcite. This induces calcite precipitation thus depleting the degree of oversaturation. The draw back below the solutus is not completely clarified, but unfortunately there was a refill of evaporation loss some days before. In equilibrium experiment (E) the IAP nearly meets the triple point where calcite, dolomite and solution are stable. The mole fraction of magnesium in solution continuously increases. The composition of the solid carbonates changes to the more stable calcite at least in the outer lattice planes that are available to heterogeneous reactions.

Saturation of minerals and the gas phase: From the calculation of saturation indices from solution composition (inverse modeling) it is to be seen, that the ion concentrations are controlled mostly by solid phase equilibria.

First, the main components are discussed. Equilibrium to gypsum and calcite is attained in all low-grade ore columns after end of percolation test, whereas equilibrium to dolomite is reached only in equilibrium test (cf. fig. 2). In column 5 (caprock) the equilibrium to gypsum is attained only in equilibrium test. Even tough few percent of gypsum are contained in the caprock (cf. table 1), there is no equilibrium with this solid in the column. The existence of preferred flow paths in the porous media might be the reason for this phenomenon. Gypsum, enriched in finer grains, is contacted only limited by the fluid, moving in wide pore canals.

Mineral equilibria to secondary heavy metal compounds are also calculated. In all solutions from low-grade ore (P and E) the solubilities of lead and zinc are limited by cerussite ($PbCO_3$) and ε-$Zn(OH)_2$ respectively, whereas smithsonite ($ZnCO_3$) is clearly oversaturated. This agrees with the found mineralogical composition. In contrast, in the carbonatic caprock zinc solubility is controlled by smithsonite equilibrium. According to solution chemical and spectroscopic investigations from Temmam et al. (2000) Zn^{2+} may isomorphic substitute Ca^{2+} in the (1014)-plane of the calcite lattice. Due to higher calcite content and lower zinc concentration in the caprock, this immobilization mechanism seems to be proximate.

The results of inverse modeling indicate a pCO_2 of 10^{-3} (P) to $10^{-2.5}$ (E). There is only limited gas exchange with the atmosphere, in particular in the closed bottles.

CONCLUSIONS

The investigated processes of water rock interaction are mostly dominated by mineral equilibria, which exhibit different adjustment times. The calcite and dolomite equilibrium determines the development of alkalinity with typical temporary oversaturation. Such complicated reaction paths are usually not identified by "crude" batch experiments.

The formation of preferred flow paths may even affect the solution composition in particular cases. In these experiments an estimation of transport parameters was not yet carried out, but is planned for the future to apply reactive transport codes for modeling these processes.

REFERENCES

Bischoff, J.L., Juliá, R., Shanks, W.C, Rosenbauer R.J. (1994): Karstification without carbonic acid: Bedrock dissolution by gypsum-driven dedolomitization. Geology 22, 995-998

Harvie, C.E., Møller, N., Weare, J.H. (1984): The prediction of mineral solubilities in natural waters: the Na-K-Mg-Ca-H-Cl-SO_4-OH-HCO_3-CO_3-CO_2-H_2O system to high ionic strengths at 25 °C. Geochim. Cosmochim. Acta 48, 723-751

Lippmann, F. (1980): Phase diagrams depicting aqueous solubility of binary mineral systems. N. Jb. Miner. Abh. 139, 1-25

Mibus, J. (2001): *Geochemische Prozesse in Halden des Kupferschieferbergbaus im südöstlichen Harzvorland.* Ph.D. thesis, Freiberg University of Mining and Technology

Temmam, M., Paquette, J., Vali, H. (2000): Mn and Zn incorporation into calcite as a function of chloride aqueous concentration. Geochim. Cosmochim. Acta 64, 2417-2430

Vehlow, J., Bergfeldt, B., Geisert, H. (2001): Wechselwirkung zwischen Wasser und Reststoffen der Abfallverbrennung. Nachrichten - Forschungszentrum Karlsruhe 33, 31-39

Wolery, T.J. (1992): EQ3/6, a software package for geochemical modelling of aqueous systems: package overview and installation guide. LLNL, Livermore

MODELING STRONTIUM SORPTION IN NATURAL AND PURIFIED BENTONITE CLAY

Mireia Molera, Trygve Eriksen and Susanna Wold

Royal Institute of Technology, Department of Chemistry, Nuclear Chemistry
SE-100 44 Stockholm, Sweden; E-mail: molera@nuchem.kth.se

ABSTRACT

To understand the effects of pH and composition of the solutions used to equilibrate untreated bentonite in feasibility studies, the sorption behavior of strontium (II) on a purified bentonite has been investigated and the results compared with those for sorption onto natural bentonite. Batch sorption experiments were performed at different $NaClO_4$ concentrations, pH range 2-10 and 10^{-5} Sr^{2+} mol/dm^3.

The resulting data are modeled by considering ion exchange and surface complexation processes. Ion exchange constants and surface complexation constants are determined in terms of 1-site structural-charge surface sites (X-layer sites) and 2-site variable-charge surface sites (edge OH groups) model using the PHREEQC code.

Sorption of strontium (II) shows pH dependence with edges at pH > 7, an inverse relation of the sorption with ionic strength and significantly higher sorption for the purified bentonite at ionic strength ≤ 0.1 M. At high ionic strength strontium (II) sorption is not affected by the impurities. At low ionic strength, the effect of the cationic inventory of natural bentonite becomes important and the modeling predicts lower sorption for the natural bentonite as found experimentally.

INTRODUCTION

Bentonite clay has low permeability, swelling capability and excellent sorption potential for cationic radionuclides (Pusch et al., 1999). However, the sorptive capabilities are very much dependent on the prevailing conditions and a further understanding of the surface chemical properties of montmorillonite, the major component in bentonite, in near-neutral and alkali media is essential for establishing a chemical model for the bentonite/water interaction applicable for repository conditions (Pusch et al., 1999; Eriksen et al., 1999; Muurinen, 1994; Melamed and Pitkänen, 1994).

Sorption of strontium on bentonite has been widely studied (Carroll et al., 2001; Chen et al., 1998; Poinssot et al., 1999) because of the potential for migration away from waste disposal and nuclear test sites into the accessible environment. Strontium retardation at low pH is assumed to take place entirely by cation exchange with the permanent-charge sites on the interlayer basal planes and less-abundant sites on the external surface, depending on solutions conditions. At high pH, strontium also sorbs at surface-hydroxyl sites at the clay edges where the crystal structure is interrupted. Assuming the major sorption processes to be ion exchange and surface complexation (Chen et al., 1998), the mean distance between the charged clay surface and a cation is expected to be strongly influenced by the charge (II) and ionic radius (1.18 Å) and thereby by hydration radius ($r_{Sr^{2+}\ (aq)}$ ~ 2.74 Å). Surface complexation is expected to be correlated to the stability of the first hydrolysis complex, $Sr^{2+} + OH^- = SrOH^+$, log K= 0.86.

Migration studies on bentonite are normally carried out with natural bentonites having an inventory of exchangeable cations and also impurities, such as $CaCO_3$ and $CaSO_4$ (Melamed and Pitkänen, 1994). To understand the effects of pH and composition of the solutions used to

equilibrate untreated bentonite in feasibility studies, the sorption of Sr on natural and purified Wyoming bentonite was experimentally studied at different $NaClO_4$ concentrations and pH.

EXPERIMENTAL

Purified Na-montmorillonite was prepared from commercial American Colloid Co. type MX-80 (Wyoming Na-bentonite). The bentonite MX-80 has a clay content (< 2 μm) of approximately 85% and a montmorillonite content of 80-90 wt % of this fraction. The remaining silt fraction contains quartz, feldspar and some micas, sulfides and oxides (Pusch et al., 1999). The mineralogical and chemical characterization of the MX-80 Wyoming bentonite, is shown in Table 1.

The major part of the accessory minerals was removed using the procedure given by Wieland et al. (1994). The solutions were prepared from analytical grade chemicals and Millipore deionized water. $HClO_4$ and NaOH 0.1 M were used to adjust the pH. ^{85}Sr was purchased from DuPont Scandinavia as strontium chloride in aqueous solution.

Table 1 Data for MX-80 and purified MX-80 (Wieland et al., 1994)

Parameter	Natural MX-80	Purified MX-80
Cation-exchange capacity, $[X]_T$	0.75 meq g^{-1}	0.85 meq g^{-1}
Amphoteric edge sites $[SOH]_T$	28.4 μmol g^{-1}	28.4 μmol g^{-1}
Edge surface area	3.0 m^2 g^{-1}	3.0 m^2 g^{-1}
Exchangeable Na	80.8 %	100 %
Exchangeable Ca	12.8 %	
Exchangeable Mg	5.5 %	
Exchangeable K	0.9 %	
Total carbonate (as $CaCO_3$)	1.5 wt %	
Total quartz	≈ 23 wt %	≈ 15 wt %
$CaSO_4$ impurity	0.58 wt %	
$MgSO_4$ impurity	0.02 wt %	
NaCl impurity	0.01 wt %	0.01 wt %
KCl impurity	0.01 wt %	
Specific density	2700 kg m^{-3}	2700 kg m^{-3}

Sorption was measured in batch experiments with 0.1 g bentonite and 20 cm^3 1 to10^{-2} M $NaClO_4$ and 10^{-5} M ^{85}Sr radionuclide spiked solution in the pH-range 2 - 10. The clay suspensions were centrifuged at 6000 rpm and solution samples analyzed by γ-counting using a germanium detector and multichannel analyzer. The distribution coefficients are calculated using the relation $K_d = ((C_i - C_e) / C_e)$ V/m where C_i, C_e denote initial and equilibrium concentrations in solution and V/m solution-to-mass ratio.

MODELING

A two-site surface complexation model including cation exchange was developed with PHREEQC code (Parkhurst, 1995) using the database *Wateq4f.dat*. The experimental results of the interaction between natural MX-80 Wyoming bentonite and purified bentonite with $NaClO_4$ solutions at different ionic strength under aerobic conditions are interpreted with the following assumptions:

(1) Initial equilibration of the natural bentonite with spiked solutions changes the concentration of the solution. pH increases because of the dissolution of calcite in natural bentonite and the ion exchange reaction.

$2\ Na\text{-}X + CaCO_3 + H_2O \leftrightarrow CaX_2 + 2\ Na^+ + HCO_3^- + OH^-$

$CaCO3(s) + H^+ \leftrightarrow Ca^{2+} + HCO_3^-$ where X is an ion-exchange site of montmorillonite.

(2) Formation of the following aqueous complexes at neutral-alkali pH has been considered: $MgOH^+$, $NaCO_3^-$, $CaCO_3$, $MgCO_3$, HCO_3^-, $NaHCO_3$, $CaHCO_3^+$, $MgHCO_3^+$, $MgOH^+$, $CaOH^+$, $SrOH^+$, $Ca(OH)_2$, $Mg(OH)_2$, $Sr(OH)_2$, $SrCO_3$, $SrSO_4$.

(3) Precipitation of the following solids has been considered: $Mg(OH)_{2\,(s)}$, $Ca(OH)_{2\,(s)}$, $Sr(OH)_{2\,(s)}$.

(4) Fitting of the data is based on the surface chemical equilibrium reactions in Table 2 as well as the parameters in Table 1.

Table 2. Surface chemical reactions and equilibrium constants for montmorillonite (Wieland et al., 1994). (SOH accounts for strong surface sites and WOH for weak surface sites. X^- represents ion exchange sites).

Reaction	log K
$SOH + H^+ = SOH_2^+$	5.4
$SOH = SO^- + H^+$	- 6.7
$WOH + H^+ = WOH_2^+$	4.5
$WOH = WO^- + H^+$	- 7.9
$Na^+ + X^- = NaX$	20.00
$K^+ + X^- = KX$	20.26
$Mg^{2+} + 2\ X^- = MgX_2$	40.17
$Ca^{2+} + 2\ X^- = CaX_2$	40.21

RESULTS AND DISCUSSION

Sorption data for Sr^{2+} on natural and purified bentonite at different supporting electrolyte concentration and pH are plotted in Figure 1. Sorption varies with the Na^+ concentration of the supporting electrolyte, is strongly dependent on the Ca^{2+} concentration in the solution and displays a sorption edge at pH > 7.

The dominating sorption mechanism for Sr^{2+} is a combination of ion exchange and outer sphere complexation (Carroll et al., 2001; Chen et al., 1998). The increase in Sr^{2+} sorption at pH > 7 is caused by surface complexation. Based on the bentonite data given in Table 1 and Table 2 the Sr^{2+} data in the pH range 2 to 10 for 0.01 to 1 M supporting electrolyte can be fairy well fitted (Figure 2) by the reactions and equilibrium constants for strontium given in Table 3.

Despite uncertainties in the amount of soluble impurities in the bentonite, the model describes successfully the experimental data. The Sr^{2+} sorption by cation exchange is influenced by the concentration of the supporting electrolyte and therefore in direct competition with Ca^{2+} and Mg^{2+}. This can be seen when comparing Figure 2(a) and (b).

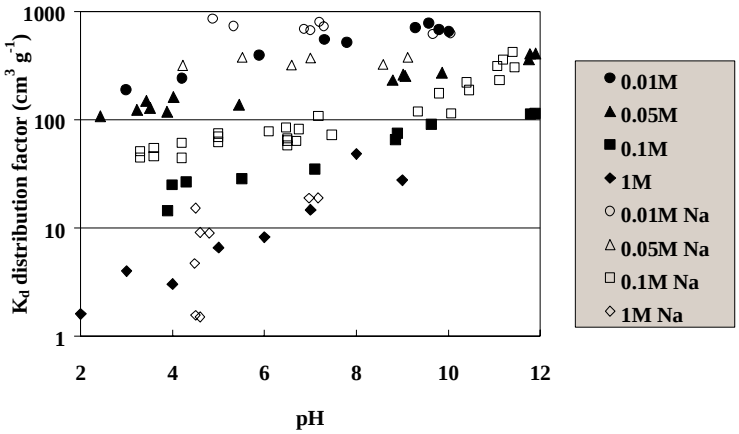

Figure 1. Sr^{2+} sorption data on natural and purified bentonite. pH effect at different ionic strength, full symbols are for data on natural bentonite and empty symbols for purified bentonite.

Table 3. Reactions and equilibrium constants used in the modeling.

Reactions	log *K*
$H^+ + X^- = HX$	21.0
$Sr^{2+} + 2\ X^- = SrX_2$	42.1
$SOH + Sr^{2+} = SOSr^+ + H^+$	6.0
$SOH + SrOH^+ = SOSrOH + H^+$	-5.0
$WOH + Sr^{2+} = WOSr^+ + H^+$	-5.5
$WOH + SrOH^+ = WOSrOH + H^+$	-9.2

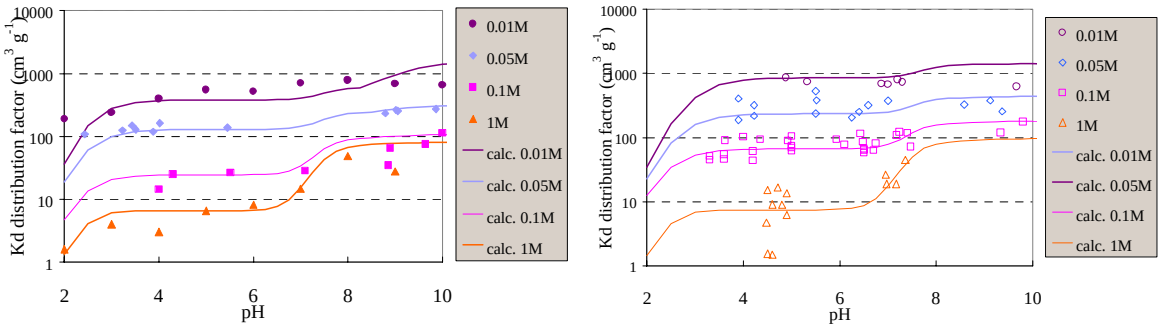

Figure 2. Experimental and calculated data for Sr sorption on MX-80. (a) Sr sorption on natural bentonite. (b) Sr sorption on purified bentonite.

Sr^{2+} sorbs much more strongly on bentonite in the absence of impurities at $I \leq 0.1$ M. At high pH the calcite ($CaCO_{3\,(s)}$) found in natural bentonite may not dissolve, and therefore Sr^{2+} is no longer in competition with Ca^{2+} but with Na^+ and displays similar Kd values with natural and purified bentonite. Deprotonation of the surface sites (SiOH/AlOH/MgOH represented as SOH or WOH, for strong or weak sites) takes place when pH increases. As can be seen at low ionic strength or in purified bentonite, there is a first sorption edge at pH around 4, due to the weak surface sites.

At high Na^+ concentrations (≥ 1 M), Na^+ can even to some extent replace Ca^{2+} on the permanently charged surface sites ($CaX_2 + 2Na^+_{(excess)} = 2NaX + Ca^{2+}$), and again similar Kd values with natural and purified bentonite are found.

CONCLUSIONS

A chemical model for the clay/electrolyte interactions, which simulates simultaneously: ion exchange, hydrolysis of clay edges and surface complexation is presented for strontium sorption on bentonite. The model can explain the sorption on natural bentonite, accounting for the amount of inventory phases competing with strontium, and on purified bentonite, where all the impurities have been depleted.

REFERENCES

Carroll, S., Roberts, S. and O'Day, P. (2001): Strontium sorption to mineral surfaces: A discussion of the importance of surface charge for outer-sphere sorption. Abstr. Pap. - Am. Chem. Soc. (2001) 221st GEOC-081.

Chen, C. C., Papelis, C. and Hayes, K. F. (1998): Extended x-ray absorption fine structure (EXAFS) analysis of aqueous SrII ion sorption at clay-water interfaces. Adsorpt. Met. Geomedia, 333-348.

Eriksen, T., Jansson, M. and Molera, M. (1999): Sorption effects on cation diffusion in compacted bentonite. Eng. Geology 54, 231-236.

Melamed, A. and Pitkänen, P. (1994): Water-Compacted Na-Bentonites interaction in simulated nuclear fuel disposal conditions: The Role of Accessory Minerals. Mater. Res. Soc. Symp. Proc. 333 (Scientific Basis for Nuclear Waste Management XVII), 919-924.

Muurinen, A. (1994): Diffusion of anions and cations in compacted sodium bentonite. Espoo, Technical Centre of Finland, VTT Publication No 168.

Parkhurst,D. L.(1995): User's guide to PHREEQC - a computer program for speciation, reaction-path, advective-transport, and inverse geochemical calculations. USGS/WRIR-95-4227: Water-resources investigations report 95-4227. 143 pp.

Poinssot, C., Baeyens, B. and Bradbury, M. H., (1999): Experimental studies of Cs, Sr, Ni, and Eu sorption on Na-illite and the modelling of Cs sorption. PSI-report 99-06.

Pusch, R., Muurinen, A., Lehikoinen, J., Bors, J. and Eriksen, T. (1999): Microstructural and Chemical Parameters of Bentonite as Determinants of Waste Isolation Efficiency. European Commission, Nuclear Science and Technology, Final Report, Contract No FI4W-CT95-0012, EUR 18950 EN.

Wieland, E., Wanner, H., Albinsson, Y., Wersin, P. and Karnland, O. (1994): A surface chemical model of the bentonite/water interface and its implications for modelling the near field chemistry in a repository for spent fuel. SKB Technical Report 94/26.

MODELLING OF LEAD MOBILITY BY COUPLING TRANSPORT AND CHEMICAL PROCESSES

H. C. Moog, D. Buhmann, T. Kühle and S. Hagemann

Gesellschaft für Anlagen- und Reaktorsicherheit mbH, Theodor-Heuss-Str. 10, 38122 Braunschweig, Germany; E-mail: moo@grs.de

Depending on the solution composition lead exhibits solubilities which differ by orders of magnitude. Assuming a non-variable element-specific solubility for lead may therefore lead to erroneous source terms in codes for the calculation of the probable outflow of lead from underground repositories.

We set up to couple an already existing code from GRS for the modelling of nuclide mobility in the near field of underground repositories with a geochemical code, which calculates mineral-solution equilibria. Thermodynamic calculations are performed on the basis of minimizing the global Gibbs Free Energy of the system. Activity coefficients of dissolved species are calculated utilizing the Pitzer formalism. Each run starts off with the total elemental composition of aqueous and solid phases. It returns the new equilibrium composition in terms of concentrations of aqueous phase constituents and discrete mineral phases.

The existing database accounts for solutions of the seawater system and lead. It will be extended for further elements of interest, such as I, Se, and Fe.

To check the performance of the new program a model was set up for a simple underground repository, which consists of three segments: a single disposal chamber for lead-containing hazardous waste, a drift filled up with brown coal fly ash, and a third one filled with rock salt. At the beginning, the disposal containing chamber is flooded with salt solution and lead is mobilized. In each segment lead solubility is calculated and, depending on the actual solution composition, defined masses of lead-containing mineral phases are formed accordingly.

The presentation gives an account about model results and the differences which turn up in comparison to calculations where non-variable element-specific solubility is assumed.

RADIONUCLIDE TRANSPORT AND SORPTION IN HETEROGENEOUS MEDIA FOR PERFORMANCE ASSESSMENT STUDIES

Ulrich Noseck and Eckhard Fein
Gesellschaft für Anlagen- und Reaktorsicherheit (GRS) mbH
Theodor-Heuss-Straße 4, 38 122 Braunschweig, Germany; E-mail: nos@grs.de

INTRODUCTION

Licensing of a nuclear waste repository in geological formations requires the demonstration of the post-closure safety of the facility. This involves the extensive use of models to assess the potential evolution of the system with respect to the behaviour of the waste, release of radionuclides, and their migration through the geosphere and the uptake by man. Hence, detailed understanding of the groundwater flow and the associated transport of radionuclides is required. For that large three-dimensional areas and long time periods have to be considered. From these requirements the numerical code d3f (distributed density-driven flow) to model density-driven flow through porous media was developed (Fein et al., 1999).
In a next step the development of a transport code was initiated with the intention to enable the model to predict besides advective, dispersive and diffusive transport all important retention effects for the pollutants (Fein et al., 2001). On that behalf the new computer code comprises linear as well as non-linear element-specific adsorption, i.e. Henry isotherms, and Langmuir or Freundlich isotherms, respectively. Equilibrium or kinetically controlled adsorption can be modelled. Precipitation processes are modelled by element-specific solubility limits. To take into account the effect of complexation the influence of agents like EDTA on Henry isotherms and solubility limits can be considered. Furthermore, pollutants may migrate into regions with immobile porewater where they are adsorbed onto the matrix material. Besides that the code comprises a module to model speciation coupled to transport processes.

APPLICATION

Up to now long-term safety analyses are performed using at best three-dimensional groundwater simulations but the transport and the retention of radionuclides through the geosphere is usually modelled one-dimensionally. The new transport code is developed to especially perform large three-dimensional areas. Currently the code is in the state of comprehensive testing. In this period the main emphasis is laid on two-dimensional test cases.

The following generic test case describes a density-driven flow pattern. It consists of two very highly conductive aquifers above a salt dome. The lower aquifer communicates with the upper through a window in the separating stratum of low permeability.

In the upper part of Fig. 1 the modelled region, its boundary conditions and the permeabilities are depicted. As is shown in the figure the inflow boundary is the upper right edge and the outflow boundary is the upper left edge. The top of the model is established as recharge area. All other boundaries are impermeable. Due to pressure distribution a flow from the inflow to the outflow boundary is induced. The bottom diagram of Fig. 1 shows the velocity field of the density-driven flow together with the salt concentration distribution

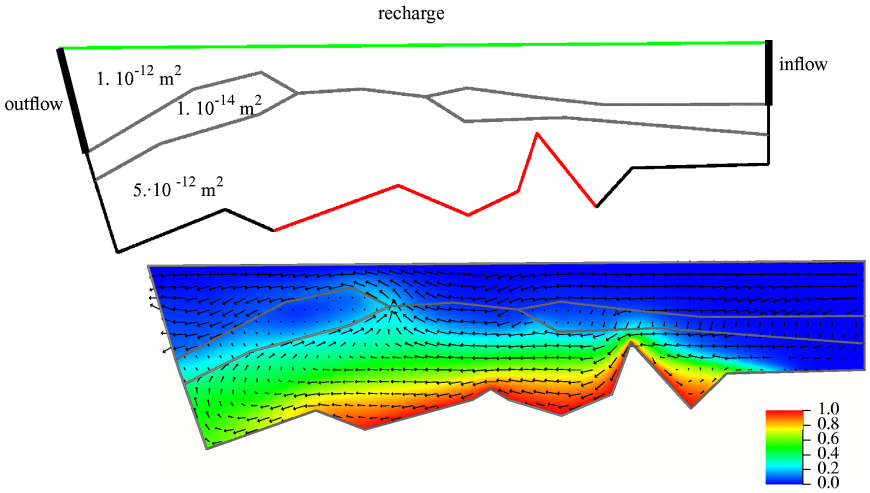

Figure 1 Modelled region and boundary conditions (top) and density-driven flow field and salt concentration distribution (bottom)

Transport calculations are performed based on a typical scenario for a radioactive waste repository in a salt formation (Brenner et al., 2000). In the considered repository concept 25000 t_{hm} (tons of heavy metal) spent fuel are disposed of in Pollux casks in five separated emplacement sections. The radionuclide flux from the repository has been calculated for a brine intrusion scenario, where it is assumed that in the surroundings of each emplacement section brine inclusions with a volume of 225 m^3 are located and brine additionally intrudes via an anhydrite vein. The radionuclide flux from the central field of the repository calculated for this case is used as radionuclide source for the transport in the far field.

Heterogeneity in the modelled area is also assumed by different sorption properties of the stratigraphic layers. Results for the transport behaviour of the radionuclide spectrum for different test cases will be presented.

CONCLUDING REMARKS

This examples illustrates the ability of the new computer code to model transport and sorption in heterogeneous media. After finishing the code development and after passing the needed tests it will become feasible to perform more realistic calculations of dilution and non-linear sorption in large and heterogeneous media even for extremely long time scales as it is required for PA. It is also intended to show first results for transport coupled with speciation.

ACKNOWLEDGEMENTS

The development of the program suite to model transport and retention of radionuclides through porous media is funded by the German Federal Ministry of Economics and Technology (BMWi) under the contract number 02 E 9148 and is still under way.
Under the overall control of GRS a team of members from four university institutes perform this development which is still in progress. The following working groups are involved: Prof. W. Kinzelbach, ETH Zürich, Prof. D. Kröner, Universität Freiburg, Prof. M. Rumpf, Universität Duisburg, Prof. G. Wittum, Universität Heidelberg.

REFERENCES

Brenner, J.; Buhmann, D.; Kühle, T.: Einfluß netzwerkartiger Strukturen der Grubenhohlräume auf die Langzeitsicherheit eines Endlagers im Salinar. Gesellschaft für Anlagen- und Reaktorsicherheit (GRS) mbH, GRS-163, Braunschweig, März 2000.

Fein, E.; Schneider, A. (eds.): d^3f - Ein Programmpaket zur Modellierung von Dichteströmungen. Gesellschaft für Anlagen- und Reaktorsicherheit (GRS) mbH, GRS-139, ISBN 3-923875-97-5, Braunschweig, 1999.

Fein, E.; Noseck, U.; Kühle, T.: Recent Developments in the Modelling of Transport and retention of Radionuclides in porous Media. 8^{th} International Conference Migration 2001, Bregenz, Austria, September 16-21, 2001.

MODELLING CEMENT-ROCK-WATER INTERACTIONS – THE INFLUENCE OF SELECTED BOUNDARY CONDITIONS

Wilfried Pfingsten
Waste Management Laboratory, Paul Scherrer Institut,
CH-5232 Villigen PSI, Switzerland; E-mail: wilfried.pfingsten@psi.ch

Repositories for low and intermediate level nuclear waste contain large amounts of cementitious material. Due to the steep geochemical gradients between the cementitious repository and the host rock, a variety of chemical reactions will occur: degradation of the cement by formation water, formation of secondary minerals and related changes of porosity and hydraulic conductivity, as well as temporal changes of mineral sorption properties for radionuclides in the near- and far-field of the repository. Many laboratory investigations focus on the cement-host-rock interaction in one-dimensional (column) experiments. Depending on the chemical composition of the water used for degrading the cement, experimental results range from clogging the one-dimensional system (mainly under CO_2 conditions due to calcite precipitation) to increased transport through the cement samples (Reardon, 1992; Bateman, Coombs et al., 1998; Pfingsten and Shiotsuki, 1998; Jakob, Sarott et al., 1999). The majority of these experiments have been modelled successfully by sophisticated one-dimensional reactive transport models and the major geochemical and transport processes have been identified. As, for example, the degradation of cement paste by deionised water in a one-dimensional set-up, where dissolution and accompanied increase of porosity and hydraulic conductivity of the sample was described successfully by coupling hydraulic, transport and chemical processes (Pfingsten and Shiotsuki, 1998). Latter shows that one-dimensional experiments and their modelling, as well as the calculation of complex reactions at the cement-host-rock interface, showed a coupling between geochemical reactions and transport parameters, e.g. the dependency of the effective diffusion coefficient or hydraulic conductivity on porosity produced by dissolution, which can be investigated in simple one-dimensional systems, too.

However, it might be inappropriate just using such one-dimensional model approaches to describe the long-term behaviour of a complex geochemical reactive, heterogeneous near-field of a cementitious repository. These one-dimensional approaches may be applicable to describe column experiments of simple geometry – a first step, in addition to batch experiments, to gain dynamic system and process understanding. A lot of approaches deal with simple boundary conditions, stimulated by well defined laboratory experiments in order to achieve or investigate individual process understanding, or, if modelling is concerned, simply by limited computer resources. However, when transferring these results to real near-field conditions, dimension, geometry, heterogeneity and boundary conditions on field-scale have to be considered carefully. The following one-dimensional modelling example shows, how the time scale and / or the general behaviour of a cement-host-rock water interaction may change due to an obviously small change of a system set-up. For the model domain, shown in Fig. 1, it is assumed that diffusion, induced by strong chemical gradients between the rock water and the cement water, is the dominant transport process; a negligible hydraulic gradient acts in x direction. Initially, a constant chemical composition is assumed along the cement area and the host rock area, which are assumed to be constant in time at the model boundaries left and right. Reactive transport is calculated using MCOTAC (Pfingsten, 1996), including advection, dispersion, diffusion, equilibrium chemical reactions for solutes and solids and an incongruent dissolution model for CSH phases (Berner, 1988). For two scenarios with different location of the cement-host-rock interface (Fig. 1), the temporal system development is calculated. In Fig. 2, results are shown for the distribution of the mineral fronts, porosity, pH and total dissolved Ca along the model domain.

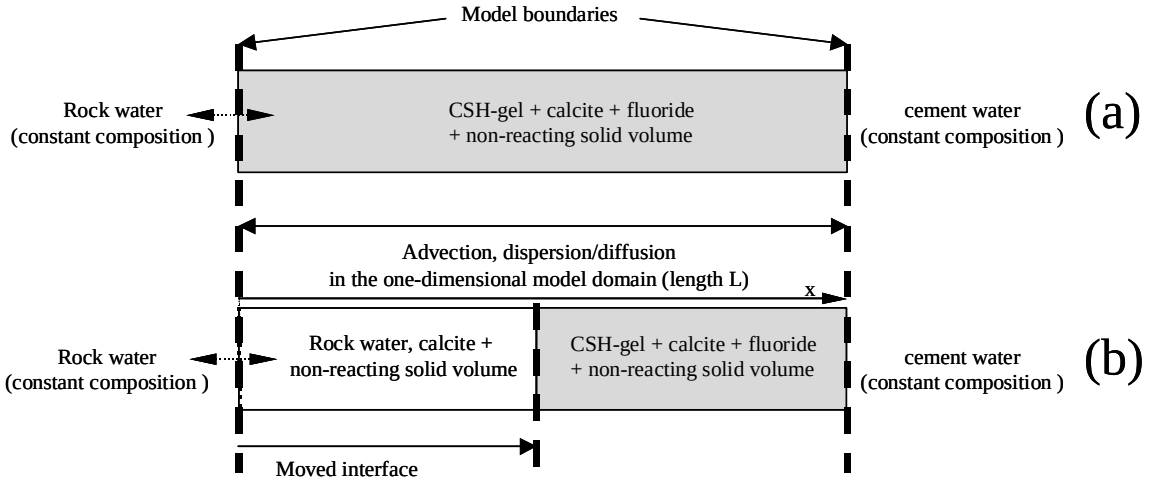

Fig. 1: One-dimensional model set-up for the degradation of hardened cement paste, represented by a Calcium Silicate Hydrate (CSH) –gel, by rock water for two different locations of the interface between the cement paste and the rock water. (a) The boundary is placed to the left of the model domain, assuming there a constant rock water composition. (b) The boundary is placed in the middle of model area, assuming constant water composition at the left (rock water) and the right (cement water).

For set-up (a) and (b), the initial compositions of cement, cement water and rock water are the same, but the model solids are allowed to precipitate or dissolve for set-up (a) only within the cement column, the model domain, whereas for set-up (b) the solids are also allowed to precipitate in the area with rock water. An initial porosity of 17.5% is assumed for the whole model domain (rock and cement area). In set-up (a), the steep chemical gradients are induced between the water compositions at the interface (here equivalent with the location of the boundary) permanently, leading to an "accelerated migration", simply induced by the choice of this boundary condition. Calcite precipitates inside the column and has to replace dissolving CSH there with the effect that a high amount of calcite is necessary first to replace the CSH volume fraction and then further to reduce the porosity. The calculations for set-up (b) give noticeable differences. Calcite precipitation is now left to the interface in the rock water area (calcite is assumed to be present in the rock initially) and the CSH dissolution is less extended inside the CSH-zone. The 60 mol/l_{fluid} level for CSH is about 0.2 m from the inlet for case (a) and only about 0.1 m for case (b). The reason is that now the chemical gradients across the interface are smoothed out slightly slowing down the transport driving forces. The Ca concentration profile is still low along the model area, not only at the left boundary. Although less CSH was calculated to dissolve during 2000 years of interaction, the porosity in the rock water area was calculated to be nearly zero, lower than for the diffusion scenario (a). That is because the locations of dissolution and precipitation are separated from each other for model set-up (b). Calcite precipitate does not have to replace dissolved CSH volume fraction first to finally decrease the initial porosity. The amount of Ca from dissolved CSH is used at a different place, in the rock water area, to precipitate calcite. This causes a local porosity reduction, spatially separated from the CSH dissolution area.

The modelling of these two diffusion examples demonstrates that the choice of the (appropriate) boundary condition and model domain will have an influence on the results of the apparently similar model set-ups. The decision, which is appropriate and applicable to a cementitious repository near-field, depends on the assumptions made with respect to hydrology, host rock and repository properties, geometry and heterogeneity of the near-field. Set-up (a) may be used if there is a large reservoir at the left boundary in contact with the

cement, which might be simple to set-up in a laboratory experiment to guarantee a simple, defined boundary condition. However, for real repository conditions, water flow to the cement-host-rock interface is limited and a set-up (a)-type boundary condition is not very likely (but is often used in one-dimensional reactive transport calculations).

It seems questionable that simple system set-ups, as described above, are sufficient to the needs of performance assessment, which should include quantitatively the timescale for degradation of repository components and the related release of radionuclides. Nevertheless, these one-dimensional approaches show results, which will help to set-up more sophisticated near-field scenarios in performance assessment studies. The extrapolation from such experiments to multi-dimensional real scenarios in nature is difficult. Results from column experiments and one-dimensional modelling indicated that, due to mineral reactions, hydraulic and transport properties, such as porosity, hydraulic conductivity, flow field and velocity, change with time. It is not possible to rigorously account for these processes in a real repository near-field with one-dimensional modelling, since e.g. the flow field is at least two-dimensional and may change locally from increased flow to zero flow. Heterogeneity and geometry together with reactive transport (mineral precipitation and dissolution and related changes for porosity, hydraulic conductivity and sorption properties for radionuclides) have to be taken into account.

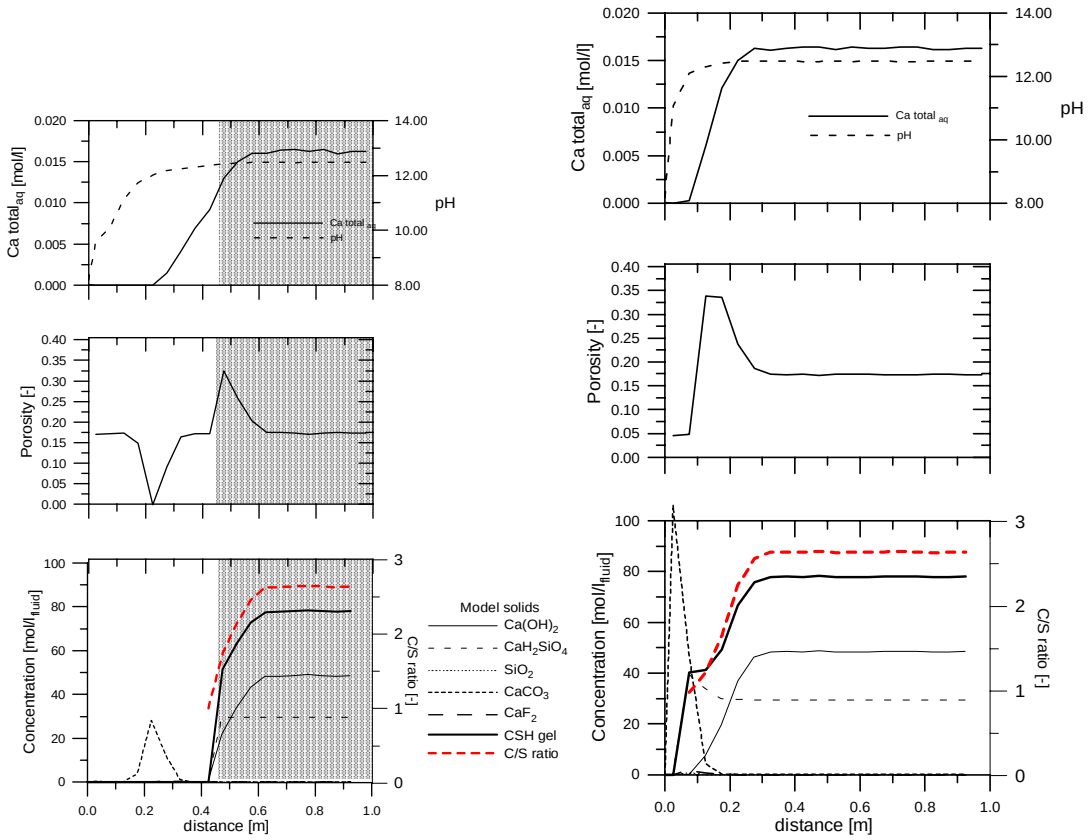

Fig. 2: Concentration distribution for Ca_{total}, pH, porosity, model solids and C/S ratio (calcium to silica ratio in cement) along the column for diffusion dominated transport for two different locations of the interface between cement and host rock: set-up (a) right, (b) left, (see Fig. 1) after 2000 years of interaction. The detailed geochemical system set-up is described in (Pfingsten, 1996).

Here, investigations were focused on the choice of the boundary conditions for a one-dimensional system set-up for reactive transport processes at a cement-host-rock interface, analogue to a near-field of a cementitious repository. A constant concentration boundary

chosen at a host rock-cement interface leads to fast degradation of a cement in a diffusion dominated system. If the interface is chosen to be within the model domain, the degradation is slower, and the porosity is calculated to be lower outside the cement due to spatially separated dissolution and precipitation. The latter is of special interest when investigating clogging processes and their related time scales. In order to overcome the limitations of one-dimensional modelling, performance assessment modelling should at least include two-dimensional coupled hydraulic and reactive transport processes, as reported by (Pfingsten, 2001) for a simplified "small-scale repository near-field".

ACKNOWLEDGEMENTS

Partial financial support by the Swiss National Cooperative for the Disposal of Radioactive Waste (Nagra) is gratefully acknowledged.

REFERENCES

Bateman, K., Coombs, P., Noy, D. J., Pearce, J. M. and P. D. Wetton (1998): Numerical modelling and column experiments to simulate the alkaline disturbed zone around a cementitious radioactive waste repository. 21st Int. Symp. on the Scientific Basis for Nuclear Waste Management, Davos, Switzerland, Mat. Res. Soc., 605-611.

Berner, U. R. (1988): Modelling the Incongruent Dissolution of Hydrated Cement Minerals. Radiochimica Acta 44/45, 387-393.

Jakob, A., Sarott, F. A. and P. Spieler (1999): Diffusion and sorption on hardened cement pastes - experiments and modelling results. PSI Bericht 99-05, Villigen, Paul Scherrer Institut.

Pfingsten, W. (1996): Efficient Modeling of Reactive Transport Phenomena by a Multispecies Random Walk Coupled to Chemical Equilibrium. Nuclear Technology 116, 208-221.

Pfingsten, W. (2001): *Indications for self-sealing of a cementitious L&ILW repository.* PSI Bericht 01-09, Villigen, Switzerland, Paul Scherrer Institut.

Pfingsten, W. and M. Shiotsuki (1998): Modeling a Cement Degradation Experiment by a Hydraulic Transport and Chemical Equilibrium Coupled Code. 21st Int. Symp. on the Scientific Basis for Nuclear Waste Management, Davos, Switzerland, Mat. Res. Soc., 805-812.

Reardon, E. J. (1992): Problems and Approaches to the Prediction of the Chemical Composition in Cement/Water Systems. Waste Management 12, 221-239.

COUPLED TRANSPORT REACTION PROCESSES IN PERFORMANCE ASSESSMENT

Budhi Sagar, Lauren Browning and Scott Painter
Center for Nuclear Waste Regulatory Analyses, Southwest Research Institute,
6220 Culebra Road, San Antonio, Texas 78238, USA; E-mail: bsagar@swri.org,
lbrowning@swri.org, spainter@swri.org

INTRODUCTION

To evaluate the performance of a geologic repository for high-level nuclear waste, at least four classes of basic processes need to be considered. These are (i) thermal (T), (ii) mechanical (M), (iii) hydrologic (H), and (iv) chemical (C) (Tsang, 1991, Manteufel, et al., 1993; Soler, 1999). There is a wide variety of related processes within each of the four classes. For example, conductive, convective, and radiative heat transfer are all included in the thermal process category. The exact rates of these processes and the interactions among them at the space and time scales of a repository are complex and depend upon the particular concept (e.g., nature of geologic medium, disposal in the saturated or unsaturated zone, backfilled or not, heat emitting or cooled waste) selected for disposal. Challenging aspects of reactive transport include formulating appropriate conceptual models of the couplings, estimating kinetic parameters needed to incorporate them in performance assessment models, and numerically solving the resulting highly non-linear equations.

In theory, all couplings should be fully included as that will assure that all effects are fully reflected in the results. In practice, including all couplings is neither possible nor necessary. The practical question then is how does one determine which couplings are to be included, why, and how. Note that exclusion of any coupling from performance assessment will be carefully scrutinized by the regulator and other stakeholders. Therefore, sufficient technical bases must be developed for any exclusions as well as for the way included processes are incorporated in performance assessment.

The challenges of capturing coupled reaction processes in performance assessment are discussed in this paper.

NATURE OF PERFORMANCE ASSESSMENT

The overall objective of building a repository is to protect human health and the environment from adverse effects of radiation. Performance assessments together with other corroborative evidence (e.g., natural analogs) are used to demonstrate the safety of the repository. Because performance is to be estimated for a very long period (thousands to millions of years), use of mathematical models to simulate the behavior of the repository is the main method for performance assessment, although other supporting evidence also plays an important part in developing an overall safety case. At the present stage of scientific understanding and the state of computational capabilities, it is impossible to precisely simulate the evolution of the repository. Not only are the mechanisms of some of the basic processes in imperfectly characterized heterogeneous geologic environment only approximately known, the condition under which the repository will be required to function in the future (e.g., future scenarios) cannot be fully known *a priori*. Therefore, current performance assessments provide neither a deterministic 'prediction' of the future states of the repository nor a calculation of the actual dose to real people. At best, performance assessment provides an estimate of the risk (dose) under possible future conditions from the repository to hypothetical people along with the likelihood of exceeding that risk (dose). Presumably, if the likelihood of exceeding a safe

dose (or regulatory limit) is acceptably small and other evidence corroborates this conclusion, then society can decide to proceed with the construction of the repository.

Despite the pessimism about the state of art of performance assessment expressed in the above paragraph, one should still conduct these analyses with as much rigor and realism as is possible. In fact, the practice of performance assessment has progressed tremendously over the years and today it is certainly capable of analyzing a wide variety of phenomena. Analysis capabilities are expected to improve even more in the future. To take advantage of such improvements, most repository programs envision a staged process including a period of performance confirmation. A time period varying from tens to hundreds of years may elapse before the repository is permanently sealed. During this period, data gathering and updates to performance assessments are expected to continue. Many repository programs allow modifications to repository design or, if new information leads to the conclusion that the project is unsafe, to reverse the waste emplacement process. The reversal of waste emplacement is obviously a costly decision, therefore, a certain minimum level of analytical sophistication and accuracy is deemed necessary for the initial decision to begin construction. Analyses of effects of coupled processes must be considered to meet the minimum requirement.

The process of assessing repository safety through simulations is often depicted as hierarchical with at least three levels. At the bottom of this hierarchy is the most detailed mechanistic investigation of individual processes. At the second level are subsystem investigations with some simplifications (generally in terms of lumping in space and or time) in representation of multiple processes. At the top of the hierarchy is performance assessment, which incorporates all components of the repository system and all relevant processes and couplings between them but in a simplified manner. The simplified performance assessment models, also called abstracted models, are obtained by one or more of (i) incorporating intermediate results of complex mechanistic process models in the form of pre-calculated tables or curves, (ii) ignoring certain processes or parts of processes by assuming some conservative value of selected parameter(s), (iii) lumping space variation into a small number of discrete homogeneous regions, (iv) lumping time variation into a small number of discrete constant process-rate, time intervals, (v) collapsing the dimensionality of the problem, (vi) including the effect of certain processes in the uncertainty range of parameters, (vii) approximating non-linear processes by linear equations, (viii) incorporating the effect of coupled processes heuristically, and (ix) simplifying based on the results of sensitivity analyses. Generally, simplifications necessary to conduct a performance assessment are justified through demonstrations that the adopted simplifications will most likely lead to a pessimistic result and hence the (unknowable) actual risk (or consequence) will most likely be less than the estimated risk (or consequence). An important consideration for the safety case is to document in a transparent and traceable manner the reasons for inclusion/exclusion of various processes and couplings.

REACTIVE TRANSPORT

Reactive transport processes manifest themselves in both the near- and the far-field of a repository. The complexity is far greater in the near field where all of the four classes (T, M, H, and C) of processes may play a significant role compared to the far field where the thermal and mechanical effects may be ignored. The near field of a repository is exceedingly important because it determines the radionuclide source term, which in turn effects all far-field dose estimates.

The basic strategy for deciding which coupled processes to include is to base it on their effect on the final safety measure (e.g., dose or health effects), if possible, or on some intermediate safety measure (e.g., container life, contaminant residence time). For example, it is not in

dispute that heat transfer in the near field can significantly affect drift stability, the rates of chemical reactions, and flow. However, the rates of heat transfer are affected only slightly by chemical reactions. If the repository is to be located in the unsaturated zone and the design does not include backfill, as is the case in the United States for the proposed repository at Yucca Mountain, then drift collapse may impede heat transfer. But if the repository is in the saturated zone (as is the case in most nations) or backfill is used in the unsaturated zone, then the effect of drift collapse (mechanical process) on heat transfer may be neglected after demonstration that these effects are indeed small. Heat transfer and water flow processes are bilaterally coupled (T⇔H) strongly (especially if above boiling temperatures are expected) in the unsaturated zone but have only significant unidirectional coupling (T→H) in the saturated zone, because flow rates are low. Rates of chemical reactions are affected both by the rates of water flow and heat transfer, therefore in the unsaturated zone one should consider T⇔H→C but in the saturated zone, one may just consider T→H→C couplings. Note that mineral dissolution and precipitation processes may alter the hydrologic regime (H←C) but such processes are generally slow (unless above boiling temperatures persist for long periods) and may be incorporated by suitable parameter changes.

A few computer codes with varying capabilities are currently available for simulating coupled reaction transport processes [e.g., TOUGHREACT (Xu and Pruess, 1998) and MULTIFLO (Painter et al., 2001)]. MULTIFLO (Painter et al., 2001) is a flexible computer code that has been developed by the Center for Nuclear Waste Regulatory Analyses on behalf of the U.S. Nuclear Regulatory Commission. This code may be used for reviewing a potential License Application from the US Department of Energy for the proposed repository at Yucca Mountain in Nevada. Note that MULTIFLO incorporates process-level models and only its selected output in the form of tables will be used as input in the Total-system Performance Assessment code (TPA code) (Mohanty et al., 2002). As stated before, it is important to justify the inclusion/exclusion of a coupling by at least approximately estimating the effect of the coupling through process-level models.

In the far field, a class of retention processes (e.g., sorption, precipitation, colloid formation, and matrix diffusion) is possibly the most important for performance assessment. This process class is strongly coupled unidirectionally with water flow rates (e.g., H→C) and the chemistry of the water and rocks. The art of mechanistic modeling of sorption processes using basic thermodynamic data has advanced significantly in recent years, but it is still too complex and computationally intensive to include directly in performance assessment models. Again, the strategies for incorporating the effects of these coupled processes may include (i) use of constant conservative sorption coefficients or (ii) the explicit effects of chemistry variation (e.g., pH) on sorption coefficients (e.g., Turner and Pabalan, 1999).

INCORPORATION OF UNCERTAINTIES

Another layer of complexity is imposed on performance assessment models by the desirability of including uncertainties in conceptual and parameter models. Because the conceptual models are eventually translated into parametric mathematical models, it is not always possible to uniquely separate these two types of uncertainties. While there are deterministic method of parameter uncertainty analysis (primarily sensitivity analyses with conservative values), the most accepted approach is to use probabilistic methods. In the probabilistic approach, the uncertain parameters are ascribed probability distributions (joint distributions for correlated parameters) rather than a single best value and the probability distributions are propagated (generally through Monte Carlo methods) through the model to obtain the probability distribution of the safety measure(s). Inclusion of uncertainties in coupled processes remains a challenge, especially at the process-level, due primarily to computational constraints. Sometimes, it is argued that data sufficient for assigning probability distributions

to parameters are not available and therefore deterministic analyses with conservative values are more appropriate. In this regard, it should be noted that the exact form of the probability distributions are not so important as their ranges and the first two moments. Normally, if there are sufficient data to justify conservative choices, then the same data will be sufficient for assigning probability distributions.

AN EXAMPLE

A number of examples related to incorporation of effects of coupled process will be included in the presentation. Table 1 below demonstrates how some reactive processes can have a significant effect on estimated repository performance. Column 2 in this table provides the measured concentrations in the pore waters in the unsaturated zone above the proposed repository at Yucca Mountain. Column 3 shows concentration calculated by the Department of Energy using a model that considers T⇔H→C processes; primarily cycles of evaporation, condensation, and mineral dissolution and precipitation. Of interest in Column 3 are the chloride and flouride concentrations which are important to corrosion processes of titanium and C22 alloy, the materials used for engineered barrier components. The flouride concentration is large enough that it must be factored into the corrosion model and if it affects the dose significantly, then it must also be included in the performance assessment model. Columns 4 and 5 show concentrations from laboratory experiments using waters of chemical composition given in column 2 and evaporated in the absence or presence of solid rock. The presence of solid rock is to study the effect of possible drift collapse.

Unsaturated Zone Environment			**Drift Environment**	
Solution Components	[1]Ambient Temperature Pore Water Composition (Reinterpreted Analytical Data) (mg/kg)	[1]Thermally Evolved Water Composition Predicted by Coupled THC Model (mg/kg)	[2]Evaporated Groundwater Composition (e.g., No Drift Collapse) (mg/kg)	[2]Evaporated Water in Presence of Tuff (e.g., Drift Collapse) (mg/kg)
pH	8.55	7.23	5.6	5.4
Na+	100.9	972.5	2,077	3,574
K+	3.6	1,548	973	1,622
Mg++	6.3	1154	1949	2889
Ca++	79.0	937.9	6,010	10,249
SiO2(aq)	86.5	2072.8	340	355
HCO3-	157.4	18.8	<37	<36
SO4-	116.2	8,914	1,564	1,516
Cl-	116.6	1318.7	19,248	30,359
NO3-	n/a	n/a	2,647	4,344
F-	5.9	63	<301	<284

[1]CRWMS M&O. "Total System Performance Assessment for the Site Recommendation." TDF-WIS-PA-00001, Revision 00. Las Vegas, Nevada: CRWMS M&O. 2000.
[2]Rosenberg et. al. "Evaporation of Topopah Spring Tuff Pore Water." UCRL-ID-135765. Livermore, California: Lawrence Livermore National Laboratory. 2000.

CONCLUSIONS

A suitable and pragmatic strategy for inclusion of effects of coupled processes in estimating the performance of a repository should be developed that is consistent with the disposal concept. Most countries have adopted a staged repository program. An important element of staged programs is the recognition that scientific knowledge will continue to progress during the period between repository construction and the decision to permanently close it. Therefore, the more complex effects such as from coupled processes may be incorporated initially only in a simplified manner and enhanced later to provide increased confidence that the safety standards are not violated. The aim of the strategy, therefore, should be to assure that the simplifications adopted have a reasonably low likelihood of leading to non-conservative results.

DISCLAIMER

This report was prepared to document work performed by the Center for Nuclear Waste Regulatory Analyses (CNWRA) for the U.S. Nuclear Regulatory Commission (NRC) under Contract No. NRC–02–97–009. The activities reported here were performed on behalf of the NRC Office of Nuclear Material Safety and Safeguards, Division of Waste Management. The report is an independent product of the CNWRA and does not necessarily reflect the view or regulatory position of the NRC.

REFERENCES

Chin-Fu Tsang, 1991, Coupled Hydromechanical-Thermochemical Processes in Rock Fractures, Reviews of geophysics (29)4, pp. 537-552.

Manteufel, R. D., et al., 1993, A Literature Review of Coupled Thermal-Hydrologic-Mechanical-Chemical Processes Pertinent to the Proposed High-Level Nuclear Waste Repository at Yucca Mountain; NUREG/CR-6021, Nuclear Regulatory Commission, Washington, D.C.

Mohanty et al., 2002, Total-System Performance Assessment (TPA) Version 4.0 Code, Center for Nuclear Waste Regulatory Analyses, San Antonio, TX.

Painter et al., 2001, MULTIFLO User's manual: Two-Phase Nonisothermal Coupled Thermal-Hydrological-Chemical Flow Simulator, Center for Nuclear Waste Regulatory Analyses, San Antonio, Texas.

Soler, J. M., 1999, Coupled Transport Phenomena in the Opalinus Clay: Implications for Radionuclide Transport, Paul Scherrer Institute, Bericht Nr. 99-07, Villigen PSI, Switzerland.

Turner, D. R. and R. T. Pabalan, 1999, Abstraction of Mechanistic Sorption Model Results for Performance Assessment Calculations at Yucca Mountain, Nevada, Waste Management Vol 19, p375-388, Elsevier Sciences Ltd., Center for Nuclear Waste Regulatory Analyses, San Antonio, Texas.

Xu, T. and K. Pruess, 1998, Coupled Modeling of Non-isothermal, Multi-phase Flow, Solute Transport, and Reactive Chemistry in Porous and Fractured Media: 1. Model Development and Validation, LBNL-42050, Lawrence Berkley National laboratory, Berkley, California.

EFFECT OF REDOX POTENTIAL ON DIFFUSION OF REDOX SENSITIVE ELEMENTS IN COMPACTED BENTONITE – SELENIUM (SE) –

Haruo Sato and Shinya Miyamoto
Japan Nuclear Cycle Development Institute (JNC), 4-33 Muramatsu, Tokai-mura, Naka-gun, Ibaraki-ken, 319-1194, Japan; E-mail: sato@tokai.jnc.go.jp

INTRODUCTION

At JNC, research has been performed to investigate the geochemistry and radionuclide migration in buffer materials and the geosphere. Experiments and modelling studies have been carried out related to the geological disposal of high-level radioactive waste (HLW) as a link in the chain of a follow-up of the second progress report (H-12 report) (JNC, 2000), which has explained the technical feasibility of the geological disposal of HLW in Japan. Although much data have been reported with respect to diffusion and sorption of radionuclides in bentonite so far, almost all data have been obtained under air condition. Data for redox sensitive elements obtained under reducing conditions, reflecting conditions for a deep geological environment, are limited. Selenium, important for dose evaluation in safety assessment (^{79}Se: half-life $T_{1/2}$ > 6.5E4y), is one of the redox sensitive elements. It is known from conventional studies that Se forms anions in solution and is slightly sorbing on bentonite (e.g. Shibutani and Yui, 1996). Selenium is found in oxidation states between –II and VI. In the pH range of natural waters, SeO_4^{2-} is predominant under strongly oxidizing conditions (Ticknor et al., 1988), while HSe^- dominates under reducing conditions (Ticknor et al., 1988, Brookins, 1988). Thus, the chemical speciation of Se depends on the redox condition and pH of the solution, which may result in a limited retardation of Se in bentonite.

The authors have proposed an experimental method to investigate non-steady state diffusion of Se in compacted bentonite under reducing conditions in a previous study (Sato, 1998), where a density dependency of the apparent diffusivities (*Da*) for Se is reported. However, quantitative data and information on the effect of redox potential on retardation properties in compacted bentonite as well as thermodynamic data for Se diffusion are lacking. Thereon, in this study, *Da* values for Se, among other redox sensitive elements, for diffusion in compacted bentonite are obtained under reducing conditions as a function of silica sand content and temperature. The effect of the redox potential on diffusion of Se is discussed.

EXPERIMENTAL

The experiments were carried out by an in-diffusion method (e.g. Sato, 1998). Table I shows the experimental conditions. A Na-bentonite, Kunigel-V1® (Kunimine Industries Co. Ltd.), of which a lot of data regarding fundamental properties have been reported, was used in a series of diffusion experiments. The major constituent clay minerals of the bentonite are Na-smectite and chalcedony, which makes up 46-49 and 37-38wt%, respectively (Ito et al., 1994). The details of the minerals are described in the literature of (Ito et al., 1994). The diffusion experiments were performed at a dry density of 1.6 Mg/m^3. Since Se is redox sensitive, all diffusion experiments were carried out in a controlled N_2 atmosphere glove box to reproduce a relevant disposal condition. The experiments were furthermore carried out at room temperature (22.5˚C) and 60˚C in order to discuss diffusion behaviour thermodynamically.

The diffusion experiments were carried out using acrylic diffusion columns, which have a cylindrical space of 20mm in diameter and 20mm in thickness. The bentonite powder dried at 110˚C more than overnight was filled into the cylindrical space together with silica sand. The diffusion columns with bentonite were evacuated for air by exchanging with N_2 gas in a

vacuum chamber and were then transferred to a controlled N_2 atmosphere glove box. The diffusion columns were immersed in degassed distilled water with $Na_2S_2O_4$ (sodium dithionate) for about 5 months to be saturated. Throughout the saturation of the bentonite, the bentonite was constantly contacted with the degassed distilled water with $Na_2S_2O_4$ in order to keep the Eh low via alumina ceramic filters with a pore size of 2μm used to prevent the bentonite from swelling.

After the saturation of the bentonite, a small volume of $Na_2{}^{75}SeO_3$ (50μl, about 22 kBq) was pipetted on the surface of one end of each cylindrical bentonite sample and a blind lid was then sealed shut. The other end of the bentonite remained in contact with degassed distilled water with $Na_2S_2O_4$ via ceramic filter. The Eh and pH of the solution contacting the bentonite were monitored throughout the saturation and diffusion experiments. Although the reductant was added to obtain initially a concentration of $[Na_2S_2O_4]$ = 5.2E-3 M, it was then added to adjust the Eh of the solution if necessary. In this case, the final concentrations of $Na_2S_2O_4$ were 8.2E-3 M at 22.5˚C and 1.2E-2 M at 60˚C, respectively. After the diffusion periods, each cylindrical bentonite sample was cut with a knife into about 1mm thick slices. Each slice was immediately weighed in order to calculate distance from the surface of bentonite specimen and was analyzed for radioactivity with a Geiger Müller (GM) counter (Aloka Co. Ltd.). Since the half-life of ^{75}Se is short (119.8d), the concentration profiles were determined by correcting for radioactive decay.

The background of βγ-radioactivity from bentonite was also measured as a function of dry density (0.8, 1.6, 1.8 Mg/m^3) and slice thickness (0.5, 1.0, 5.0mm).

Table 1 Experimental conditions for diffusion experiments

Item	Condition
Method	In-diffusion method
Bentonite	Kunigel-V1® (content of Na-smectite: 46-49wt%)
Dry density of bentonite	1.6 Mg/m^3 (sample size: ϕ20mmx20mm)
Silica sand content	0, 30, 50wt% (mixed with silica sand with particle sizes of 1–5mm and 0.1–1mm at a mixture ratio of 1:1)
Tracer solution	^{75}Se (Na_2SeO_3 solution: 2.63 MBq/5ml (1.3E-8 M))
(carrier concentration)	50ppm-Se (6.3E-4 M)
Introduced tracer quantity	50ml/sample (21.96 kBq/sample)
Temperature	22.5±2.5˚C, 60±0.1˚C
Atmosphere	N_2 atmosphere (O_2 concentration < 1ppm)
Saturated solution	Degassed distilled water + $Na_2S_2O_4$ (initial $[Na_2S_2O_4]$ = 5.2E-3 M)
pH of contacted solution	7–7.5 (pH of solution contacted with bentonite)
Diffusing period	1–14 days
Repeatability	n = 2

RESULTS AND DISCUSSION

Effect of redox potential on Da values of Se in compacted bentonite

The obtained counts per minute (cpm) were approximately at the same level as for natural radioactivity during the measurements and it became clear that the obtained cpm values were not originated from bentonite. Therefore, an average value was used in the calculations for the Se concentration profiles.

Although the Eh of the solution contacted with bentonite rose a little as time evolved for the diffusion experiments at 60˚C, it was stable at around –400mV at 22.5˚C throughout the saturation and diffusion experiments. The dominant species of Se in the porewater of bentonite under these conditions is predicted from Eh-pH diagrams to be HSe^- (Ticknor et al., 1988, Brookins, 1988).

The *Da* values for Se were determined based on the Fickian law (Crank, 1975) considering radioactive decay. Since the tracer solution includes 50ppm of Se (6.3E-4 M) as a carrier, it is considered that Se precipitated at the surface of bentonite and that the boundary concentration was controlled by the solubility of Se. The *Da* values for Se were determined by a least squares fits to the concentration profiles. In the actual calculations of *Da* values, IDBENTO1, a numerical analysis code for a least squares fitting based on a difference method, was used. The details of this code are described in (Sato and Miyamoto, 2001).

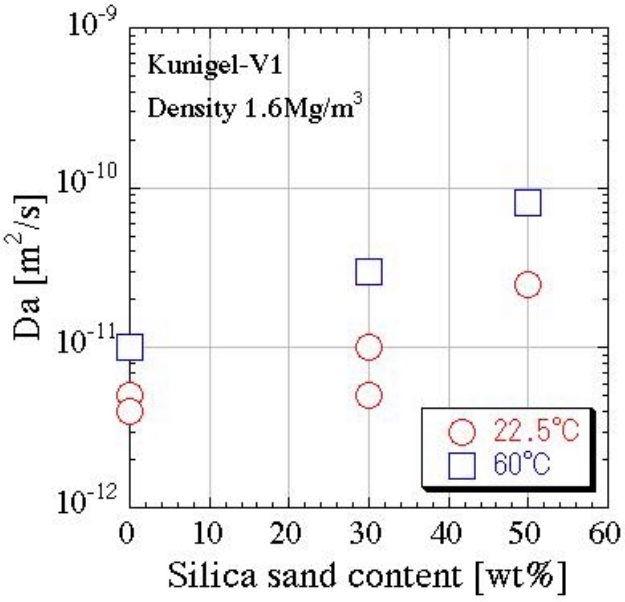

Figure 1 Dependencies of Da values for Se on silica sand content and temperature

Figure 1 shows dependencies of *Da* values for Se on silica sand content and temperature. The effects of silica sand content and temperature on *Da* are overall summarized as follows:
(1)The *Da* values show a tendency to increase with increasing silica sand content.
(2)The *Da* values show a tendency to increase with increasing temperature.
(3)The increasing rate of *Da* with temperature is approximately constant, independent on silica sand content.

Figure 2 shows *Da* values for various elements previously reported together with new data for Se with respect to Kunigel-V1® as a function of dry density. The *Da* values obtained for Se under reducing conditions are about one order of magnitude smaller than those for SeO_3^{2-} obtained under anaerobic conditions (Sato and Shibutani, 1994). Therefore, Se is strongly retarded under reducing conditions. The reason might be explained by the fact that different sorption processes for different species in the porewater are related to different redox potentials.

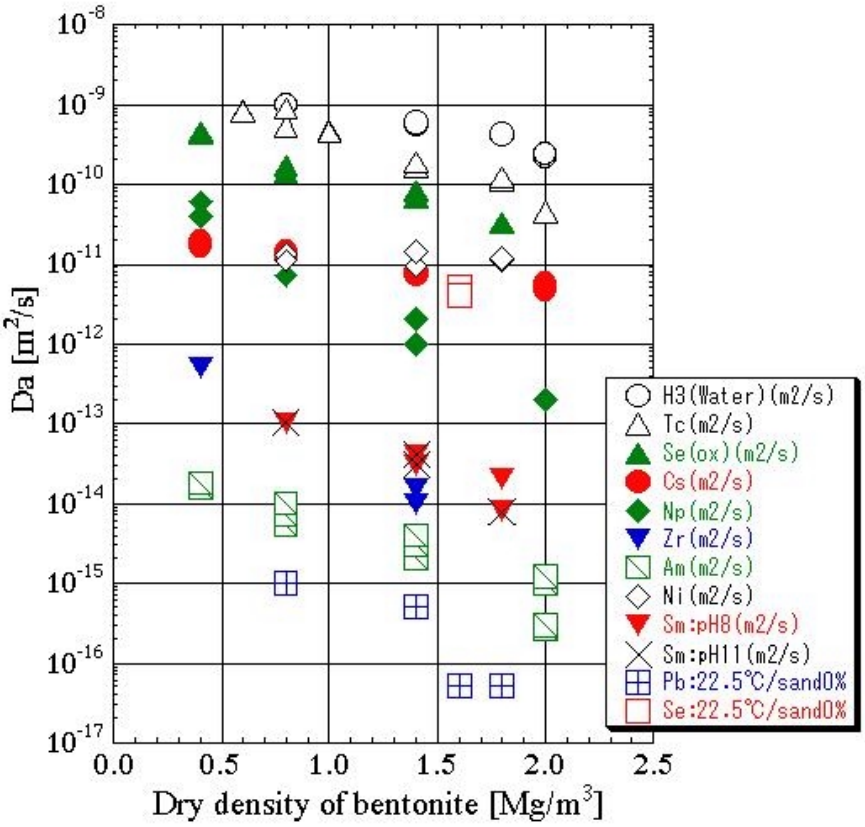

Figure 2 Dependencies of *Da* values for various elements reported to date together with new data for Se on the dry density. Selenium marked (ox) was measured under anaerobic conditions, but not under reducing conditions.

Correlations between Da values and smectite partial density

Figure 3 shows correlations between *Da* values for Se and smectite partial density, which was defined only by density of the smectite aggregates in bentonite (Sato and Miyamoto, 2001). The *Da* values were well correlative with smectite partial density for both temperatures. This indicates that Se diffusion is predominantly controlled by the properties in part of smectite.

Activation energy (ΔEa) for Da

Activation energies for *Da* values of Se were calculated from the temperature dependency of the *Da* values. The calculated *ΔEa* values were in a range of 17 to 32 kJ/mol and no systematic tendency with respect to smectite partial density was found. The *ΔEa* values of ionic diffusivities in free water (D^o) for popular ions are generally 15 to 25 kJ/mol and *ΔEa* values obtained in this study are similar to those, although *ΔEa* values obtained in this study

are slightly higher. A reason might be that the properties of the porewater of compacted bentonite are different from that of free water.

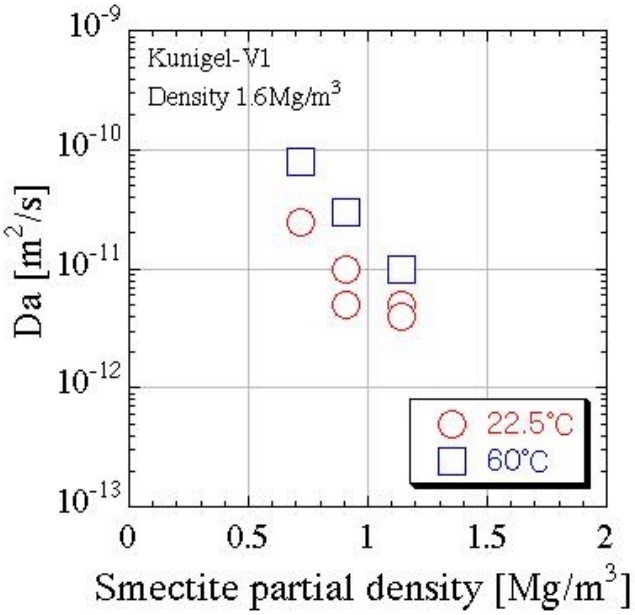

Figure 3 Correlations between *Da* values for Se and smectite partial density

CONCLUSIONS

The *Da* values for Se in compacted Na-bentonite were obtained at a dry density of 1.6 Mg/m^3 as a function of silica sand content and temperature under reducing conditions. The conclusion is summarized as follows.

(1)The *Da* values for Se obtained under reducing conditions are about one order of magnitude smaller than those for SeO_3^{2-} obtained under anaerobic conditions and it was found that Se was strongly retarded under reducing conditions

(2)The *Da* values increased with increasing silica sand content and temperature.

(3)The *Da* values were well correlated to the smectite partial density, which indicates that Se diffusion is predominantly controlled by the properties of smectite.

(4)The ΔEa values for *Da* values of Se, in a range of 17 to 32 kJ/mol, were similar to those for D^o values of popular ions.

REFERENCES

Brookins, D. G., Eh-pH Diagrams for Geochemistry, Springer-Verlag, Berlin Heidelberg (1988).

Crank, J., The Mathematics of Diffusion, 2nd ed., Pergamon Press, Oxford (1975).

Ito, M., Okamoto, M., Suzuki, K., Shibata, M. and Sasaki, Y., J. At. Energy Soc. Japan, Vol.36, No.11, pp.1055-1058 (1994), in Japanese.

Japan Nuclear Cycle Development Institute, JNC TN1410 2000-001 (2000).

Shibutani, T. and Yui, M., PNC TN1410 96-071, pp.153-155 (1996), in Japanese.

Sato, H., Radiochimica Acta 82, pp.173-178 (1998).

Sato, H. and Miyamoto, S., JNC TN8400 2001-018 (2001).

Sato, H. and Shibutani, T., PNC TN8410 94-284, pp.71-89 (1994), in Japanese.

Ticknor, K. V., Harris, D. R. and Vandergraaf, T. T., Atomic Energy of Canada Limited Research Company, TR-453 (1988).

EFFECT OF COLLOIDAL IRON HYDROXIDE TRANSFORMATION ON ACTINIDE MOBILITY IN GORLEBEN GROUNDWATER

Thorsten Schäfer, Robert Artinger, Kathy Dardenne, Andreas Bauer and Jae Il Kim
Institut für Nukleare Entsorgung (INE), Forschungszentrum Karlsruhe, P.O. Box 3460, D-76021 Karlsruhe, Germany; E-mail: schaefer@ine.fzk.de

INTRODUCTION

In natural aquifers, aquatic colloids are ubiquitous and take part in geochemical solid-water-interface reactions (Kim, 1986; McCarthy & Zachara, 1989). Colloidal transport of inorganic nanophases is strongly correlated to the presence of humic substances, either for colloidal stabilization via surface charge reversal (Kretzschmar & Sticher, 1997) or by initiating dissolution of sediment grain coatings (iron oxyhydroxides) and mobilization of clay colloids (Swartz & Gschwend, 1998). The metastable, low crystalline iron oxyhydroxide 2-line ferrihydrite (2LFh) is frequently found as the dominant inorganic Fe-colloid species in aquatic systems including the Gorleben system, but appears also as sediment grain surface coatings determining therefore the sorption properties of the sediment. Sorption experiments reveal that actinides such as Np(V) are reversibly bound onto 2LFh (Girvin et al., 1991), whereas ^{239}Pu (V/VI) shows a very slow desorption rate from iron oxide surfaces (Lu et al., 1998). Coprecipitation studies from Grigoriev et al. (2001) have demonstrated, that Pu(IV) and Np(IV) produce mixed hydroxides with Fe(III). Due to the metastable nature of 2LFh, a possible structural entrapment of actinides in colloidal stable secondary phases (goethite/hematite) might lead to an irreversible actinide binding. Np(V) binding changes with 2LFh alteration have been observed by Sakamoto et al. (1994) and Nagano et al. (1999) showed by Rietveld refinement analysis a substitution of structural Fe by the Am homologue Nd in the hematite structure.

The aim of this study is to discuss the influence of 2LFh and its thermal transformation product (i. e. hematite) on the mobility of Am(III) by colloid stability, batch and column migration experiments.

MATERIALS AND METHODS

For the preparation of ^{59}Fe spiked 2-line-ferrihydrite (2LFh), the synthesis described in Schwertmann & Cornell (1991) was modified using an irradiated 99.99+ % pure iron foil (GoodFellow, Germany). 2LFh/Am coprecipitates (later referred to as 2LFh/Am) were synthesised by adding 2ml of the ^{59}Fe stock solution (pH < 1) to a 3 ml aliquot of ^{241}Am(III) stock solution and adjusting the suspension to pH 6 with 1 M KOH. Washing up to five times with Milli-Q water was performed to purify the synthesized 2LFh/Am precipitates. Tempering 2LFh/Am over a period of 7d at 70°C in an oven generated the transformation products (later referred as Hae/Am). The pH value was set to 6 and adjusted once a day. X-ray diffraction analysis of the transformations products indicate hematite as major mineral component. Photon Correlation Spectroscopy (PCS) analysis showed an intensity weighted mean colloid size of 259 ± 127 nm for the 2LFh/Am sample and a slightly lower colloid size of 180 ± 80 nm for Hae/Am. To determine the fraction of exchangeable, poorly crystalline (bioavailable) and total ^{241}Am in the colloidal phases an operational three-step extraction scheme selective for iron oxides was used (Loeppert & Inskeep, 1996). The influence of humic substance concentration on the coagulation kinetics of 2LFh was investigated with PCS by adding 2LFh colloids to the untreated Gorleben groundwater with a dissolved organic carbon (DOC) range from 0.9 to 81.6 mgC/dm^3. The 2LFh colloid concentration was adjusted to 1.8 mg/L or 5.6 mg/L.

Column experiments were performed under inert gas atmosphere (Ar + 1 % CO_2) in a glove box. For the flow-through column experiments the Pleistocene quartz sand (Artinger et al., 1998) was equilibrated in separate columns with Gorleben groundwater and circulated for a period of 3 months. Continuous injection of approximately one pore volume of Am/2LFh spiked groundwater was initiated. The contact time of Am with colloids (2LFh/humics) is varied in a single column experiment by continuous injection of approximately one pore volume Am spiked groundwater into the column. In the case of the quantitative tritiated water (HTO) elution, dispersion effects in the column could be neglected and the Am recovery was directly detectable from the breakthrough curve. Isotopes under investigation (^{241}Am, ^{243}Am, ^{59}Fe and HTO) were detected by γ-spectrometry and/or liquid scintillation counting.

RESULTS AND DISCUSSION

The PCS measurements on the coagulation kinetics of 2LFh in the different Gorleben groundwater revealed a strong dependence of aggregation on the DOC concentration (Fig. 1). Fast coagulation of 2LFh colloids could be observed for the groundwater of low (0.9-5.0 mgC/L) DOC concentration (GoHy-182, -412), whereas the colloids were stabilized in groundwater of higher DOC content (GoHy-532,-2227) with 22.6-81.6 mgC/L. Zetapotential (ζ) measurements of the purified 2LFh revealed, that the isoelectrical point is at pH_{IEP} 8.7 and a positive ζ-potential of +22 mV was found at pH 6.5 (GoHy-182) and +16 mV at pH 7.5 (GoHy-532), respectively. The 2LFh-humic associations showed a decrease of the positively charged 2LFh surface to more negative values with increasing DOC content from -5 mV in GoHy-182 to -30 mV in GoHy-2227. Similar results were obtained from fatty acid and Suwannee humic/fulvic acid sorption experiments on hematite colloids (Liang & Morgan, 1990). The results revealed that the negatively charged humics sorbed onto the 2LFh surface force, via charge neutralization, a 2LFh colloid destabilization in Gorleben groundwater of low DOC concentration, whereas higher DOC concentrations were sufficient to exceed the critical coagulation concentration (CCC) and stabilize 2LFh colloids in the mg/L range.

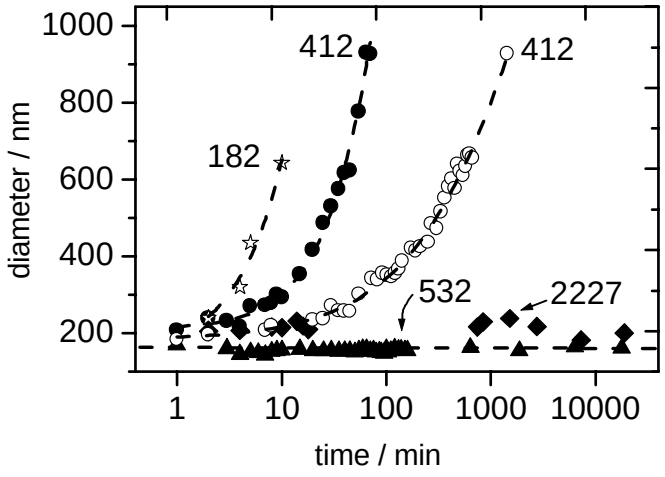

Figure 1: Time dependent 2LFh colloid hydro-dynamic diameter (d_H) change by dynamic light scattering (PCS) analysis in Gorleben groundwater (☆ GoHy-182: 0.9 mg/L DOC; ●,○ GoHy-412: 5.0 mg/L DOC; ▲ GoHy-532: 22.6 mg/L DOC; ◆ GoHy-2227: 81.6 mg/L). 2LFh colloid concentration adjusted to 5.6 mg/L (filled symbols) or 1.85 mg/L (open symbols).

The results of the migration experiments including the Am and 2LFh recoveries are shown in Fig. 2. ^{59}Fe was used as an indicator for iron colloids in the migration experiments. HTO breakthrough is quantitative and in the range of quantitative HTO elution the $[Am]/[Am]_0$ ratio corresponds directly to the recovery of colloid-borne Am. The migration velocity for the iron colloids is 13 % higher (retardation factor R_f = 0.87) than that of HTO in GoHy-532 due to their larger colloid size (Fig. 2) and therefore, a pronounced pore size exclusion effect. The breakthrough of 2LFh/Am colloids in groundwater GoHy-182 (0.9 mgC/L) could not be determined due to the low concentration of ^{241}Am and ^{59}Fe in the column outlet fractions, but

the total ^{241}Am recovery of 0.5% showed no enhancement of Am mobility by 2LFh addition. The unretarded Am mobility in GoHy-532 groundwater changed from 7.9 % total recovery for humic colloid-borne migration to 10.2 % Am recovery after addition of 2LFh with a 2LFh recovery of 31.3 %. In all conducted experiments using GoHy-532 groundwater ^{59}Fe was detectable in the column outlet fraction showing that initially positively charged 2LFh colloids are partly mobile in near neutral pH of Gorleben groundwater rich in humic substances. However, the Am mobility is not significantly enhanced compared to humic colloid borne migration. This can be explained by the total ^{241}Am/^{59}Fe recovery ratio of 0.33 (Fig. 3). This ratio shows that a large fraction of the 2LFh bound Am (67 %) dissociates from the iron colloid surface and afterwards adsorbs to the column sediment. The experiments with 2LFh/Am colloids revealed higher recoveries for ^{241}Am and ^{59}Fe, but the total Am/Fe recovery ratio increased only from 0.33 to 0.41. These results show that also a major part of the Am on 2LFh/Am colloids is reversibly bond. The Hae/Am colloids show a completely different effect on Am mobility, with an increase of ^{241}Am recovery to 39.0 % and a ^{59}Fe recovery of 46.0 %. The Am/Fe total recovery ratio thus increased to 0.85 indicating a reduced exchangeable Am fraction of ~ 15 %. Contrary to the unaltered 2LFh experiments, the Am/Fe ratio in the column outlet fractions decreased from almost 1 to a plateau value of 0.8, which could be attributed to a kinetically controlled Am desorption from 2LFh onto humics during the initial stage of the experiment.

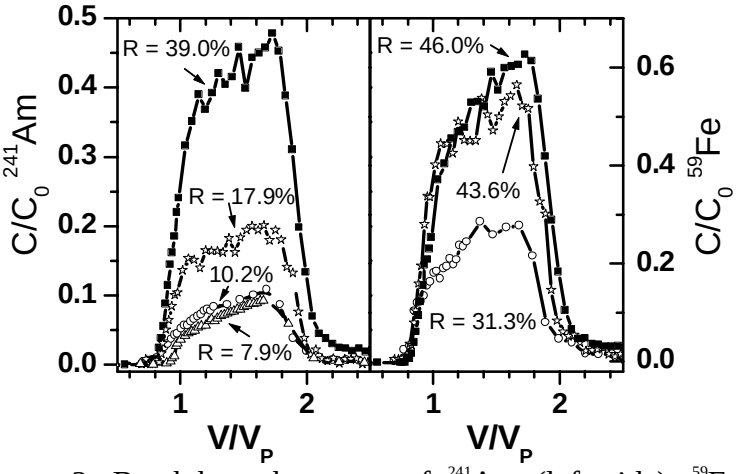

Figure 2: Breakthrough curves of ^{241}Am (left side), ^{59}Fe (right side) and recoveries R as a function of colloid type (Δ: humic bond Am, ○: Am sorbed on 2LFh, ☆: 2LFh/Am, ■: Hae/Am). Here, C/C_0 is the ratio of the outlet to inlet concentration of ^{241}Am and ^{59}Fe, respectively.

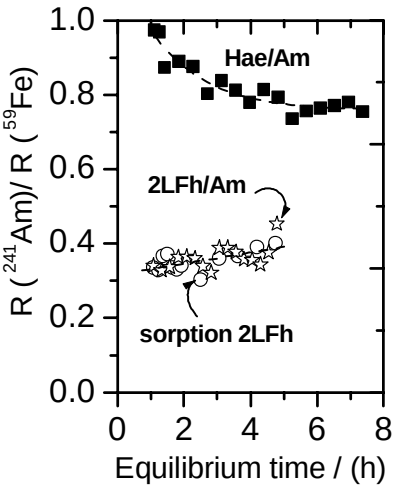

Figure 3: The recovery ratio variation of ^{241}Am /^{59}Fe as a function of equilibrium time. Equilibrium time is the calculated contact time prior to column injection of the spiked groundwater.

The selective extraction procedures on the iron oxide/hydroxide colloids prior to injection validate the changes in Am binding. The NH_4-oxalate-oxalic acid extractable $Fe_{(O)}$ changes from 99 % for 2LFh

over 77 % in the 2LFh/Am sample to 33 % in the Hae/Am sample, therefore documenting the change in iron colloid mineralogy.
The parallel measured release of ^{241}Am via selective iron phase dissolution showed that 90 % of the 2LFh sorbed Am is salt exchangeable ($Am_{(E)}$), with a slight decrease to 78 % $Am_{(E)}$ in the 2LFh/Am sample and a strong decrease to 19 % in the Hae/Am sample. However, the results also revealed, that the Am in the Hae/Am sample is mostly $Fe_{(O)}$ extractable (76%) whereas the major fraction of iron is citrate-dithionite-bicarbonate ($Fe_{(T)}$) extractable. The extraction results suggest a preferential binding of Am in the 33% $Fe_{(O)}$ of lower crystallinity and demonstrate that 2LFh recrystallization and secondary mineral formation (i.e. hematite) changes drastically the Am/mineral interaction kinetics. This point is of crucial importance for the Am mobility, either for sediment fixation via crystal entrapment or as shown in this work via colloidal mobilization enhancing the Am mobility in a near natural system.

CONCLUSIONS

The relevance of colloidal transport to enhance the actinide mobility in the natural environment depends, among others on the reversibility of metal ion colloid binding. In this paper, the influence of the metastable, low crystalline precursor phase 2-line ferrihydrite (2LFh) and the possible structural entrapment of Am(III) in transformation products (thermal treatment at 70°C over 7d) on the colloidal mobility of Am was investigated in batch and column migration experiments. Laser light scattering analysis (PCS) demonstrated a fast 2LFh aggregation (1.8-5.6 mg2LFh/L) in Gorleben groundwater of low humic content (1-7 mgC/L), which can be attributed to surface charge neutralization detected via zeta potential measurements. The results demonstrated that humic substances can intervene in the aquatic subsurface actinide interaction not only as immediate actinide carrier but also as stabilizing agent for an inorganic colloid mediated mobilization. The column experiments showed in groundwater with low humic content no significant enhancement of humic colloid bond Am recovery (R = 0.5 %). Contrary to this, in humic rich groundwater (30-90 mgC/L) the 2LFh colloids remained stable and showed an almost fivefold increase of the unretarded Am mobility in the case of transformed 2LFh (mainly hematite). Iron oxide/hydroxide selective extractions indicated a strengthening of Am from salt exchangeable in 2LFh to NH_4-oxalate-oxalic acid extractable in transformed 2LFh. Additionally, batch experiments revealed no equilibrium state for 2LFh colloid and ^{241}Am sorption onto Gorleben sand after 165 days, therefor indicating that metal colloid association/dissociation and colloid sediment attachment kinetics are a key issue for the actinide mobility.

REFERENCES

Artinger, R.; Kienzler, B.; Schüßler, W.; Kim, J.I. J. Contam. Hydrol. 1998, 35 , 261.

Girvin, D.C.; Ames, L.L.; Schwab, A.; McGarrah, J.E. J. Colloid Interface Sci. 1991, 141(1), 67.

Grigoriev, M.S.; Fedoseev, A.M.; Gelis, A.V.; Budantseva, N.A.; Shilov, V.P.; Perminov, V.P.; Nikonov, M.V.; Krot, N.N. Radiochim. Acta 2001, 89 , 95.

Kim, J.I. In Handbook on the Physics and Chemistry of the Actinides, A.J. Freeman; C. Keller, Eds.; Elsevier Science Publication, 1986; Chap. 8.

Kretzschmar, R.; Sticher, H. Environ. Sci. Technol. 1997, 31 , 3497.

Liang, L.; Morgan, G.G. Aquatic Sci. 1990, 52 (1), 32.

Loeppert, R.H.; Inskeep, W.P. In Methods in Soil Analysis. Part 3. Chemical Methods, J.M. Bartels, Ed.; SSAS & ASA, Inc.: Madison, WI, 1996; Vol. 5, pp 639.

Lu, N.; Triay, I.R.; Cotter, C.R.; Kitten, H.D.; Bentley, J. Reversibility of sorption of Plutonium-239 onto colloids of hematite, goethite, smectite, and silica; Report LA-UR-98-3057; Los Alamos National Laboratory: Los Alamos, 1998.

McCarthy, J.F.; Zachara, J.M. Environ. Sci. Technol. 1989, 23 (5), 497.

Nagano, T.; Mitamura, H.; Nakayama, S.; Nakashima, S. Clays Clay Minerals 1999, 47(6), 748.

Sakamoto, Y.; Ohnuki, T.; Senoo, M. Radiochim. Acta 1994, 66/67 , 285.

Schwertmann, U.; Cornell, R.M. Iron Oxides in the Laboratory (Preparation and Characterization); VCH Verlagsgesellschaft mbH: Weinheim, 1991; p 137.

Swartz, C.H.; Gschwend, P.M. Environ. Sci. Technol. 1998, 32 , 1779.

PROGRAM SYSTEM TRANSREAC

Frank Schmidt-Döhl
Materialprüfanstalt für das Bauwesen / Testing laboratory for civil engineering,
TU Braunschweig, Beethovenstraße 52, 38106 Braunschweig, Germany;
E-mail: f.schmidt-doehl@tu-bs.de

GENERAL

Transreac is a software to simulate corrosion processes of structures made of mineral building materials. It is characterized by single modules representing the most important partial processes of a corrosion process combined in an algorithm incremental in time and space. Fig. 1 gives an overview.

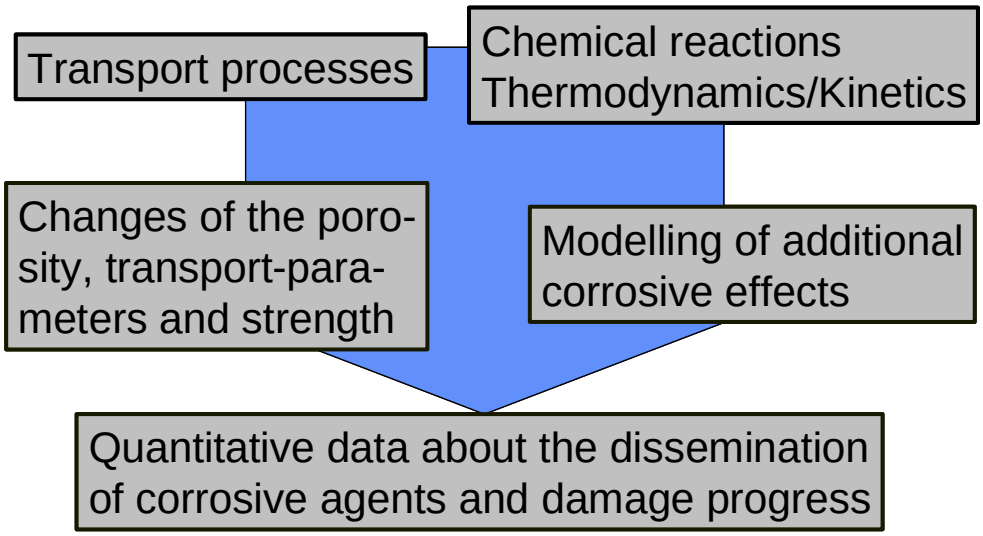

Fig. 1. General structure of Transreac

INTERNAL STRUCTURE

The following partial processes of a corrosion process are incorporated:

- Transreac contents a module for the calculation of transport processes. The program is able to calculate the transfer of heat and moisture, the heat conduction, water vapour diffusion, capillary suction of a solvent and solved species, diffusion of different solved species, the transport of ions by the diffusion potential caused by the different diffusive velocities of the ions and the flow of solvent and solved species by a seepage pressure.

- Another essential module of the algorithm deals with the calculation of the chemical reactions caused by the transport processes which change the chemical compositions at the volume elements. They are quantitatively determined by the repeated calculation of the thermodynamic and kinetic stable phase assemblage at the individual volume elements. To determine the thermodynamic stable phase assemblage, an algorithm that optimize the Gibbs free energy at the volume elements in combination with a Pitzer module for the determination of the activity coefficients of the solved species is used.

- The precipitation or dissolution of solid phases leads to a change of porosity and results in an alteration of the transport parameters and the material strength. This changes are also considered.

- In another module the resulting corrosive effects, for example the loss of bearing capacity, loss of mass from the surface and the rise of cracks are calculated.

This program structure is the basis to calculate very different corrosion processes without change of the underlying model. Transreac is also able to simulate the corrosion behaviour of concrete in contact with solutions with very complex and variable chemical compositions and under variable and changing environmental conditions.

SCIENTIFIC MODELS

A detailed description of the underlying scientific models is given in (Schmidt-Döhl, 1996; Schmidt-Döhl and Rostásy, 1999a; 1999b). In addition to this papers the following information is necessary.

In the meantime it is possible to calculate all transport processes as 2 D processes. It is possible to calculate the transport processes of heat and moisture now on the basis of the model of Künzel (1994) with some simplifications. In addition to Schmidt-Döhl (1996) and Schmidt-Döhl and Rostásy (1999a; 1999b) it is possible now to calculate the flow of solvent and solved species by a seepage pressure. The actualisation of the permeability coefficient K in the corroded volume elements of the structure is based on the following equation of Gaber (1989). r_e is an equivalent pore radius. The coefficient a was used by Gaber (1989) to adjust experimental and calculated values. During simulations with Transreac the factor $r_e^2 \cdot a$ is determined by the permeability coefficient and the porosity parameters of the uncorroded material and is assumed to be unaffected. The relevant porosity of the corroded material ε is determined by the concentrations of the solid phases and their densities.

$$K = \varepsilon^8 \cdot r_e^2 \cdot a$$

EXPERIMENTAL VERIFICATION AND APPLICATION

Transreac was experimentally tested for the simulation of chemical attack on concrete and cement mortar by acid, sulfate, ammonium-, magnesium- and chloride-solutions and on sandstone by acid with and without sulfate. Fig. 2 shows as an example an experimental result of a corrosion experiment with cement mortar in contact with Na_2SO_4-solution resulting in the new formation of ettringite. The corresponding simulations, using only the properties of the uncorroded material, resulted in a good correspondence of measured and calculated data.

ACTUAL AIMS OF RESEARCH

In connection with Prof. Triantafyllidis (Lehrstuhl für Grundbau und Bodenmechanik, Universität Bochum) the time dependent maximum load of ground anchors in soils containing aggressive carbon dioxide is modeled. In addition to experimental examinations Transreac is used to simulate the dimension of the corroded zone of the injection mortar as a function of time and to interpolate and extrapolate the experimental results.

In Germany all disposal sites for very hazardous waste are located in former salt mines. In such disposal sites mineral building materials can be attacked by salt solutions if such solutions arise. Their corrosion behaviour is therefore of great importance for the safety

concept. Because of the long interesting time span, this problem is unsolvable without computer simulations. Because of its structure and comprehensive functions Transreac is very well suitable for such simulations. Transreac was able to calculate the dimension of the corroded zone of concrete structures in contact with high concentrated salt solutions as a function of time. These simulations cover a time span of some thousand years. Of course the correct function of the algorithm in this special chemical system was tested by comparing calculated results with results of short time laboratory experiments. In an actual project the change of the permeability of structures made of some special mineral building materials during percolation with aggressive solutions is prognosticated.

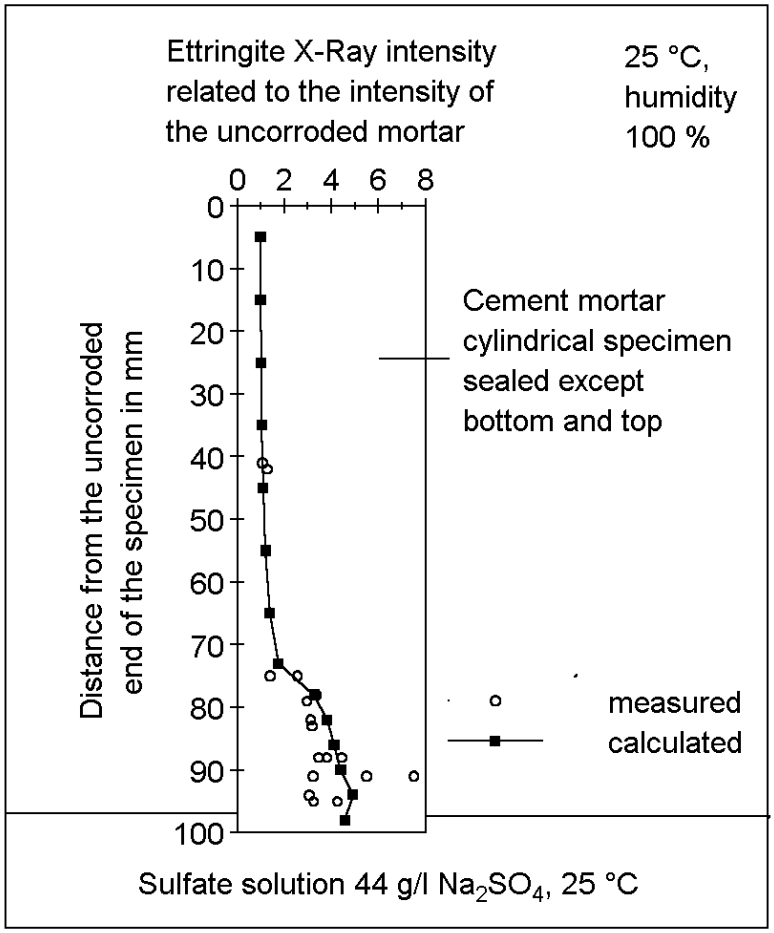

Fig. 2: Ettringite-profile of cement mortar after 303 days of sulphate attack (from Schmidt-Döhl and Rostásy (1999c)).

The aim of another project is, to extend Transreac to an adaptive model. Adaptive model in this case means that the model is able to improve its accuracy itself by the use of measured data from the structure. This concept of an adaptive durability prognosis therefore needs a time span for observing the structure. But it takes into account the real properties of the built structure. Another advantage is, that the accuracy of the durability prognosis is improved, in spite of the possibility to use only crude estimated initial material properties. This research is a part project of the collaborative research center SFB 477 (http://www.sfb477.tu-bs.de) "life cycle assessment of structures via innovative monitoring" of the Deutsche Forschungsgemeinschaft. The extension of Transreac to an adaptive model and first results are described in detail in Schmidt-Döhl et al. (2000).

Another project has the aim to extend Transreac to a probabilistic model by combining it with a Monte-Carlo-simulation. A precondition for this extension is the reduction of calculation time by using more efficient algorithms. In addition, the extended program will allow the simulation of redox-reactions, which is not possible at the moment, because of the incorporated GEM-module. This research is part of the priority program "prognosis of the time dependent chemical-physical damage of mineral building materials" of the Deutsche Forschungsgemeinschaft.

REMARKS, OPERATION AND TERMS OF DELIVERY

Transreac is available for MS-Windows-systems. The program system, the source code of the post-processor (Fortran), a simulation example and the manual are available without charges. Support is with costs. The output-language of the program and the manual is in German. The pre-processor does not include an automatic examination of the input data for completeness and to be plausible. It is therefore absolutely necessary to understand and examine every input parameter of Transreac when starting to simulate a new problem. The initial period to get familiar with the program system is at least 6 months. Good knowledge of physical chemistry is necessary. It is therefore highly recommended to charge the testing laboratory for civil engineering in Braunschweig to solve a corrosion problem with Transreac.

REFERENCES

Gaber, K. (1989): *Einfluß der Porengrößenverteilung in der Mörtelmatrix auf den Transport von Wasser, Chlorid und Sauerstoff im Beton*. Dissertation, Technische Hochschule Darmstadt (in German)

Künzel H.M. (1994): Verfahren zur ein- und zweidimensionalen Berechnung des gekoppelten Wärme- und Feuchtetransportes in Bauteilen mit einfachen Kennwerten, Dissertation, Universität Stuttgart (in German)

Schmidt-Döhl, F. (1996): *Ein Modell zur Berechnung von kombinierten chemischen Reaktions- und Transportprozessen und seine Anwendung auf die Korrosion mineralischer Baustoffe*, Dissertation, Technische Universität Braunschweig, Heft 125, Schriftenreihe des Instituts für Baustoffe, Massivbau und Brandschutz der TU Braunschweig, ISBN 3-89288-104-9 (in German)

Schmidt-Döhl, F., Bruder, S. and Budelmann, H. (2000): Adaptive model for the prognosis of durability during the monitoring of concrete structures. In: Proceedings of the 14. Internationale Baustofftagung ibausil, Weimar, 20.-23.9.2000, Vol.1, 1001-1008

Schmidt-Döhl, F. and Rostásy, F.S. (1999a): A model for the calculation of combined chemical reactions and transport processes and its application to the corrosion of mineral building materials. I. Simulation model, Cement and Concrete Research, 29, 1039-1046

Schmidt-Döhl, F. and Rostásy, F.S. (1999b): A model for the calculation of combined chemical reactions and transport processes and its application to the corrosion of mineral building materials. II. Experimental Verification, Cement and Concrete Research, 29, 1047-1054

Schmidt-Döhl, F. and Rostásy, F.S. (1999c): A model for the simulation of chemical attack on mineral building materials. In: Proceedings of the RILEM-ACI-OECD 8th International Expertcentrum Conference on life prediction and aging management of concrete structures, Bratislava, 6.-8.7.1999 (RILEM, 1999) 50-55

HUMIC COLLOID BORNE AMERICIUM MIGRATION: A STRONGLY COUPLED TRANSPORT/REACTION PROCESS

W. Schüßler, R. Artinger, B. Kienzler and J.I. Kim
Forschungszentrum Karlsruhe, Institut für Nukleare Entsorgungstechnik, P.O. Box 3640
D-76021 Karlsruhe, Germany; E--mail: wolfram@ine.fzk.de

The Gorleben salt dome (Lower Saxony, Germany) has been investigated for disposal of high level radioactive waste (HLW). In the aquifer system overlying the salt dome, dissolved organic carbon (DOC) concentrations up to 200 mg/L are found (Buckau, 1991). This DOC mainly consists of colloidal humic and fulvic acids. As humic colloids strongly bind multivalent metal ions (Czerwinski et al., 1996), their potential impact on the migration of radionuclides, especially actinides, has to be determined for performance assessment.

Laboratory investigations on humate mediated metal ion transport has been conducted by both column and batch experiments (e.g. (Zeh, 1993, Randall et al., 1994, Klotz and Lazik, 1995, Artinger et al., 1998). The results of these experiments are attributed to and modeled by three different approaches:

(1) Filtering of metal ion bearing colloids.

(2) Sorption/exchange of metal ion bearing colloids with sediment bound humic matter.

(3) Dissociation of colloid bound metal ions followed by sorption onto the sediment.

Filtration processes of colloids are functions of flow velocity and particle size. Therefore, if one assumes filtration of metal ion bearing colloids, a change in the flow velocity in column experiments would be expected to have considerable influence on the size distribution of the of humic colloid in the effluent. Under the same assumption a variation of the reaction time prior to the pulse injection could only affect the metal recovery, if the size distribution of the humic colloid bound metal ion is changed.

Assuming local equilibrium, sorption or exchange of metal ion bearing colloids with sediment bound humic matter, and dissociation of colloid bound metal ions followed by sorption onto the sediment results always in a retardation of the metal ion breakthrough compared to an ideal tracer. Taking into account kinetically controlled reactions for both mechanisms allows to account for retarded and unretarded fractions.

Attempts to model humic colloid/actinide migration experiments by means of thermodynamic equilibrium have not been successful. This is due to the lack of identification and quantification of unambiguous equilibrium.

The Ca breakthrough of an experiment of Klotz and Lang, 1996 in a humic rich groundwater by means of thermodynamic equilibrium can be modeled with Ca surface interaction or without Ca surface interaction. Calculations using the first assumption results in non retarded Ca breakethrough ($R_f = 1$) with a recovery of 100 %. Using the second assumption a retarded Ca fraction is calculated. In contradiction the observed Ca breakthrough curve showed a minor peak with a retention factor of 1 and a major peak with a retention factor of approximately 8. The only way to model this experiment with an equilibrium approach is the ad hoc assumption of the existence of two different non interacting Ca species. The distribution between these two species can not be defined prior to the experiment, and consequently, no prediction of the elution behavior is possible.

Using actinide sorption experiments to predict actinide migration experiments arises another problem. Distribution coefficients (K_d values) determined in batch experiments can only be used to predict the retention factors observed in column experiments, if local equilibrium can be assumed. Zeh,1993 predicted from Am-batch-K_d-values an Am-breakthrough with a retention factor of 250. In contradiction the column experiments showed about 70 % of the Am to elute unretarded (R_f = 1). Consequently, he suspected kinetically controlled processes to be involved in the metal ion humic acid association/dissociation reactions. Also several other experimentalists (Choppin and Nash, 1981, Yu et al., 1996, Cacheris and Choppin, 1987, Bonifazi et al., 1996, Rao et al., 1994) discussed kinetically controlled metal ion humic acid interactions.

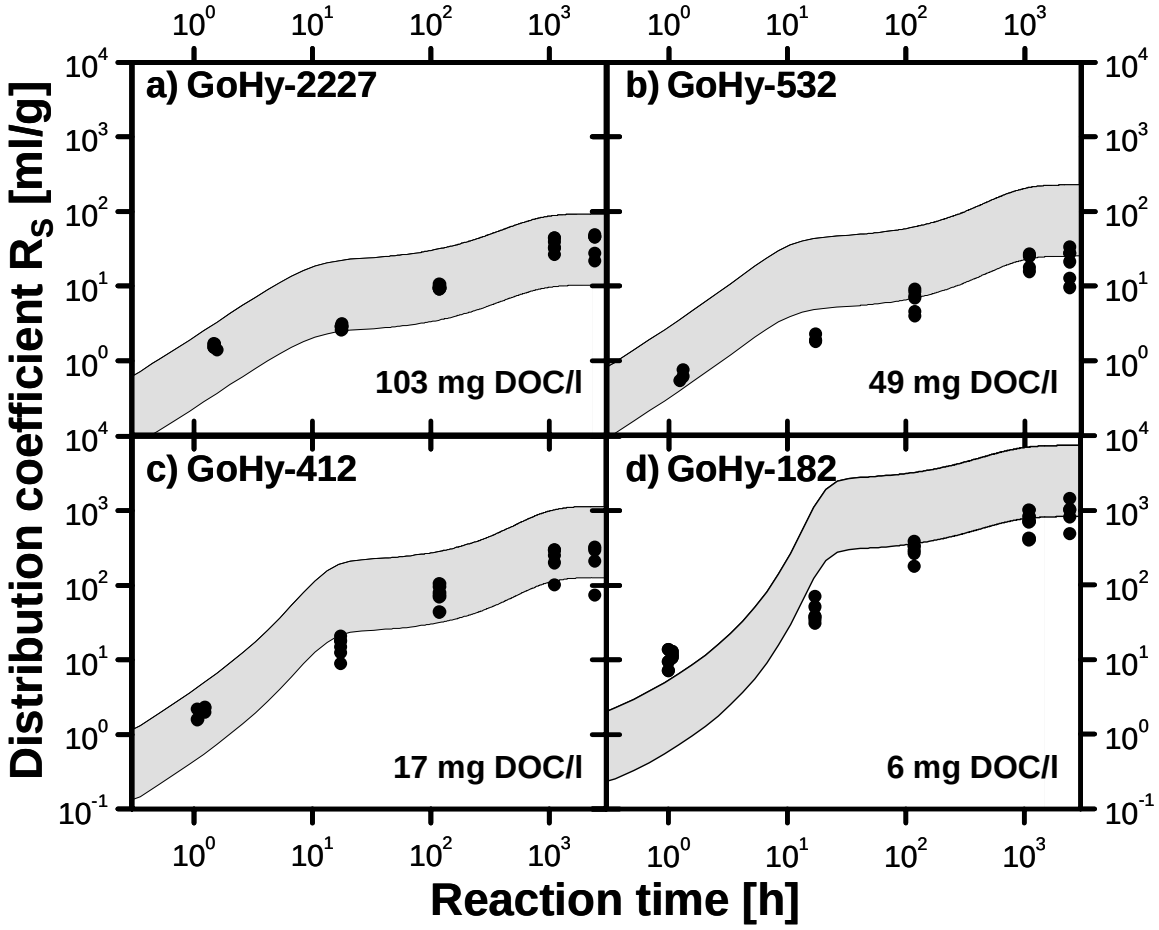

Figure 3: Experimental and modeling results of the temporal development of the distribution coefficient in four Gorleben groundwater sand systems The shaded area corresponds to the model results (KICAM), taking into account the model uncertainty of a factor of 3.

At our institute the colloid borne Am(III) transport was investigated in laboratory for Gorleben groundwater/sand systems. Both batch and column experiments were performed for 4 different groundwaters with humic substance concentrations from 6 to 100 mg/l (DOC). In the batch experiment, the sorption equilibrium was not attained up to a reaction time of 250 days (Fig. 1). The determined sorption coefficient increased during the reaction period by two orders of magnitude. Enhanced humic substance concentrations were found to reduce the sorption onto the sediment.

The column experiments were performed varying the pore water flow velocity, the column length and the Am/groundwater contact time prior to injection onto the column from one experiment to another. The recovery of Am(III) was found to increase with increasing pore water flow velocity (Fig. 2), with decreasing column length, with increasing Am/groundwater contact time, and with increasing DOC.

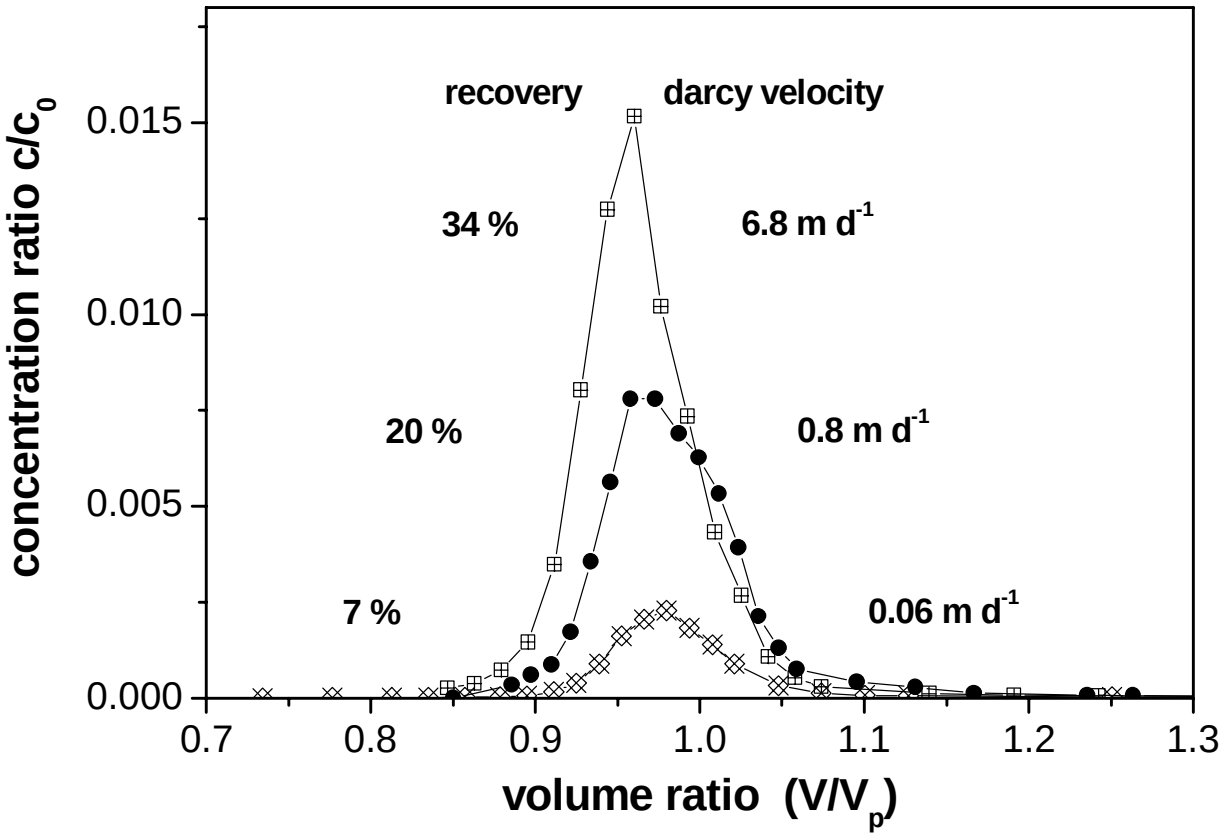

Figure 4: Am breakthrough curves and recovery in column experiments for a Gorleben groundwater/sand system (GoHy-2227) rich in humic colloids (100 mg DOC dm^{-3}) for different pore water flow velocities in the column.

Attempts to model these results by means of thermodynamic equilibrium in combination with filtration of humic colloids were not successful. Consequently, a kinetic model, i.e. Kinetically Controlled Availability Model (KICAM, Fig. 3), was developed to adequately describe actinide sorption and transport in laboratory batch and column experiments. The KICAM is based on the kinetics of the reactions of Am with humic colloids.

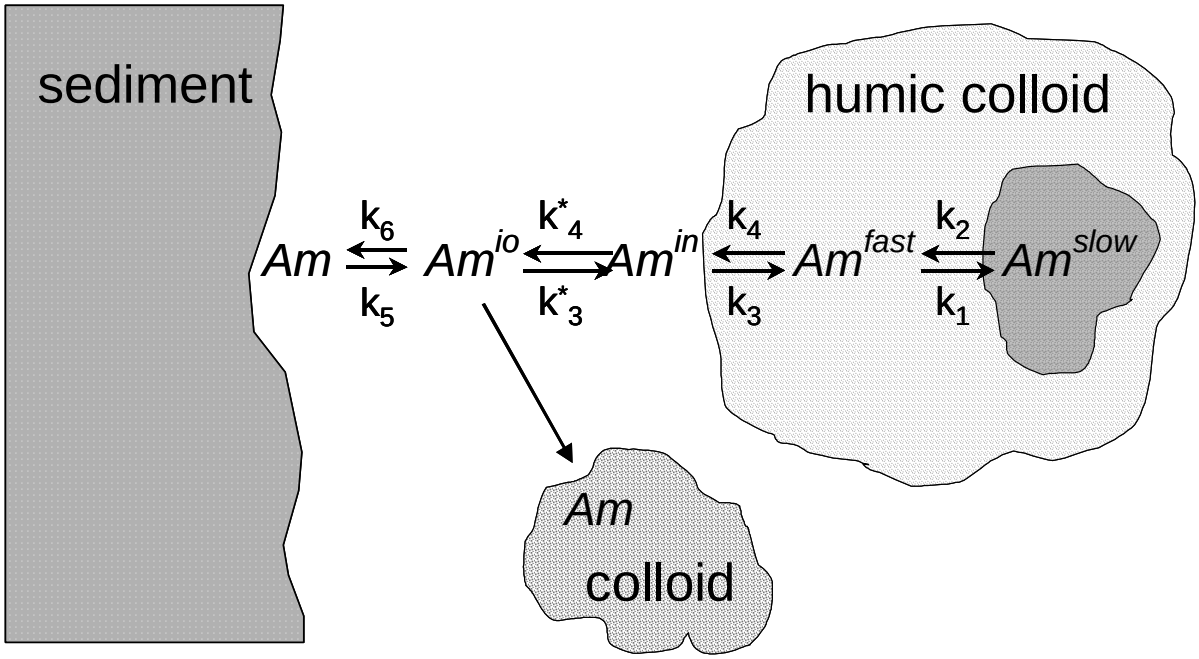

Figure 5: Concept of the refined Kinetically Controlled Availability Model (KICAM)

Model parameters are determined by fitting to experimental data. The result is an adequate and consistent description of both column and batch experiments (see Fig. 1 shaded areas) under various conditions and verifies the predominant impact of humic colloids on the chemical behavior of actinide ions in groundwater. The approach appears to be a major achievement compared to previous attempts applying equilibrium approaches in combination with filtering of colloids.

REFERENCES

Buckau, G.; Freie Universität: Berlin, **1991**; p 167.

Czerwinski, K. R.; Kim, J. I.; Rhee, D. S.; Buckau, G. *Radiochim. Acta* **1996**, *72*, 179-187.

Zeh, P.; TU Munich: Munich, **1993**; p 170.

Randall, A.; Warwick, P.; Lassen, P.; Carlsen, L.; Grindrod, P. *Radiochim. Acta* **1994**, *66/67*, 363-368.

Klotz, D.; Lazik, D. *Isotopes Environ. Health Stud.* **1995**, *31*, 61-75.

Artinger, R.; Kienzler, B.; Schüßler, W.; Kim, J. I. *J. Contam. Hydrol.* **1998**, *35*, 261-275.

Klotz, D.; Lang, H. Institute of Hydrology, GSF-National Research Center for Environment and Health, **1996**.

Choppin, G. R.; Nash, K. L. *J. inorg. nucl. Chem.* **1981**, *43*, 357-359.

Yu, Y. S.; Bailey, G. W.; Xianchan, J. *J. Environ. Qual.* **1996**, *25*, 552-561.

Cacheris, W. P.; Choppin, G. R. *Radiochim. Acta* **1987**, *42*, 185-190.

Bonifazi, M.; Pant, B. C.; Langford, C. H. *Environ. Tech.* **1996**, *17*, 885-890.

Rao, L.; Choppin, G. R.; Clark, S. B. *Radiochim. Acta* **1994**, *66/67*, 141-147.

HIGH-pH PLUME. REACTIVE TRANSPORT SIMULATIONS

Josep M. Soler[1] and Urs K. Mäder[2]
1-Institut de Ciències de la Terra "Jaume Almera" (CSIC), Lluís Solé i Sabarís s/n,
E-08028 Barcelona, Spain; E-mail: jsoler@ija.csic.es
2-Rock-Water Interaction Group, University of Bern, Baltzerstrasse 1, CH-3012 Bern,
Switzerland; E-mail: urs@mpi.unibe.ch

INTRODUCTION

Cement is a major component of the engineered barrier system in proposed underground repositories for low- and intermediate-level radioactive waste. The interaction between the hyperalkaline solutions derived from the degradation of cement and the rocks hosting such repositories may change the physical and chemical properties of the host rock.

Two examples of reactive transport modeling of the evolution of such systems will be shown. One corresponds to the case of the proposed repository at Wellenberg (Switzerland), where the host rock is a fractured marl. The other one has to do with the GTS-HPF project (Grimsel Test Site - Hyperalkaline Plume in Fractured Rock), where the rock is a fractured granodiorite.

In all the cases a modified version of the GIMRT software package (Steefel and Yabusaki, 1996) has been used for the reactive transport calculations. Both diffusive/dispersive and advective solute transport are taken into account in the calculations. Mineral reactions are described by kinetic rate laws. The reaction rates for the primary minerals are based on experimentally-determined rates published in the literature and geometric considerations regarding mineral surface areas. Relatively fast rates for the secondary minerals have been used, so the results resemble the local equilibrium solution for these minerals.

THE CASE OF WELLENBERG

Calculations simulating the interaction between hyperalkaline solutions and a fractured marl, at 25^{o}C, have been performed. Solute transport and chemical reaction are considered in both a high permeability zone (fracture), where advection is important, and the wall rock, where diffusion is the dominant transport mechanism.

The primary minerals that make up the rock in the simulations are calcite, dolomite, quartz, and muscovite (as a surrogate for illite, illite/smectite, and chlorite). The fluid flow system under consideration is a two-dimensional porous medium (marl, 1% porosity), with a high permeability zone simulating a fracture (10% porosity) crossing the domain. The fracture starts right at the flow inlet boundary, which is equivalent to the assumption of a worst case scenario, with a highly conductive feature starting right at the repository. The dimensions of the domain are 6 m per 1 m, and the fracture width is 10 cm. The fluid flow field is updated during the course of the simulations by solving the equation of conservation of fluid mass with the updated porosities and permeabilities. Permeabilities are updated according to Kozeny's equation.

The composition of the solutions entering the domain is derived from modeling studies of the degradation of cement under the conditions at the proposed underground repository at Wellenberg (Neall, 1994). These are high-pH solutions at equilibrium with calcite and undersaturated with respect to the other primary minerals.

Four different cases have been considered. These four cases are representative of the two different types of groundwater (a more dilute $NaHCO_3$-type and a more saline NaCl-type) present at Wellenberg and two different stages in the process of degradation of cement (pH 13.5 and pH 12.5).

The results of the calculations show only small differences between the $NaHCO_3$ system and the NaCl system. However, the results with the two different pH values are quite different. In both cases, the flow velocity in the fracture diminishes with time, due to a decrease in porosity. However, the decrease in porosity and flow velocity is much more pronounced in the lower pH case. Also, the extent of the zone of mineral alteration along the fracture is much more limited in the lower pH case (1 to 2 m along the fracture after 20000 years). For the higher pH case, mineral alteration affects the whole length of the flow domain along the fracture (6 m) after only 5000 y.

One of the main mineral reactions in these systems is the dissolution of the dolomite initially present in the rock (fracture) and its replacement (partial or total) by calcite. A markedly advancing reaction front is defined by this reaction in the higher pH system.

The magnesium released by the dissolution of dolomite is taken by the precipitation of brucite and sepiolite (a Mg-phyllosilicate). Brucite dominates near the fracture inlet and at earlier stages of the process. Sepiolite is the dominant Mg-containing phase further from the fracture inlet and also at later stages (brucite tends to dissolve and be replaced by sepiolite with time in the lower pH cases).

Other secondary minerals that precipitate during the simulations are analcime and natrolite (zeolites) and tobermorite (a CSH phase). The amount of reaction affecting quartz (dissolution) and muscovite (dissolution and precipitation) is relatively minor.

Since the biggest source of uncertainty for the reaction rates arises from the value of the surface areas used for the primary minerals, additional calculations making use of smaller values of these areas have also been performed. The results show that the smaller surface areas result in a smaller reactivity of the system and smaller porosity changes. These smaller porosity changes mean that porosities near the fracture inlet are larger than in the calculations with larger surface areas. The larger porosities translate into larger Darcy velocities along the fracture (less favorable for the performance of a repository), showing that the coupling between chemical reaction, which drives the changes in porosity, and fluid flow is very important.

In summary, the results of the simulations suggest that the net result of the interaction between the high-pH solutions derived from the degradation of cement and the fractured marl is a reduction of porosity and water velocity along the fractures. This result would actually be highly beneficial for the performance of a repository hosted by the Valanginian marls at Wellenberg. However, the magnitude and scale (spatial and temporal) of this evolution is open to a large degree of uncertainty.

THE HPF PROJECT AT THE GRIMSEL TEST SITE

One of the objectives of the GTS-HPF project is to study the alteration of the Grimsel granodiorite due to the circulation of high-pH solutions derived from the degradation of cement through the fractures present in the rock. A K-Na-Ca-rich high-pH solution is currently being continuously injected through a borehole into a fracture. An extraction borehole is located about one meter away from the injection borehole. The planned duration of the experiment is one year. A laboratory version of the experiment was performed at the University of Bern.

(a)One-dimensional simulations. The primary minerals that make up the rock in the simulations are quartz, albite, microcline, phlogopite and muscovite. A number of possible secondary phases have been considered in the calculations (brucite, ettringite, gibbsite, kaolinite, portlandite and several zeolites, CSH and CASH phases). Maximum available mineral surface areas are estimated from BET measurements of fault gouge. The initial

surface areas for the secondary minerals in the model are about 10000 times smaller than for the primary minerals. Temperature is 12^{o}C.

The fluid flow system under consideration is a one-dimensional porous medium simulating a single flow path through a fracture which is filled by fault gouge.

The model results show that the circulation of the hyperalkaline solution through the fracture causes the dissolution of albite, microcline and quartz in the fault gouge (the solutions reach saturation with respect to microcline in a relatively short distance). Muscovite dissolves close to the injection borehole and precipitates further away. Phlogopite does not react. Regarding the secondary minerals, there is precipitation of tobermorite (a CSH phase) close to the injection borehole and prehnite (a CASH phase) further away. There is also minor mesolite (a Na-Ca-zeolite) precipitation towards the end of the prehnite zone.

Maximum surface areas in the model are constrained by BET measurements of the specific surface area of fault gouge material (8 m^2/g). However, this only provides maximum available surface areas. It is possible that the solutions do not have access to all the mineral surface area. The extension of the reaction zones and the amount of mineral that reacts depends on the available surface area for reaction. The results (magnitude, mineralogy and extension of the reaction zones) from both the field experiment and the small-scale laboratory experiment should provide constraints regarding the values of the surface areas to be used in the calculations.

All the results show a decrease in porosity close to the injection borehole and an increase in porosity further away. Such an evolution of the porosity of the fracture infill would be beneficial for the performance of a repository, and it is consistent with the results of the laboratory experiment, which indicate a decrease in the permeability of the fracture with time.

(b)Two-dimensional simulations have been performed making use of the heterogeneous flow field calculated from the results of conservative tracer tests at the Grimsel Test Site (Pfingsten and Soler, 2002). The domain of the simulations is a square region of the fracture plane including the injection and extraction boreholes (Fig. 1). Mineral surface areas (ranges of values) are calculated from specific surface areas (BET) measured on the fine-grained fault gouge filling the fractures and geometric considerations.

The interaction between the injected hyperalkaline solution and the rock (fault gouge filling the fracture) causes a series of mineral reactions. The main processes are the dissolution of albite and precipitation of tobermorite (CSH phase), prehnite (CASH phase) and mesolite (Na-Ca zeolite) close to the injection borehole, which causes a decrease in porosity, and the precipitation of natrolite and analcime (Na-zeolites) farther away down the flow field. Figure 1 shows the pH distribution in the fracture after one year since the start of injection of the high-pH solution (the planned duration of the experiment). The two plots correspond to two different values of the initial surface areas of the primary minerals. A single value of porosity (30%) was used in the calculations. Also, the flow field was not updated during the calculations (Darcy velocities were assumed to be constant with time). Even with these simplifications, the results show that a large degree of spatial heterogeneity is expected, given the heterogeneous nature of the flow field. Also, the amount of reaction (reflected in the figure by changes in pH) is greatly dependent on the available reactive surface area.

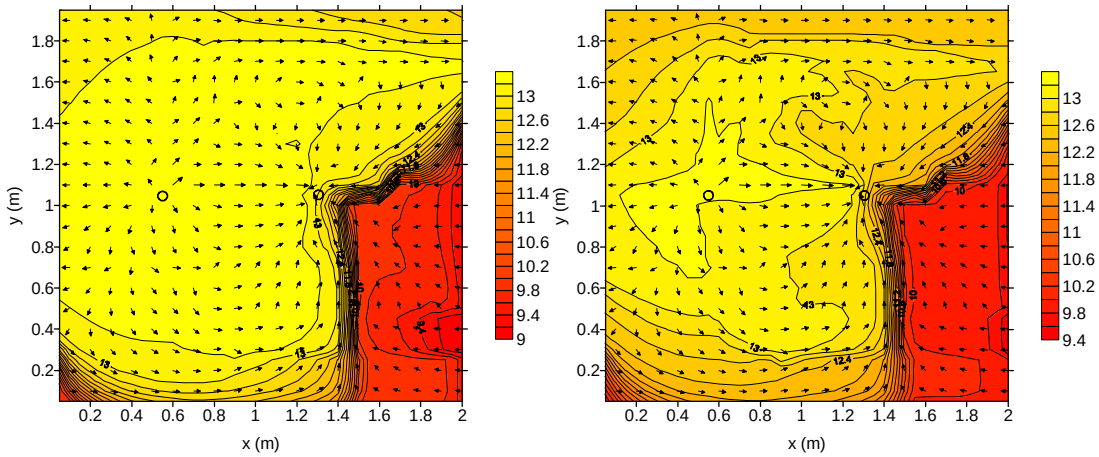

Figure 1: pH distribution in the fracture after one year since the start of injection of the high-pH solution. The circles show the location of the injection and extraction boreholes. The arrows show the flow field in the fracture. The two figures correspond to initial surface areas for primary minerals of the order of 10^6 m^2/m^3rock (left) and 10^7 m^2/m^3rock (right).

CONCLUSIONS

The results of reactive transport calculations simulating the interaction between the hyperalkaline solutions derived from the degradation of cement and potential host rocks for repositories of low- and intermediate-level radioactive waste suggest that mineral reaction will tend to progressively seal the pores of the rocks and diminish the hydraulic conductivity of these systems. The results from small-scale laboratory experiments with Grimsel granodiorite and Opalinus Clay (Adler, 2001) support these modeling conclusions.

REFERENCES

Adler M. (2001) *Interaction of Claystone and Hyperalkaline Solutions at 30°C: A Combined Experimental and Modeling Study*. Ph.D. Thesis, University of Bern, Switzerland.

Neall F. B. (1994) Modelling of the Near-Field Chemistry of the SMA Repository at the Wellenberg Site. PSI Bericht 94-18. Also published as Nagra Technical Report NTB 94-03.

Pfingsten W. and Soler J. M. (2002) Modelling of Non-Reactive Tracer Dipole Tests in a Shear Zone at the Grimsel Test Site. Journal of Contaminant Hydrology (submitted).

Steefel C. I. and Yabusaki S. B. (1996) OS3D/GIMRT, Software for Multicomponent - Multidimensional Reactive Transport: User's Manual and Programmer`s guide. PNL-11166, Pacific Northwest National Laboratory, Richland WA.

COLONBO : A DIFFUSION-BASED MODEL TO ASSESS RADIONUCLIDE RELEASE AND MIGRATION DURING DEEP GEOLOGICAL DISPOSAL OF BITUMINIZED WASTE

C. Tiffreau[1], B. Simondi-Teisseire[1], I. Felines[1], S. Camaro[1], P.P. Vistoli[1] and V. Blanc[2]

1- CEA Centre d'Etudes de Cadarache, Département d'Etudes des Déchets,
13108 St Paul lez Durance, France; E-mail: tiffreau@desdsud.cea.fr
2- COGEMA, 1 rue des hérons, 78182 St Quentin en Yvelines cedex, France

Bitumen is being used for many years in France as an embedding matrix for the conditioning of low and medium level activity waste resulting from nuclear effluent treatment. Long term management options for this kind of waste include at present deep geological disposal. As a consequence, research programmes are being conducted by CEA and COGEMA in order to assess the long-term leaching behaviour of bituminized waste in deep geological conditions. For this purpose, the COLONBO model has been developed to predict the release of chemical species through the bitumen matrix and the subsequent radionuclide migration in the deep geological near field.

Several assumptions have been used to enable the build-up of the COLONBO model. Radionuclides initially present in the waste package are associated with a mixture of soluble ($NaNO_3$ and Na_2SO_4) and slightly soluble (mainly $BaSO_4$) salts. These salts resulting from the effluent insolubilization treatment, are considered to be homogeneously dispersed in the bitumen matrix. Under leaching, adsorption and solubilization of water in the bitumen occur at the wasteform surface, followed by diffusive transport of water through the bitumen matrix. As a consequence, the soluble salts are progressively dissolved by water accumulation, resulting in a local swelling of the waste package. This swelling itself induces a local alteration of the diffusive properties of the bitumen matrix, allowing an outward diffusion of inactive dissolved salts and radionuclides. Although radionuclides are supposed to be associated with the least soluble salts used in the coprecipitation process, precise knowledge about their speciation are still lacking. Therefore, the release of each radionuclide is described by a lump solubility parameter. Chemical species can then diffuse through the storage facility near field (clay or concrete engineered barrier). The COLONBO model enables to account for up to three different barriers described by their respective porosity, diffusion and retention (Kd) parameters. In the whole system, water concentration profiles, the position of salt dissolution fronts and radionuclide near field migration are described by water conservation and Fickian diffusion equations in each area (waste package + barriers) of the wasteform. Due to the diffusive character of the transport, the alteration and radionuclide release proceed with the square root of time (provided that the salt concentration outside the system is kept constant). Our paper details the model specifications and gives some typical numerical results. Some related experimental issues will be also discussed in order to statue on the model validity.

« PÔLE GÉOCHIMIE TRANSPORT » - BENCHMARK II - : A STUDY OF THE EFFECTS OF IRON INJECTION IN A REACTIVE POROUS MEDIUM, IN THE SCOPE OF HLW NEAR-FIELD INTERACTIONS.

L. Trotignon[1], M.-E. Stoeckel[2] , J. Van der Lee[3], P. Montarnal[1], E. Piault[1], O. Bildstein[1], and F. Renard[4]
1- CEA/DEN France; E-mail: laurent.trotignon@cea.fr
2- EDF/LNH France
3- ENSMP/CIG France
4 – CEA/DAM France

The simulation of redox fronts has often been a numerical challenge for coupled transport-chemistry codes, because they display sharp contrasts of aqueous and mineral speciation pushing numerical solvers to their limits. The « Pôle Géochimie Transport », grouping several research institutes in France (CEA, IRSN, EdF, ENSMP), has proposed a stepwise benchmark from a 1-D purely diffusive test-case to a 2-D configuration, coupling diffusion, convection and the development of redox fronts.

The geochemical scenario is based on the injection of iron, simulating a canister corrosion, at one limit of a porous medium in which alumino-silicates and carbonates react and transform to new iron bearing phases.

First results of the benchmark in 1-D configurations, obtained with Hytec and Chemtrap are presented and commented.

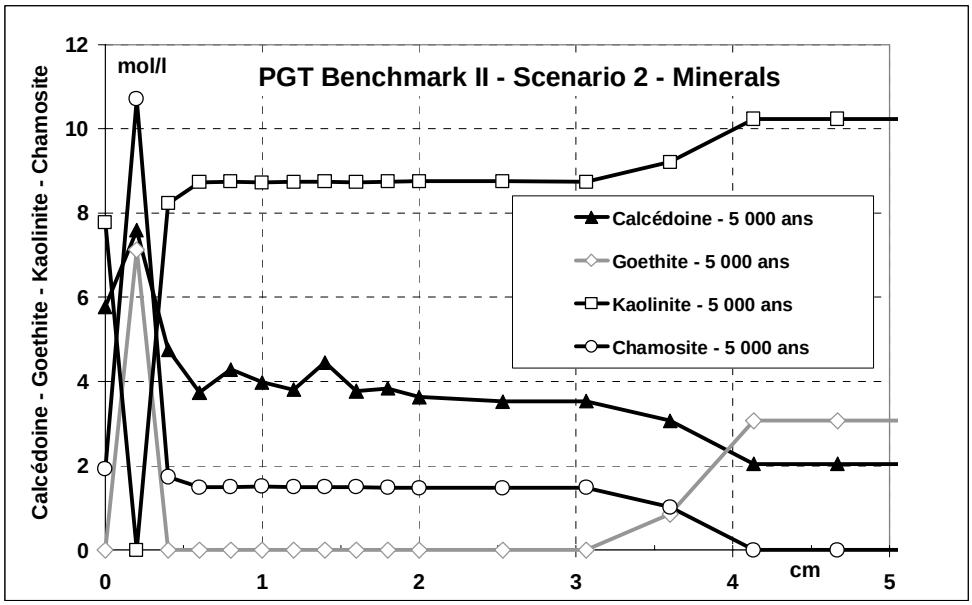

Spatial profiles of main minerals after 5000 years of iron injection (scenario 2). The iron is injected at x = 0 cm. Upon the injection of iron, goethite is reduced and transformed with kaolinite to produce chamosite. When the initial goethite is exhausted, the excess iron forms an internal zone with accumulation of secondary goethite together with chamosite. The excess silica precipitates as chalcedony.

COLLOIDS IN FRACTURED AND POROUS HYDROGEOLOGIC MEDIUM

Jan van der Lee and Laurent De Windt

Centre d'Informatique Géologique
École des Mines de Paris
35, rue Saint Honoré,
77300 Fontainebleau, France

ABSTRACT

The mobility, apparent solubility and toxicity of heavy or hazardous metals and radionuclides in subsurface aquifers strongly depends on the solution chemistry as well as on interactions with mineral and colloidal phases. Organic and inorganic colloids are omnipresent in natural media and notably in subsurface systems and are often considered as potentially rapid vehicles for pollutants. Whether colloidal transport is effective, however, critically depends on the strength of the bond formed with the contaminant and also on the actual mobility of the colloidal species. Reactive transport models are increasingly used for groundwater pollution studies. They couple microbiological and/or geochemical reactions with hydrodynamic migration of species and, sometimes, include colloidal transport. Due to a certain lack in scientific knowledge and consensus on the matter, retention mechanisms of colloidal species are generally disregarded. Here we address this issue in terms of a theory for colloidal retention in porous media.

INTRODUCTION

Organic and inorganic colloids are omnipresent in natural media and notably in subsurface systems. One of the first colloidal alerts has been given two decades ago by researches who found that radionuclides such as plutonium and americium traveled over a significant distance in colloidal form (Champ et al., 1982; Travis and Nuttall, 1985). These conclusions have been confirmed more recently by Kersting et al.(Kersting et al., 1999) and colloidal transport has been recognized as an important mechanism for migration of chemicals in natural systems in general. Multi-component transport codes which also account for reactive colloidal species are nevertheless scarce.

Part of the absence of colloidal migration in reactive transport models is related to the absence of databases including colloids and reactions with surfaces in general. Except for the surface complexation data for hydrous ferric oxide proposed more than a decade ago

(Dzombak and Morel, 1990), no equivalent dataset for other solid phases, colloidal or mineral, has been published since. Another part of the problem of colloidal transport modeling is retention. Colloidal retention is, due to the size and surface properties of the colloids, subject to short and long range (electrostatic) forces, which do not fit into the common framework of thermodynamic equilibrium models. Moreover, when the transported matter is composed of larger species, such as organic macro-molecules (e.g., fulvic and humic-bound contaminants, herbicides, pesticides), industrial solvents, phosphate complexes and contaminated inorganic colloidal particles (e.g., clay particles, silica colloids, hydroxides), kinetics starts to play a role which affects adsorption, especially in column experiments at relatively high flow rates (Bouchard et al., 1988; Brusseau, 1992). Although important, in the present context we propose to focus on the retention only.

ADSORPTION OF COLLOIDS

A simplified size-related classification of retention mechanisms for colloidal particles is illustrated by Fig. 1. Here we distinguish constriction (filtration) and gravitational sedimentation for relatively large particles, i.e. with diameters superior to 1 μm. Accumulation in stagnant zones (*cul-de-sac*) may become significant for smaller sized particles. The overall effect of this type of retention is, however, mainly an additional tailing of the breakthrough curve, generally explained by kinetic retention and/or double-porosity approaches. Electrostatic forces always exist and may lead to retention of colloids. In most natural media, colloids are expected to be small: otherwise, filtration and sedimentation would have immobilized them in time. Electrostatic retention with, eventually, additional effects of stagnant zones and other kinetic processes related to thermal motion, is therefore probably the predominant retention process.

ELECTROSTATIC RETENTION

The retention of colloids is determined by the *retention capacity* of the medium, a function of short- and intermediate range interface forces. It is important to stress the dynamic nature of the retention capacity: electrostatic forces depend on the local geochemical conditions such as pH, ionic strength and mineral surface characteristics such as site-density. They therefore vary in time and space, especially in chemically very reactive systems such as cement-clay interfaces (De Windt et al., 2001). The following surface energies (from which the forces result) can be considered:

- electrostatic energy due to surface (de)protonation, complexation;
- electromagnetic molecular energy (van der Waals forces)
- short-range Born energies
- surface hydration energy
- energy resulting from a preferential orientation of (bipolar) water molecules

The first two energies are likely to dominate the attachment process but very short-range Born forces may play a significant role with respect to the fixation reaction. Surface roughness is an important factor with respect to reversibility or to fixation forces in general (Israelachvili and Wennerström, 1996). For example, Figure 2 illustrates surface roughness at molecular level due to protruding functional groups of a silica surface with neutral ≡Si—OH and negatively charged ≡Si—O^-. As a result, the point of action of electrostatic forces is slightly advanced with respect to the one of van der Waals and Born forces, which reduces the overall attractive force very close to the surface.

Mathematical expressions are available to simulate the energies mentioned above, leading to so-called *total interaction energy profiles* valid for two surfaces (van der Lee, 1997). Direct measurement of the resulting forces is possible via the atomic force microscope. For relatively pure materials such as colloidal silica, a rather good agreement is observed between the theory and experimental results (e.g. Fig. 3). When the two surfaces approach very closely, the agreement is less convincing which is possibly due to the effect of protruding surface groups as illustrated by Fig. 2.

The fixation capacity, s, is defined by the maximum number of colloids accumulated in a single layer on the medium surface (e.g. a sand grain, a fracture wall) and given by:

$$s = \frac{\chi}{2\sqrt{3}(\ell a)^2} \tag{1}$$

where a is the colloid radius (assuming spherical colloids) and ℓa represents an *effective* radius of the colloid, including eventual repulsive forces between the colloids. χ is the overall fixation probability, $\chi \in [0..1]$ and a complex function of electrostatic, van der Waals and Born energies and the thermal motion of the colloid. More precisely, $\chi = \chi_p + \chi_s$, where subscripts p and s refer to primary (strong) and secondary (weak) binding forces:

$$\chi_p = \Theta(V_b - V_s)[1 - \Theta(V_b - V_p)] \tag{2}$$

$$\chi_s = [1 - \Theta(V_{sb} - V_s)][1 - \chi_p] \tag{3}$$

with:

$$\Theta(\xi) = \exp\left[-\left(\frac{\xi}{\vartheta kT}\right)^2\right]. \tag{4}$$

V_b is the energy of the repulsive barrier, V_p the energy of the primary minimum and V_s the energy of the secondary minimum. Subsequent energy maxima and minima are ignored since they are generally very small. The unknown parameter is ϑ, the *escape coefficient*, yielding $\sim$1 for a thermal energy of kT J/K and 0 if the probability to escape from the primary minimum is inexistent. A value higher than 1 generally implies an external source of energy capable of desorbing the colloid, such as hydrodynamic forces. The probabilistic nature of χ originates from the randomness of thermal motion. Parameter ℓ is a function of electrostatic forces between particles. Hence both χ and ℓ vary with the chemistry of the solution.

So far, only a mono-layer of colloids is covered by the fixation capacity. As soon as coagulation occurs, the effective fixation capacity dramatically increases. A theoretical development of s under coagulating conditions is available and takes the following form:

$$s = [1 + p\chi'] \frac{\chi}{2\sqrt{3}(\ell a)^2} \tag{5}$$

where χ' denotes the coagulation probability (developed similarly to χ) and p is the number of layers possible in the current system, related to the pore-geometry but also to the coagulation probability, henceforth to electrostatics.

Since surface forces are the result of surface complexation reactions, the theory very briefly outlined above allows us to express colloidal fixation and coagulation as a function of true geochemical parameters, such as pH and ionic strength. The theory has been implemented in the geochemical code CHESS and illustrated for a simple system of colloidal ferric oxide in contact with quartz grains (van der Lee, 1998). Table 1 summarizes the system, defined by relatively well known, thermodynamic entities only: despite the complexity of the theory, only very few unknowns are left for which good estimates can be made. Figure 4 shows the fixation capacity as a function of two key-variables, pH and ionic strength. The figure shows an increased capacity around the pH of zero charge, and an overall increase of the amount of fixed colloids with ionic strength. This is expected, since at high ionic strength, repulsive forces tend to weaken.

Hence we dispose of a geochemical model which accounts for colloidal retention. CHESS is the geochemical reaction module of HYTEC, hence HYTEC can use this feature to simulate migration of reactive colloids.

COLLOID MIGRATION

In perfect analogy to aqueous species, colloids in natural aquifers are subject to advection, dispersion and diffusion. They are therefore readily incorporated in transport models, but that is generally not sufficient to account for colloidal effects with regard to pollutants and metals in particular. Indeed, colloids act as reactive surfaces, like mineral surfaces, but they are mobile, unless retained by processes as outlined above. Moreover, colloids can be created at chemical fronts (e.g. redox fronts), thus forming a new mobile phase with, eventually, new reactive surfaces. Inversely, colloids may dissolve as they enter zones where they are thermodynamically unstable, or coagulate and precipitate.

HYTEC is a reactive transport code currently used for groundwater pollution studies, safety assessment of nuclear waste disposals, geochemical studies and interpretation of laboratory column experiments (van der Lee et al., tion). HYTEC integrates most of the specific processes for inorganic and organic colloidal species and therefore allows to quantify the effect of colloids in geochemically complex systems. During the workshop, we will outline some aspects of HYTEC and show examples of colloid-enhanced migration in porous media.

REFERENCES

Bouchard, D., Wood, A., Campbell, M., Nkedi-Kizza, P. and Rao, P. (1988): Sorption nonequilibrium during solute transport. *J. Contam. Hydrol.*, 2:209–223.

Brusseau, M. (1992): Nonequilibrium transport of organic chemicals: the impact of pore-water velocity. *J. Contam. Hydrol.*, 9:353–368.

Champ, D., Merrit, W. and Young, J. (1982): Potential for the rapid transport of plutonium in groundwater as demonstrated by core column studies. In Lutze, W., editor, *"Scientific Basis for Radioactive Waste Management"*, 5:745–754, New-York.

De Windt, L., Pellegrini, D. and van der Lee, J. (2001): Reactive transport modeling of pH buffering in cement - clay systems. In Cidu, editor, *Water-Rock Interactions*, pages 1315–1318, Sardaigne (Italie):

Dzombak, D. and Morel, F. (1990): *Surface Complexation Modeling. Hydrous Ferric Oxide.* John Wiley & Sons, New York.

Israelachvili, J. and Wennerström, H. (1996): Role of hydration and water structure in biological and colloidal interaction. *Nature*, 379:285–295.

Kersting, A., Efurd, D., Finnegan, D., Rokop, D., Smith, D. and Thompson, J. (1999): Migration of plutonium in ground water at the Nevada Tet Site. *Nature*, 397:56–59.

Travis, J. and Nuttall, H. (1985): A transport code for radiocolloid migration: with assessment of an actual low-level waste site. In *Mat. Res. Soc.*, volume 44 of *symp. proc.*, pages 969–976.

van der Lee, J. (1997): *Modélisation du comportement géochimique et du transport des radionucléides en présence de colloïdes.* PhD thesis, École des Mines de Paris, Paris, France.

van der Lee, J. (1998): Thermodynamic and mathematical concepts of CHESS. Technical Report LHM/RD/98/39, CIG, École des Mines de Paris, Fontainebleau, France.

van der Lee, J., De Windt, L., Lagneau, V. and Goblet, P. (2002, submitted for publication): Module-oriented modeling of reactive transport with HYTEC. *Computers & Geosciences.*

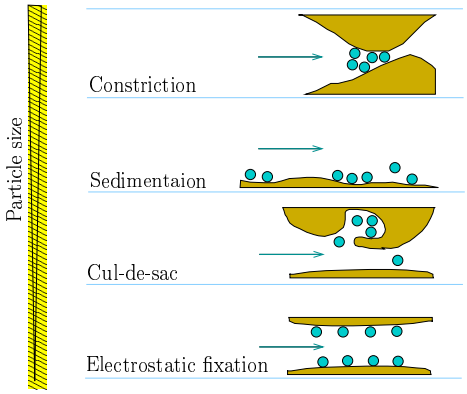

Figure 1: Different retention mechanisms for particles in porous or fractured media with an approximate dependence on size.

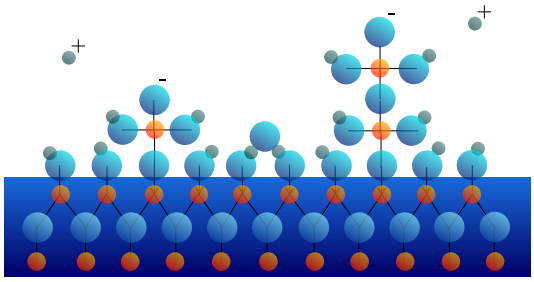

Figure 2: Schematic illustration of molecular roughness by protruding surface groups for a silica surface.

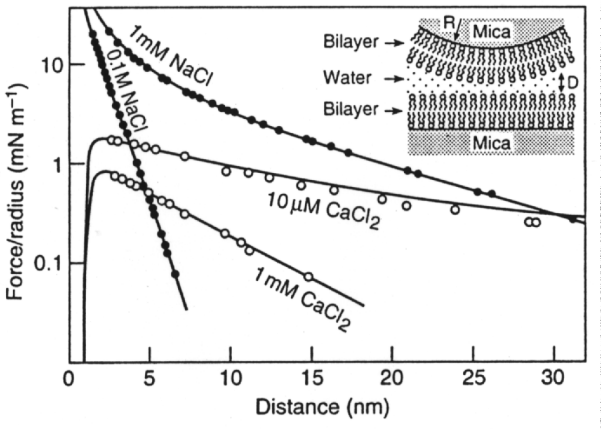

Figure 3: Direct measurement (atomic force microscope) of interaction forces for two lipid bi-layers and comparison with theoretically calculated curves. After (Israelachvili and Wennerström, 1996).

$Fe(OH)_3$(s) :		
concentration	: 1	g/l
site density of $\equiv Fe(OH)_3^s—OH$	: 0.093	μeq/m^2
site density of $\equiv Fe(OH)_3^w—OH$	: 3.745	μeq/m^2
radius	: 10	nm
specific surface	: 69.34	m^2/g
volumic mass	: 3114	kg/m^3
major reactions:		
$\equiv Fe(OH)_3^s—OH + H^+ \rightleftharpoons \equiv Fe(OH)_3^s—OH_2^+$		$\log(K) = 7.29$
$\equiv Fe(OH)_3^w—OH + H^+ \rightleftharpoons \equiv Fe(OH)_3^w—OH_2^+$		$\log(K) = 7.29$
$\equiv Fe(OH)_3^s—OH \rightleftharpoons \equiv Fe(OH)_3^s—O^- + H^+$		$\log(K) = -8.93$
$\equiv Fe(OH)_3^w—OH \rightleftharpoons \equiv Fe(OH)_3^w—O^- + H^+$		$\log(K) = -8.93$
Quartz :		
concentration	: 1	kg/l
site density of $\equiv$Quartz—OH	: 4	μeq/m^2
volumic mass	: 2648	kg/m^3
specific surface	: 0.001	m^2/g
major reactions:		
$\equiv$Quartz—OH $\rightleftharpoons \equiv$Quartz—$O^- + H^+$		$\log(K) = -7.0$
$\equiv$Quartz—ONa $\rightleftharpoons \equiv$Quartz—$OH - H^+ + Na^+$		$\log(K) = -6.7$
General :		
electrolyte	: NaCl	
dissolution	: *disabled*	
precipitation	: *disabled*	

Table 1: Parameter configuration for the simulation of fixation in presence of coagulation of a hydrous ferric oxide suspension in a quartz medium (flat surfaces).

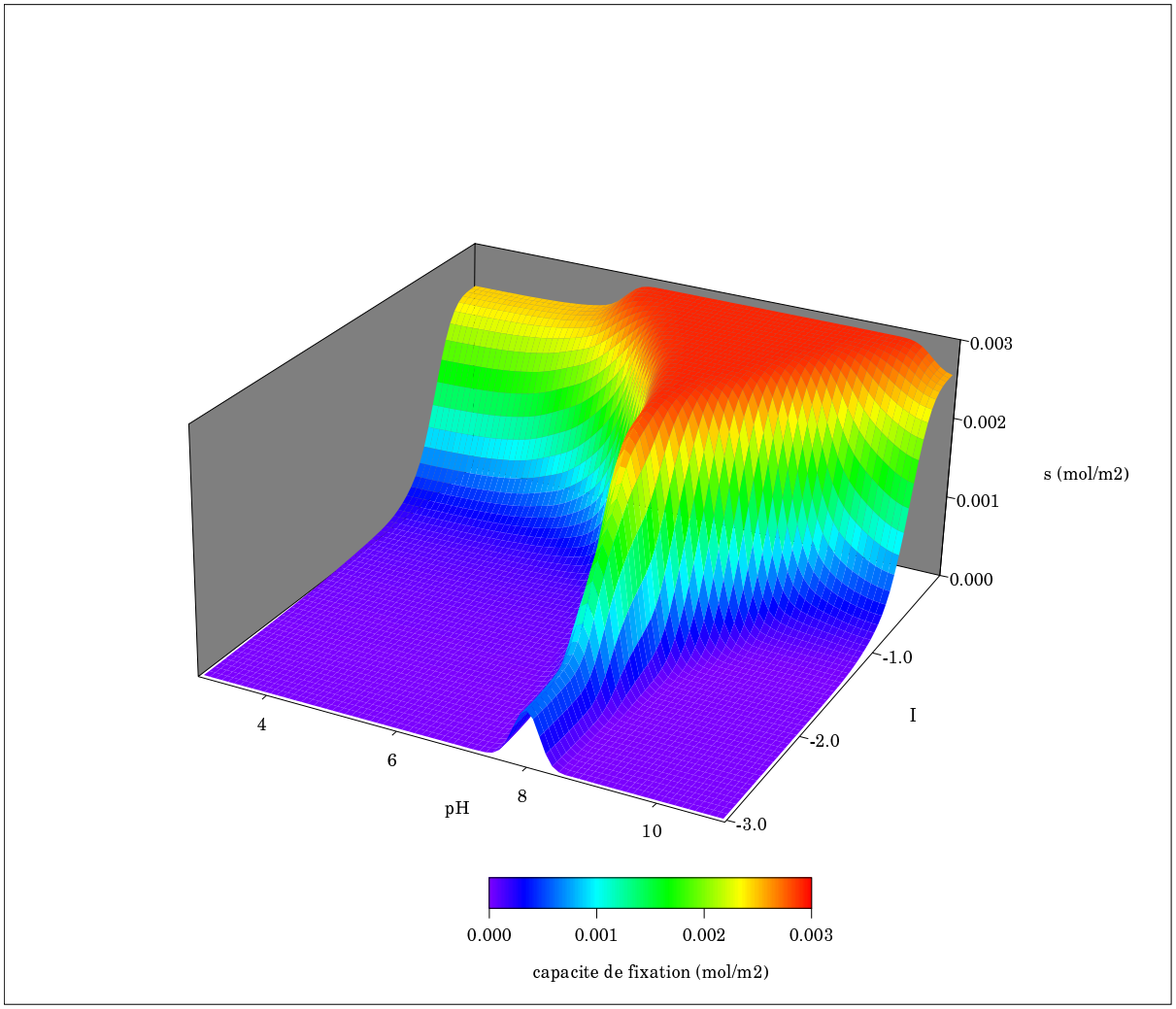

Figure 4: Fixation capacity diagram (s) for a colloidal hydrous ferric oxide suspension and a plane quartz surface. Calculated by CHESS using the parameter configuration of Table 1, $\vartheta = 1$, $p = 10$.

SORPTION AND REACTIVE TRANSPORT A MULTICOMPONENT PROBLEM?

W.H. van Riemsdijk
Department of Environmental Sciences, Subdepartment of Soil Quality,
P.O.Box 8005 6700 EC Wageningen, Wageningen University, The Netherlands
E-mail: Willem.vanriemsdijk@bodsch.benp.wag-ur.nl

In order to be able to make reasonable predictions about transport of chemicals in the environment one should have insight in a quantitative sense in the (multiple) interactions which affect the distribution of the compound of interest over the solution and the solid phase during the transport. The interaction of a toxic substance present at trace levels will in general not affect the chemistry of the solution of the porous medium, other than the concentration of the toxic trace compound. In that ideal situation one might use a mono-component reactive transport approach. In case of non-linear adsorptive interaction one can easily predict the transport if the adsorption curve is known for the medium and compound of interest if an equilibrium approach is justified. The transport velocity of an acid or base front at constant salt level can for instance be treated as a pseudo mono-component problem if the adsorption of H and OH with the solid phase determine the interaction between solid and solution.

The next step which may complicate the problem is when reaction kinetics are of relevance. Calculation of the Damkohler number, which depends on the rate constant of the reaction, the flow velocity of the groundwater and the transport distance, will give an idea whether kinetics are of relevance. It will also give an idea of the time scale of the adsorption/desorption experiment which may be required to follow the reaction. Especially for reactions which may need very long time periods to reach equilibrium it is important to realize how long one should follow the reaction kinetics in order to be of relevance for the problem one wants to study or calculate. Such problems are already quite complex to study, although we still assume that we can simplify the problem to a mono-component transport problem. One example is the (simplified) transport of phosphate present in liquid manure which is spread in high amounts over the soil. The difference in the measured phosphate adsorption to a sandy soil at a given phosphate concentration between a reaction time of one day or one year can easily be a factor two.

Also in the area of colloid facilitated transport, the kinetics and reversibility of the reaction are of paramount importance for the predicted mobility of the trace element which supposedly is bound to the mobile colloid like dissolved organic carbon (DOC).

The mobility of DOC itself may also be an important issue in case of risk assessment if the concentration of DOC varies during transport. One should in that case know what the interaction is between the DOC and the porous matrix through which the aqueous solution is being transported and in addition to knowledge on the interaction between the chemical of interest and the DOC. It is rather common in the literature on DOC transport to treat the DOC as if it is one substance with (average) properties which interacts with the solid phase. However DOC is a complex mixture of Humic acids (HA), Fulvic acids (FA) and other organic molecules. In principle each type of organic molecule will have its own interaction behavior with the solid matrix and the chemical of interest. The adsorption affinity and kinetics of the various types of organic molecules may differ, which can lead to competitive multi component interactions. I will give some examples of the phenomena which one can

encounter in studying DOC adsorption/desorption and transport and I will give examples how such problems can be tackled.

I will also show some very recent results on transport data of HA and FA through soil columns and show the multiple type of interactions which occur. The main mechanisms which can be observed in such experiment will also be discussed

WORKSHOP PROGRAMME

Wednesday, March 20

9:00 - 9:15 **OPENING AND WELCOME ADDRESS**
P. Fritz, Forschungszentrum Karlsruhe (Germany)

Session PA **COUPLED TRANSPORT REACTION MODELING IN PERFORMANCE ASSESSMENT**
Presiding: B. Sagar (USA) and B. Kienzler (Germany)

9:15 - 10:00 **COUPLED TRANSPORT REACTION MODELING IN PERFORMANCE ASSESSMENT**
B. Sagar (invited), L. Browning and S. Painter, Center for Nuclear Waste Regulatory Analyses, San Antonio, USA

10:00 - 10:30 **RADIONUCLIDE TRANSPORT AND SORPTION IN HETEROGENEOUS MEDIA FOR PERFORMANCE ASSESSMENT STUDIES**
U. Nosek and E. Fein, Gesellschaft für Anlagen- und Reaktorsicherheit (GRS), Braunschweig, Germany

10:30 - 11:00 **COFFEE BREAK**

Session A **COUPLING OF SORPTION PROCESSES AND TRANSPORT**
Presiding: W. van Riemsdijk (Netherlands) and J. Lützenkirchen (Germany)

11:00 - 11:45 **SORPTION AND REACTIVE TRANSPORT A MULTICOMPONENT PROBLEM?**
W. van Riemsdijk (invited), University of Wageningen, The Netherlands

11:45 - 12:15 **CHARACTERIZATION OF NONLINEAR TRANSPORT BEHAVIOR IN HETEROGENEOUS POROUS MEDIA BY MEANS OF BREAKTHROUGH CURVES**

J. Dimitrova, S. Attinger and W. Kinzelbach, Institute of Hydromechanics and Water Resources Management, ETH Zürich, Switzerland

12:15 - 13:45 **LUNCH**

13:45 - 14:15 **TOWARDS OBTAINING THE EXCHANGE COEFFICIENTS OF SYNTHETIC ZEOLITE NAP1; MULTICOMPONENT ION EXCHANGE TO BE COUPLED TO TRANSPORT**

J. Cama, A. Garrido, X. Querol and C. Ayora, Institute of Earth Science “Jaume Almera”, CSIC, Barcelona, Catalonia, Spain

14:15 - 14:45 **MODELING STRONTIUM SORPTION IN NATURAL AND PURIFIED BENTONITE CLAY**

M. Molera, T. Eriksen and S. Wold, Royal Institute of Technology, Department of Chemistry, Stockholm, Sweden

14:45 - 15:15 **SPREADING OF REACTIVE CHEMICALS IN NATURAL POROUS MEDIA: FROM THE ATOMIC TO THE FIELD SCALE.**

D. Grolimund, J.A. Warner, X.X. Carrier, G.E. Brown, Jr. Swiss Light Source (SLS) and Waste Management Laboratory, PSI, Switzerland, USA, France

15:15 - 15:45 **MONTE CARLO SIMULATION OF THE SWELLING BEHAVIOUR OF MX-80 WYOMING MONTMORILLONITE**

A. Meleshyn and C. Bunnenberg, Center for Radiation Protection and Radioecology (ZSR), Hannover, Germany

15:45 - 16:15 **COFFEE BREAK**

Session B **COUPLING OF REDOX PROCESSES AND TRANSPORT**

Presiding: M. Isenbeck-Schröter (Germany) and W.Schüßler (Germany)

16:15 - 17:00 **COUPLING OF REDOX PROCESSES AND TRANSPORT: TRACER TESTS WITH ARSENIC (III) AND ARSENIC (V) AT THE CAPE COD SITE**
M. Isenbeck-Schröter et al. (invited) , Institute of Environmental Geochemistry, University of Heidelberg, Germany, USA, Denmark

17:00 - 17:30 **EFFECT OF REDOX POTENTIAL ON DIFFUSION OF REDOX SENSITIVE ELEMENTS IN COMPACTED BENTONITE – SELENIUM (Se)**
H. Sato and S. Miyamoto, Japan Nuclear Cycle Development Institute (JNC), Tokai-mura, Japan

17:30 - 18:00 **CODE DEVELOPMENT FOR MODELING OF COUPLED EFFECTS AT CORROSION OF CARBON STEEL CONTAINERS UNDER REPOSITORY CONDITIONS**
E. Korthaus, Institute for Nuclear Waste Management, Forschungszentrum Karlsruhe, Germany

18:30 - 22:00 **POSTER SESSION WITH BUFFET**

Thursday, March 21

Session C **COUPLING OF DISSOLUTION / PRECIPITATION PROCESSES AND TRANSPORT**
Presiding: J. Soler (Spain) and W.Pfingsten (Switzerland)

9:15 – 10:00 **HIGH-pH PLUME. REACTIVE TRANSPORT SIMULATIONS**
J. Soler (invited) and U.K. Mäder, Institute of Earth Science “Jaume Almera”, CSIC, Barcelona, Catalonia, Spain, Switzerland

10:00 - 10:30 **COFFEE BREAK**

10:30 - 11:00 **FULLY COUPLED MODELING OF CS AND U MIGRATION IN A CLAYEY ROCK DISTURBED BY ALKALINE PLUME**

L. De Windt, D. Pellegrini, J. van der Lee and V. Lagneau, École des Mines de Paris, Fontainbleau, France

11:00 - 12:00 **REACTIVE TRANSPORT MODELLING OF INTERACTION BOOM CLAY – CEMENT WATER: EXPERIMENTAL DATA AND PRELIMINARY MODELLING RESULTS**

D. Jacques, SCK□CEN, Mol, Belgium

12:00 - 13:15 **LUNCH**

Session D **INFLUENCE OF COLLOIDS ON TRANSPORT PHENOMENA**

Presiding: J. van der Lee (France) and D.Grolimund (Switzerland)

13:15- 14:00 **COLLOIDS IN FRACTURED AND POROUS HYDROGEOLOGIC MEDIUM**

J. van der Lee (invited) and L. de Windt, École des Mines de Paris, Fontainbleau, France

14:00 - 14:30 **EFFECT OF COLLOIDAL IRON HYDROXIDE TRANSFORMATION ON ACTINIDE MOBILITY IN GORLEBEN GROUNDWATER**

T. Schäfer, R. Artinger, K. Dardenne, A. Bauer and J.-I. Kim, Institute for Nuclear Waste Management, Forschungszentrum Karlsruhe, Germany

14:30 - 15:00 **QUANTITATIVE MODELLING OF COLLOID FACILITATED TRANSPORT IN NATURAL POROUS MEDIA**

D. Grolimund and M. Borkovec, Analytical and Biophysical Environmental Chemistry,University of Geneva, Switzerland

15:00 - 15:30 **COFFEE BREAK**

15:30 - 16:00 **HUMIC COLLOID BORNE AMERICIUM MIGRATION: A STRONGLY COUPLED TRANSPORT/REACTION PROCESS**

W. Schüßler, R. Artinger, B. Kienzler and J.-I. Kim, Institute for Nuclear Waste Management, Forschungszentrum Karlsruhe, Germany

16:00 - 16:15 **WORKSHOP SUMMARY AND CONCLUSIONS**
B. Sagar, Center for Nuclear Waste Regulatory Analyses, San Antonio, USA

16:15 - 17:00 **DISCUSSION**

17:00 **CLOSING OF WORKSHOP**

Poster

REACTIVE TRANSPORT MODELLING OF RADIONUCLIDES ALONG A SINGLE FRACTURE IN GRIMSEL GRANITE (CRR PRJECT).

A. Delos, L. Duro and J. Guimerà. Enviros QuantiSci S.L., Av. Universitat Autònoma, Barcelona, Spain

A MICROSCOPIC SCALE LOW PARAMETER MODEL FOR SIMULATION OF FLOW AND TRANSPORT IN POROUS MEDIA

F. Enzmann, M. Kersten and T. Hofmann, Institute of Geosciences, University of Mainz, Germany

DIFFUSION-LIMITED SORPTION OF STRONTIUM BY MICROPOROUS HYDROUS FERRIC OXIDE: MODELLING ELECTROSTATIC CONSTRAINTS

A. Hofmann, W. van Beinum, J. C. L.. Meeussen and R. Kretzschmar, Institut für Terrestrische Ökologie, ETH Zürich, Switzerland

MIGRATION OF AMD WATER IN CARBONATE BUFFERED AQUIFERS - COLUMN FLOW EXPERIMENTS AND THEIR MODELLING

N. Hoth, J. Hutschenreuter and F. Häfner, Institute of Drilling Engineering and Fluid Mining, Technical University of Freiberg, Germany

MODELLING OF COLLOID TRANSPORT IN A GRIMSEL SHEAR ZONE

G.Kosakowski, Waste Management Laboratory, PSI, Switzerland

COMPARISON OF DOUBLE LAYER MODELS IN TRANSPORT PROBLEMS

J. Lützenkirchen and B. Kienzler, Institute for Nuclear Waste Management, Forschungszentrum Karlsruhe, Germany

COLUMN EXPERIMENTS WITH HEAP MATERIAL OF KUPFERSCHIEFER MINING AND THERMODYNAMIC INTERPRETATION

J. Mibus, Forschungszentrum Rossendorf, Dresden, Germany

MODELLING OF LEAD MOBILITY BY COUPLING TRANSPORT AND CHEMICAL PROCESSES

H. C. Moog, D. Buhmann, T. Kühle, and S. Hagemann, Gesellschaft für Anlagen- und Reaktorsicherheit (GRS), Braunschweig, Germany

MODELLING CEMENT-ROCK-WATER INTERACTIONS - THE INFLUENCE OF SELECTED BOUNDARY CONDITIONS

W. Pfingsten, Waste Management Laboratory, PSI, Switzerland

PROGRAM SYSTEM TRANSREAC

F. Schmidt-Döhl, Testing Laboratory for Civil Engineering, Braunschweig, Germany

COLONBO: A DIFFUSION-BASED MODEL TO ASSESS RADIONUCLIDE RELEASE AND MIGRATION DURING DEEP GEOLOGICAL DISPOSAL OF BITUMINIZED WASTE

C. Tiffreau, B.Simondi-Teisseire, I. Felines, S. Camaro, P.P. Vistoli and V. Blanc, CEA Centre d'Etudes de Cadarache, Département d'Etudes des Déchets, St Paul lez Durance, France

PÔLE GÉOCHIMIE TRANSPORT - BENCHMARK II - : A STUDY OF THE EFFECTS OF IRON INJECTION IN A REACTIVE POROUS MEDIUM, IN THE SCOPE OF HLW NEAR-FIELD INTERACTIONS

L. Trotignon, P. Montarnal, E. Piault, O. Bildstein, M.-E. Stoeckel, J. Van der Lee, CEA Centre d'Etudes de Cadarache, Département d'Etudes des Déchets, St Paul lez Durance, France

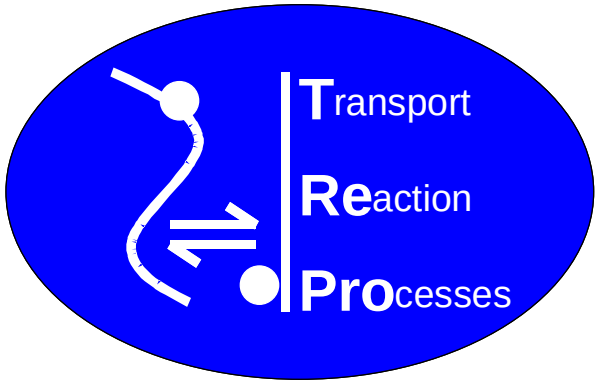
Transport
Reaction
Processes